



FACULTY OF MARITIME STUDIES

Siniša Martinić-Cezar

FUEL CONSUMPTION AND EXHAUST EMISSIONS REDUCTION OF A MARINE ELECTRIC POWER PLANT WITH FOUR STROKE DUAL-FUEL ENGINES

DOCTORAL THESIS





FACULTY OF MARITIME STUDIES

Siniša Martinić-Cezar

FUEL CONSUMPTION AND EXHAUST EMISSIONS REDUCTION OF A MARINE ELECTRIC POWER PLANT WITH FOUR STROKE DUAL-FUEL ENGINES

DOCTORAL THESIS

Supervisors:

Full Prof. Nikola Račić, Ph.D. Asst. Prof. Zdeslav Jurić, Ph.D.

Split, 2025.

IMPRESUM/BIBLIOGRAPHICAL DATA

The doctoral thesis is submitted to the University of Split, Faculty of Maritin	ne
Studies in fulfilment of the requirements for the degree of Doctor of Philosophy.	

Supervisor: Full Prof. Nikola Račić, Ph.D., University of Split, Faculty of Maritime Studies, Croatia

Co-supervisor: Assist. Prof. Zdeslav Jurić, Ph.D., University of Split, Faculty of Maritime Studies, Croatia

The doctoral thesis consists of: 132 pages, including Literature, Lists and Attachments.

Doctoral thesis no.:

This Ph.D. thesis was prepared at the Department of Marine Engineering of the Faculty of Maritime Studies.

DATA ON EVALUATION AND DEFENSE OF THE DISSERTATION

Doctoral dissertation evaluation committee:

- 1. Assoc. Prof. Tina Perić, Ph.D., University of Split, Faculty of Maritime Studies, Faculty of Maritime Studies in Split.
- 2. Full Prof. Peter Vidmar, Ph.D., University of Ljubljana, Faculty of Maritime Studies and Transport, Portorož, Slovenia.
- 3. Full Prof. Gojmir Radica, Ph.D., University of Split, Faculty of Electrical Engineering, Mechanical Engineering and Naval Architecture Studies in Split.

Doctoral Dissertation Defence Committee:

- 1. Assoc. Prof. Tina Perić, Ph.D., University of Split, Faculty of Maritime Studies, Faculty of Maritime Studies in Split.
- 2. Full Prof. Peter Vidmar, Ph.D., University of Ljubljana, Faculty of Maritime Studies and Transport, Portorož, Slovenia.
- 3. Full Prof. Gojmir Radica, Ph.D., University of Split, Faculty of Electrical Engineering, Mechanical Engineering and Naval Architecture Studies in Split.

Dissertation defended on:

SUPERVISOR BIOGRAPHY

Full Professor Nikola Račić, PhD, obtained his BSc and MSc degrees in Marine Engineering at the Faculty of Maritime Studies in Split. He later completed his PhD degree at the University of Rijeka - Faculty of Engineering in 2008. He is a full professor/scientific advisor in a permanent position in the Department of Marine Engineering at the Faculty of Maritime Studies, University of Split. At the Faculty, he has held almost all leadership positions at all levels, from Head of Studies, Head of Department and Director of the Centre to Vice Dean and Dean for two mandates. He is currently the Assistant Dean at the Faculty of Maritime Studies, University of Split.

He is the head of the following courses: Marine Engines, Marine Energy Systems, Marine Steam Generators and Heat Turbines, Marine Engineering Machinery Complex and Modelling and Simulation of Ship Systems. His research interests include numerical analysis of operating parameters of heat engines, marine energy systems and especially slow-speed diesel engines, for which he has developed a number of mathematical models and their numerical solutions. He is the author of 71 scientific and professional papers, many of which are in international peer-reviewed journals indexed in the Web of Science (CC, SCIE, ESCI).

CO-SUPERVISOR BIOGRAPHY

Assistant Professor Zdeslav Jurić, PhD, obtained his Bachelor's and master's degrees in marine engineering at the Faculty of Maritime Studies in Split. He received his PhD from the University of Split, Faculty of Electrical Engineering, Mechanical Engineering and Naval Architecture in 2010. He is an assistant professor and head of the Department of Marine Engineering at the Faculty of Maritime Studies, University of Split.

Since 2002, he has been continuously active as a course leader or lecturer in the following subjects: Thermodynamics and Heat Transfer, Heat and Mass Transfer, Marine Refrigeration and Air Conditioning Systems, Thermodynamics I, and Thermodynamics II and others. He has been involved in nine scientific research projects.

His research interests are energy efficiency, focused on marine energy systems. He is the author of 14 scientific and technical articles published in international peer-reviewed journals indexed in the Web of Science.

ACKNOWLEDGMENTS

This doctoral voyage is the culmination of decades of professional and personal seafaring, both literally and academically. After more than thirty years at sea, the transition from the engine rooms to the research papers has been challenging, but also very rewarding.

First and foremost, I would like to express my deepest gratitude to my wife Vesna for her tireless patience, encouragement and belief in me throughout this endeavor. Her understanding and perseverance, not only during my time at sea, but also during the countless hours I spent at home immersed in research, were the silent force behind this achievement. In moments of doubt, her constant encouragement served as a compass that always guided me onwards.

I thank our children for their patience, support and understanding during the many moments when I was physically present but mentally engrossed in academic thoughts. Now that this chapter is coming to an end, I look forward to calmer waters and calmer sailing together, as a family.

My sincere thanks go to my supervisor, Full Prof. Nikola Račić, Ph.D., and my cosupervisor Assistant Prof. Zdeslav Jurić, Ph.D., whose guidance, constructive feedback and constant support have been instrumental in shaping this work. Their experience and clarity helped guide the research to meaningful results, and their commitment to academic excellence is an example I will continue to follow.

I would also like to thank my colleagues and collaborators at the Faculty of Maritime Studies in Split, whose expertise, co-operation and generous sharing of time contributed significantly to the quality and feasibility of this research. Their insights and support were crucial at every stage.

And finally, I would like to thank the many shipmates and engineers I have worked with over the years. This thesis is also in part a reflection of the countless shared experiences, lessons and conversations I have had during long watches and maintenance routines. They helped plant the seeds of curiosity that eventually grew into research questions. I also owe special thanks to my parents, whose calm guidance and enduring values have helped shape the person I have become. To all who have helped me navigate this journey thank you.

ABSTRACT

This dissertation addresses the critical issue of fuel consumption and the reduction of exhaust emissions in marine power plants powered by 4-stroke Dual Fuel Diesel Electric (DFDE) propulsion system, with a focus on liquefied natural gas (LNG) tankers application. As international environmental regulations such as MARPOL Annex VI, Energy Efficiency Existing Ship Index (EEXI), and the Carbon Intensity Indicator (CII) become increasingly stringent, optimizing the energy efficiency of propulsion systems has become a priority for the maritime sector. Despite the theoretical advantages of DFDE systems in terms of flexibility and environmental performance, the Power Management Systems (PMS) commonly used on LNG vessels distribute loads evenly across all active engines, which does not necessarily correspond to optimal fuel consumption or emission behavior.

In this research, a novel, data-driven optimization model for the dynamic load distribution of the engines is developed and validated, which improves both fuel efficiency and emissions performance. The model integrates real-time operational data and specific performance characteristics of three fuel types, namely liquefied natural gas (LNG), marine diesel oil (MDO) and heavy fuel oil (HFO), with the aim of intelligently and adaptively distributing engine loads. Two iterations of the model are presented. The first version focuses on minimizing fuel consumption, while the extended model applies a multi-criteria optimization strategy that also considers nitrogen oxide (NOx) and carbon dioxide (CO₂) emissions.

Comprehensive empirical data was collected from a full-size LNG tanker equipped with five DFDE engines. Measurements included specific fuel oil consumption (SFOC), exhaust gas concentrations (NOx, CO₂) and operational power requirements in various ship modes (e.g. cargo loading/unloading and ballast/laden passage). This data formed the basis for the development and refinement of the optimization algorithms, which were implemented and tested in MATLAB using advanced interpolation and constraint-based solution methods.

Model validation was performed through a comparative analysis between optimized and standard PMS-controlled load distributions in both simulated and real-world environments. The results consistently showed fuel savings and reductions in NOx and CO₂ emissions, depending on the load scenario and fuel type. The improved model also allows the weighting of economic and environmental priorities, enabling adaptive optimization tailored to operational and regulatory requirements.

The results show that the implementation of this optimization model can significantly improve the environmental and economic sustainability of LNG ship operations. To complement the fuel and emissions optimization model, an exergy-based assessment was carried out to provide a deeper thermodynamic insight into energy quality and system efficiency.

In addition, the modular design of the model enables integration into existing ship energy management systems, providing a scalable and practical tool for meeting future emissions targets in maritime transport.

Keywords: Dual-Fuel Diesel-Electric (DFDE) power propulsion, Load Distribution Optimization, Fuel Consumption Reduction, Exhaust Emissions, LNG Marine Power Plant, Power Management System (PMS), Optimization Modeling, Exergy.

CONTENTS

1. INTR	CODUCTION	1
1.1. DE	EFINITION OF THE PROBLEM, SUBJECT OF RESEARCH	5
1.2. RE	SEARCH HYPOTHESIS	6
1.3. TH	IE RESEARCH PURPOSE AND OBJECTIVE(S)	9
1.4. CA	SE STUDY CONTEXT	10
1.5. BO	DIL-OFF GAS MANAGEMENT AND DFDE ENGINE INTEGRATION	I 13
2. LITE	RATURE REVIEW	17
2.1. MI	ETHODOLOGY OF THE LITERATURE SEARCH	17
2.2. LI	TERATURE REVIEW AND STATE-OF-THE-ART	18
3. RESE	EARCH METHODOLOGY AND MODEL DEVELOPMENT	24
3.1. PR	ELIMINARY ANALYSIS USING SHIP SIMULATOR DATA	24
	MISSION MEASUREMENTS IN REAL CONDITIONS OF	
EXPLOI	TATION	30
3.2.1.	Comparison of generator systems with constant and variable speed	36
3.3. OP	PTIMIZATION MODEL	38
3.3.1.	Overview of the development of the optimization model	38
3.3.2.	Initial model: Fuel consumption optimization model	38
3.3.3.	Enhanced model: Multi-criteria optimization model (Fuel and Emissions)	42
4. RESU	JLTS AND DISCUSSION OF THE OPTIMIZATION MODE	L 45
4.1. OV	VERVIEW OF THE APPLICATION OF THE MODEL AND ANALYTI	ICAL
APPROA	ACH	45
4.2. IN	ITIAL OPTIMIZATION MODEL (FUEL CONSUMPTION ONLY)	47
4.2.1.	Heavy Fuel Oil (HFO) Optimization Example	47
4.2.2.	Marine Diesel Oil (MDO) Optimization Example	51
4.2.3.	Liquefied Natural Gas (LNG) Optimization Example	54
4.3. EN	HANCED OPTIMIZATION MODEL (FUEL AND EMISSIONS)	58
4.3.1.	Liquefied Natural Gas (LNG) Optimization Example	58
4.3.2.	Marine Diesel Oil (MDO) Optimization Example	60
4.3.3.	Heavy Fuel Oil (HFO) Optimization Example	61
4.3.4.	Heavy Fuel Oil (HFO) Optimization Example across a wide load range	62
4.3.5.	Overview of the tested operating scenarios	66

4	.4.	EXAMPLE OF MODEL VALIDATION WITH CONSUMPTION	AND
E	EMISS	SION ANALYSIS BASED ON WEIGHTING FACTOR FOR HFO AT H	IGH
I	LOAD	DEMAND	67
4	.5.	VALIDATION OF THE OPTIMIZATION MODEL WITH LNG ACR	OSS
T	THE S	SHIP DIFFERENT OPERATING MODES	70
	4.5.1	1. Loaded passage optimization example (24,000 kW)	73
	4.5.2	2. Ballast passage optimization example (17,500 kW)	75
	4.5.3	3. Discharging the cargo optimization example (8,000 kW)	78
	4.5.4	4. Loading cargo optimization example (4,000 kW)	80
	4.5.5	5. Summary of observations and environmental impact	82
5.	EX	ERGY ASSESSMENT OF FUEL UTILISATION IN MAR	INE
PO	WEI	R PLANTS	85
5	5.1.	FUEL EXERGY AND THERMODYNAMIC ASSESSMENT	85
	5.1.1	1. Comparison of energy and exergy concepts	86
5	5.2.	EXERGY-BASED OPTIMIZATION OF ENERGY SYSTEMS	88
5	5.3.	EXERGY EFFICIENCY AND SECOND LAW THERMODYNAMICS	88
5	5.4.	METHODS FOR QUANTIFYING FUEL EXERGY	89
	5.4. 1	1. Approximate exergy calculation using the lower heating value (LHV)	89
	5.4.2	2. Stoichiometric combustion and fuel heating values	90
	5.4.3	3. Standard chemical exergy	92
5	5.5.	CARBON DIOXIDE EMISSIONS IN THE CONTEXT OF EXERGY	AND
R	REGU	JLATIONS	95
5	5.6.	HEAT UTILISATION IN HEAT ENGINES	96
6.	EX	PECTED SCIENTIFIC CONTRIBUTION	100
7.	CO	NCLUSION	102
Lľ	TERA	ATURE	104
		OF FIGURES AND DIAGRAMS	
		OF TABLES	
		OF ABBREVIATIONS	
		OF SYMBOLS	
BI	OGR	APHY	121

1. INTRODUCTION

The dual-fuel diesel-electric (DFDE) propulsion systems used in liquefied natural gas (LNG) tankers offer opportunities for significant improvements in energy efficiency and the reduction of emissions. Observations from actual ship operation have shown that the standard integrated Power Management Systems (PMS), which distribute the load evenly between the engines, do not always lead to optimal fuel consumption or exhaust emissions. This realization has sparked an increasing interest in alternative load distribution strategies that are aligned with both operational requirements and environmental regulations.

There is evidence from the field that manual adjustments to engine load distribution can outperform PMS-controlled distributions in terms of fuel consumption and emissions control. This observation led to the formulation of the research presented in this dissertation, which focuses on the development and validation of an intelligent load optimization model for engine distribution in marine power plants.

The model utilizes real-time operational data and considers multiple fuel types of Marine Diesel Oil (MDO), Heavy Fuel Oil (HFO) and Liquefied Natural Gas (LNG) at different ship operating modes. This research builds on previous work [1–4] published in peer-reviewed studies and extends it through refined model development, validation against on-board measurements and integration with emission reduction frameworks compliant with IMO regulations, including MARPOL Annex VI, the Energy Efficiency Existing Ship Index (EEXI) and the Carbon Intensity Indicator (CII).

To support this research, real-time data collection was carried out using the "Testo 350 Maritime" exhaust gas analyzer, a precision instrument designed to monitor emissions from marine diesel engines. This scientific equipment was procured as part of the project "Functional integration of the College of Split, PMF/PFS/KTF through the development of scientific research infrastructure in the building of the three faculties (KK.01.1.1.02.0018)"

The analyzer was used on board an LNG vessel to measure engine operating parameters and exhaust gas concentrations, including NOx and CO₂. The measurements were collected over the entire load range of the engine in order to develop an optimization model to determine the ideal load distribution per engine for each desired electrical output. The main goal was to improve overall energy efficiency and minimize fuel consumption and exhaust emissions.

The results confirmed the initial hypothesis that the load distribution managed by the ship's PMS could be significantly improved. The data obtained under real operating conditions

served as the basis for further refinement of the model. These results underscored the need for advanced load optimization methods tailored to DFDE engines in LNG propulsion systems.

Further validation was carried out as part of the project "Increasing efficiency, reducing pollutant emissions and hybridization of the marine energy system – MOPTHYB (IP-2020-02-6249)" as part of this initiative, specific fuel oil consumption (SFOC), engine performance and exhaust emissions (NOx and CO₂) were analyzed through comparative tests conducted both in a simulator and onboard. The results were used to refine an optimization algorithm suitable for real-time application.

In accordance with the International Convention for the Prevention of Pollution from Ships (MARPOL 73/78) and with particular reference to Annex VI on the Prevention of Air Pollution from Ships, this study examines the fuel savings of DFDE engines in liquefied natural gas (LNG) ships power plants. With the rapid expansion of the maritime sector and the increasing demand for pollution control, attention is increasingly focused on improving the energy efficiency of propulsion systems on LNG carriers. In this study, the optimal engine load configuration is investigated by analyzing the power requirements in the different operating modes and assessing in detail the specific fuel consumption and pollutant emissions taking into account port safety standards and operational constraints. In accordance with the MARPOL Convention, the study also examines the performance of on-board energy management systems, particularly in relation to engine load distribution, in order to propose strategies that effectively reduce both fuel consumption and pollutant emissions in line with international regulations.

This study examines the performance of integrated PMS, which typically distribute electrical loads evenly across all connected engines without taking into account variations in fuel consumption or emissions. The focus is on the evaluation of manual load sharing strategies that aim to improve energy efficiency and minimize pollutant emissions. A thorough comparative analysis of the collected data shows that manual adjustment of engine loads leads to better results, both in terms of fuel consumption and environmental impact.

An evaluation of the functions of the PMS shows that while it fulfils its primary operational tasks, it may not offer the most economical or environmentally sustainable solution under all typical operating conditions. This limitation is particularly evident in certain scenarios, such as navigation in rough seas, prolonged maneuvers or extended port calls where multiple engines are operating at low load, resulting in sub-optimal efficiency. Previous studies [1–4] suggest that optimization of engine deployment on a daily basis is essential, particularly through strategic reallocation of power between engines. In some operating scenarios, manual fine-tuning of load distribution is required to improve fuel efficiency and reduce NOx and CO₂

emissions accordingly. With increasing pressure on the environment and international targets to reduce greenhouse gas emissions, improving fuel efficiency has become a key priority in the maritime sector. This need forms the basis for the development of an optimization model capable of determining the most efficient load distribution for each engine, with the overall aim of minimizing fuel consumption and consequently reducing exhaust emissions.

For the marine power plants under consideration, there is currently no reliable algorithm which identifies the most efficient number of engines to be operated, and the ideal distribution of their loads based on the defined power demand, taking into account both fuel consumption and emission levels. This dissertation demonstrates the benefits of implementing a specially developed optimization model to improve fuel consumption and increase the overall energy efficiency of DFDE propulsion systems on LNG carriers.

A series of fuel consumption and exhaust emissions measurements were carried out under real operating conditions and in different operating regimes with three fuel types: LNG, HFO and MDO in accordance with Annex 4 of the NOx Technical Code 2008 [5]. The measurements covered an engine load of 20 % to 90 %, with the data initially recorded at 10% intervals. Analysis of this data set revealed that reducing fuel consumption and emissions requires a more balanced and optimized power allocation among the DFDE engines. To enhance the precision and dependability of the findings, additional measurements were conducted at intermediate load levels, incorporating 5% increments between the initially recorded intervals. These refined data points were then incorporated into the optimization model. During data collection, the automatic load sharing function was manually overridden, and the engine load was gradually increased in 5% increments to capture accurate performance data. When the desired measurement point was reached, the load was kept in this mode for some time and when all operating parameters were stable, the recording was started (according to the requirements of 6.4.9.2 and 6.4.9.3 of the NOx Technical Code 2008) [5].

The fuel consumption measurements were performed using a "145 PROFLOW Series "J" Vane meter" a mass flow meter that is calibrated and verified to maintain an accuracy of $\pm 0.2\%$ during the measurement period.

For the exhaust gas measurements, the exhaust gas analyzer for emission measurements on marine diesel engines "Testo 350 Maritime "was used, which was also used for recording the emissions on the test bench.

Steps have been taken to ensure that the accuracy of the measuring instruments is within the acceptable limits specified in section 1.3.1 of Annex 4 of the 2008 Technical Code. Careful attention was also paid to the placement of the gas sampling probes, which were positioned

either at least 0.5 meters or three times the diameter of the flue pipe, whichever was greater, upstream of the exhaust outlet. The probes were installed into the exhaust pipe, downstream of the turbocharger outlet but upstream of the exhaust outlet, ensuring sufficient gas mixing and a temperature above 343K (70°C) in accordance with the test procedures described in section 3.2 of the 2008 Technical Code [5].

The engine's key operating parameters, including NOx and CO₂ emissions and specific fuel oil consumption (SFOC), were monitored and analyzed by collecting discrete data across the engine's entire load spectrum (20% to 90%). This dataset formed the basis for the development of an optimization model to identify the most efficient load distribution for each diesel generator to match the different electrical requirements of the vessel. The main objective was to improve overall energy efficiency by reducing fuel consumption and minimizing harmful gas emissions. The research results confirmed the initial hypothesis and showed that improvements to the current PMS logic for controlling individual generators are both feasible and beneficial. In addition, the analysis of real operating data provided a basis for defining directions for future investigations.

The results of the model were re-evaluated by the author under the actual operating conditions on board the vessel and showed a high degree of reliability. Environmental variables such as weather, humidity and other external influences were not specifically analyzed, but these conditions generally remained the same throughout the validation period. The results confirmed that optimizing the load distribution to the DFDE engines integrated into the ship's electrical network is crucial to improve overall efficiency and minimize both fuel consumption and harmful exhaust emissions.

In addition to the optimization of fuel consumption and emissions, Chapter 5 also presents an exergy-based assessment of the marine power plant. This thermodynamic analysis provides a deeper insight into the quality of the energy conversion and supports the development of more comprehensive and sustainable optimization strategies.

To further validate the effectiveness of the optimization model and eliminate possible biases, this dissertation presents a detailed analysis of its effects on fuel consumption and exhaust emissions in different operating modes of the ship. These operating modes include all common ship operating modes, including cargo loading, loaded passage, cargo discharge and ballast passage, each of which places different demands on the power of the ship's power plant. The study first analyzed fuel consumption and emissions under real operating conditions using the ship's existing PMS, which distributes power evenly across the engines (uniform load). The simulation model was then applied under identical load conditions to compare fuel consumption

and emissions. To check the accuracy of the model, real load redistributions of the engines based on the optimization model were carried out on board the ship in all possible operating modes, allowing a direct comparison of the simulated and real results. In addition to validating the model, this process provided valuable insights that led to the refinement and improvement of the model, including the incorporation of exergy analysis. The second law of thermodynamics has enabled a more comprehensive assessment of efficiency by considering not only the quantity but also the quality of (fuel) energy. If this extended approach is integrated, it can contribute to further optimization of on-board energy management strategies. This analysis will quantify the fuel savings and emission reductions for each mode of operation and calculate the overall impact over the entire voyage and on an annual basis.

1.1. DEFINITION OF THE PROBLEM, SUBJECT OF RESEARCH

In recent years, the shipping industry has come under increasing regulatory and environmental pressure to reduce greenhouse gas emissions and improve energy efficiency, particularly in the propulsion systems of merchant vessels. Among the emerging technologies, Dual-Fuel Diesel-Electric (DFDE) propulsion systems have gained prominence as they can run on cleaner fuels such as liquefied natural gas (LNG) while being compatible with conventional fuels such as marine diesel oil (MDO) and heavy fuel oil (HFO).

Despite their potential for environmental and operational benefits, DFDE systems are often managed with standard PMS that distribute the electrical load evenly across all engines in operation, regardless of their individual fuel efficiency curves or emissions characteristics. While this even load distribution is operationally straightforward, it often results in suboptimal fuel consumption and unnecessarily high emissions of nitrogen oxides (NOx) and carbon dioxide (CO₂), especially under varying engine loads and vessel operating conditions.

The core problem addressed by this research is the inefficiency of PMS control at the uniform load levels in marine power plants using DFDE engines and the lack of a reliable algorithm or model that dynamically adjusts the engine's load distribution based on actual operating data, fuel type and environmental goals. This inefficiency is particularly evident in real-world conditions, such as rough seas, manoeuvrings in port or prolonged low-load operation, where PMS logic cannot optimize performance.

The subject of this study is the optimization of power distribution in an electric propulsion system for ships consisting of five 4-stroke DFDE engines (type 8L51/60DF). This study investigates and analyses:

- The effects of different engine load distribution strategies on fuel consumption and exhaust emissions
- The development and implementation of an optimization model using real operating data from LNG ships
- The comparison of optimized vs. standard PMS-controlled load distributions in terms of environmental and operational efficiency
- The integration of multiple fuel types (LNG, MDO, HFO) into the model for a comprehensive emissions and efficiency assessment.

In this study, a novel approach for an algorithm-based load dispatch model is proposed, which is capable of dynamically assigning optimal loads to each generator engine in response to real-time demand and operating conditions. The study uses extensive on-board fuel consumption and emissions measurements validated under real operating conditions to develop and refine the optimization framework.

The goal is to determine whether strategic, data-driven load allocation can significantly reduce fuel consumption and pollutant emissions, thereby contributing to regulatory compliance (e.g. MARPOL Annex VI, EEXI and CII) and more sustainable practices in maritime transportation.

1.2. RESEARCH HYPOTHESIS

The hypothesis is derived from the research purpose and is fully formulated when the research objectives have been defined. The hypothesis is formulated:

The existing power distribution system in LNG marine diesel electric power plants can be optimized by implementing a load distribution algorithm that strategically adjusts engine loads based on fuel consumption and emissions data. This approach will result in significant fuel savings and reduced exhaust emissions compared to the conventional method of even load distribution currently applied by standard Power Management Systems (PMS).

This hypothesis is based on the observation that the load balancing logic built into the PMS does not take into account the efficiency characteristics of individual engines, nor does it adapt to changing operating conditions or fuel types. In contrast, an algorithmic model driven by real-time data and validated by empirical testing can distribute loads dynamically and more intelligently, improving the overall performance of the system.

The hypothesis was tested by developing an optimization model, measuring on-board emissions and fuel consumption, and making direct comparisons between standard PMS-driven load distribution scenarios and optimized load distribution scenarios. The expected outcome is a validated model that delivers measurable improvements in both the energy efficiency and environmental impact of DFDE powered LNG vessels.

To support the main research hypothesis, several auxiliary hypotheses were formulated to structure the analytical process and clarify the scope of the investigation. These auxiliary hypotheses break down the central assertion into testable components and provide the methodological framework for the study.

- The first auxiliary hypothesis states that optimising engine load distribution based on specific fuel consumption (SFOC) data tailored to the different fuel types can lead to a measurable reduction in overall fuel consumption compared to standard practice based on uniform load sharing as implemented by standard PMS. By using detailed SFOC curves and real engine performance data, this hypothesis aims to demonstrate the efficiency gains of intelligent, non-uniform load distribution.
- The second auxiliary hypothesis extends the first by proposing that the inclusion of exhaust emissions, particularly nitrogen oxides (NOx), as an additional criterion in the optimization framework can further improve the environmental performance of DFDE-powered systems. This hypothesis assumes that prioritisation of emission reduction through a weighted multi-criteria optimization algorithm can be achieved without significantly compromising fuel efficiency, thereby meeting both economic and regulatory objectives.
- A third auxiliary hypothesis addresses the feasibility of applying the proposed optimization model to real-time operating scenarios. The hypothesis states that realworld data collected through onboard measurements across a range of engine loads and

fuel types can be used to develop a model that performs reliably under different vessel operating modes and generator configurations. This hypothesis underpins the practical relevance and adaptability of the model under real maritime conditions.

• The fourth auxiliary hypothesis builds on the previous ones by introducing a thermodynamic perspective. It states that the inclusion of an exergy-based assessment provides additional insight into the energy efficiency of DFDE marine power plants by quantifying the quality of energy conversion. This approach complements the traditional analysis of fuel consumption and emissions and enables a more comprehensive and robust optimization strategy.

However, the formulation and testing of these hypotheses are subject to several important limitations that determine the scope of this study.

- First, it is assumed that the engines considered are of the same type and have similar performance characteristics, which allows the generalisation of SFOC and emissions data across different units.
- Secondly, the influence of environmental variables such as sea state, weather and
 ambient temperature is not explicitly considered in the model. These factors are held
 constant to isolate the impact of load distribution strategies on fuel consumption and
 emissions.
- Thirdly, the model does not include economic variables such as fluctuating fuel prices, carbon taxation or the financial costs of non-compliance with emission limits that could influence decisions on implementation have minor variations due to installation constraints and environmental influences.
- Finaly, while emission measurements were performed using standardised procedures and calibrated equipment, minor inaccuracies may occur due to installation constraints and environmental conditions.

Together, these additional assumptions and constraints provide a structured framework for the development, testing and evaluation of the optimization model. They ensure that the study remains focused on its core objectives while recognizing the limitations within which its conclusions can be applied.

1.3. THE RESEARCH PURPOSE AND OBJECTIVE(S)

The purpose of this research is to develop and validate an advanced load distribution optimization model for Dual-Fuel Diesel-Electric (DFDE) marine power plants on LNG vessels. This model aims to improve energy efficiency and reduce exhaust emissions by dynamically allocating engine loads based on real operational data, fuel type, and engine specific performance characteristics. The study addresses the limitations of conventional PMS that rely on uniform load distribution, which often leads to unnecessary fuel consumption and higher emissions.

Through a combination of real-world data collection, simulation, and on-board validation, this research aims to demonstrate that intelligent load distribution algorithms can significantly improve both the environmental and economic performance of LNG-powered vessels.

The objectives of the research are:

- To analyse the limitations of standard PMS-based uniform load distribution in DFDE power systems.
- To develop an optimization model that allocates engine loads based on real-time data on fuel consumption and emissions.
- To measure and compare of fuel consumption and exhaust emissions (CO₂ and NOx) under standard and optimized load conditions.
- To validate of the optimization model under real operating conditions on an LNG ship.
- To quantify of the potential fuel savings and emissions reductions that can be achieved in the various operating modes of the ship (e.g. cargo loading, sailing, manoeuvrings, cargo unloading).
- To evaluate of the feasibility of integrating the optimization algorithm into existing energy management systems on board.
- To broaden the scope of the optimization approach, an exergy-based assessment is included to quantify the quality of energy use and provide a thermodynamic insight that goes beyond traditional metrics for fuel consumption and emissions

1.4. CASE STUDY CONTEXT

This research is based on a case study of a modern LNG carrier powered by a DFDE propulsion system as shown in Figure 1.1. The vessel has five main diesel gensets, each powered by a MAN 8L51/60DF engine with an output of 8,000 kW, delivering a total installed electrical power of 40 MW.

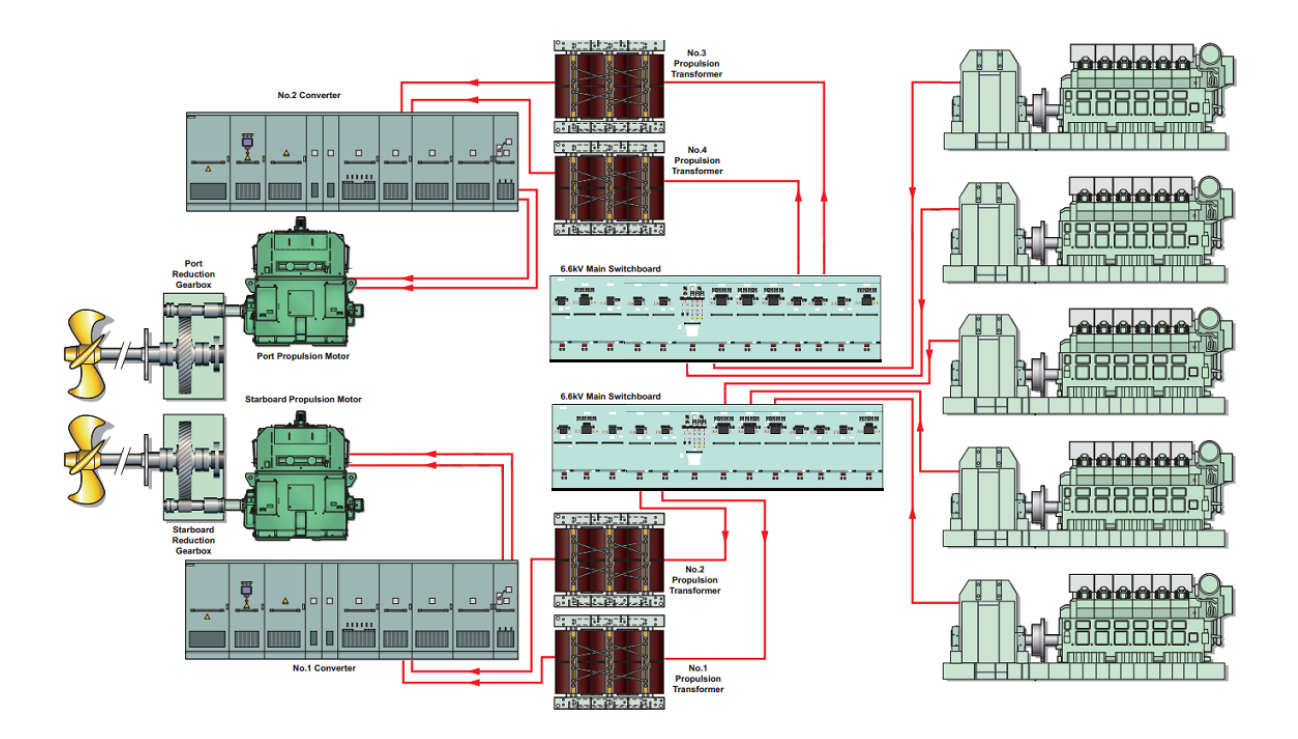


Figure 1.1 Simplified connection arrangement of diesel generators, main switchboards and propulsion systems [6]

These engines are designed so that they can be operated with boil-off gas (LNG), marine diesel oil (MDO) or heavy fuel oil (HFO) without any loss of power when changing fuel. Switching between fuel types can be done without load interruption thanks to the engine's micro-pilot injection system, which uses a small amount of diesel (less than 1%) [6] fuel to ignite the gas-air mixture in gas mode.

The DFDE engines are directly coupled to generators that provide power for both propulsion and auxiliary system. The drive system uses electric motors driven by a reduction gearbox. This allows for flexible power allocation and improved efficiency in different operating modes.

The main electrical network comprises two 6.6 kV high-voltage switchboards, which play a central role in the distribution of power throughout the ship, as shown in Figure 1.2. The connections between the generators and the high-voltage switchboard are dynamically adapted

to the real-time power requirements of the ship. Although the generators can be manually activated and connected to the switchboard, their operation, together with the main functions of the switchboard, is usually controlled automatically by the PMS.

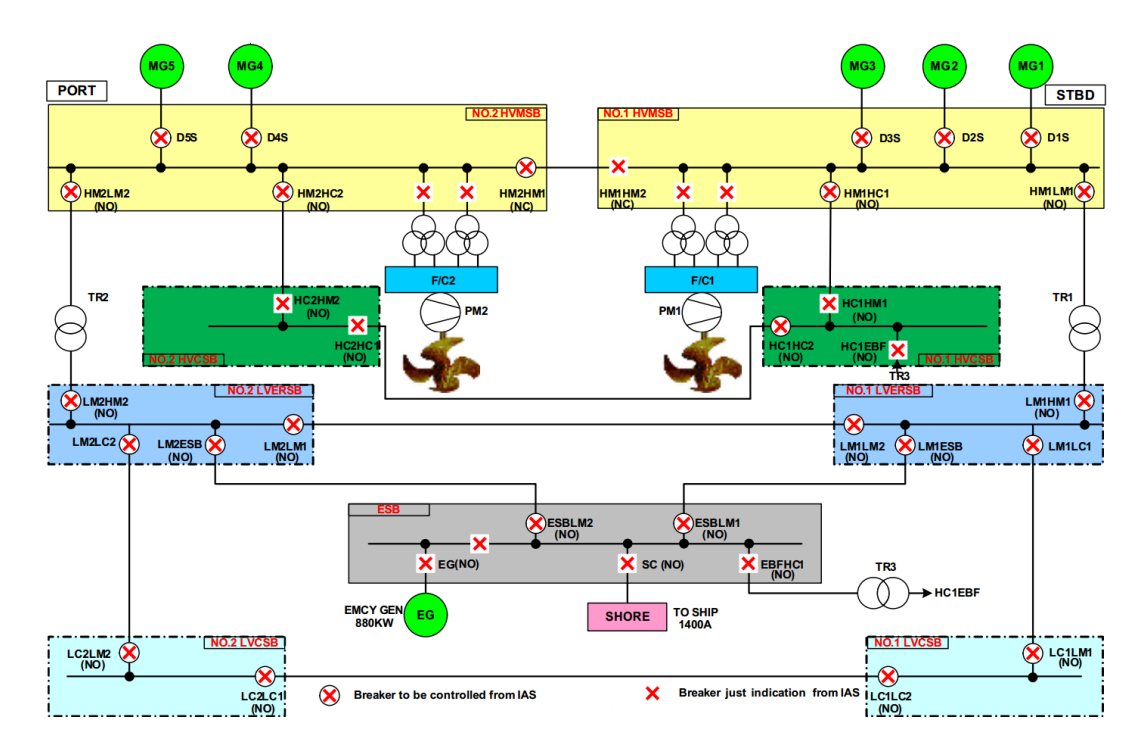


Figure 1.2 Layout of the electrical power distribution for a DFDE-powered LNG ship [7].

The intermediate distribution boards are designed to ensure redundancy and an uninterruptible power supply, thus protecting the system from possible failures. This arrangement allows the electrical consumers on the port side to be supplied by the generators on the starboard side and vice versa. The specific configuration of the electrical network is adapted according to the current operating status of the vessel and is largely based on the crew's operating experience and is generally as follows:

- During normal sea voyages, 4 or 5 diesel generators are usually in use (5 when laden, 4 when in ballast).
- During maneuverings, 2 or 3 generators are used.
- Two generators are active for cargo handling (loading and unloading).
- At berth or anchorage, 1 generator is usually sufficient.

The Power Management System (PMS) is an automated digital platform responsible for monitoring and regulating the operation of the main switchboard and the ship's generators.

It contains important control functions required for efficient energy coordination, including safety monitoring functions such as alarms and emergency shutdowns via the motor control

interface. In addition, it manages the protection and tripping of circuit breakers via dedicated control panels. The system also monitors the operation of the main switchboards and all five primary diesel generators, including their start-up, shutdown, grid connection and load balancing. It can be controlled from the workstations of the Integrated Automation System (IAS). In the event of a failure of the IAS, manual control of the motors and systems can still be carried out directly via the control panels. The PMS is responsible for several important functions, including:

- Synchronization of generators to the electrical grid.
- Regulation of system frequency.
- Automatic distribution of electrical load among active generators.
- Load-dependent start and stop of generator units.
- Automatic restart in the event of a blackout.
- Prevention of large consumer start-up under unstable conditions.
- Selection and management of standby generator units.

This system ensures that the PMS provides a reliable infrastructure for managing power flow and enforcing safety protocols on board. However, automatic load balancing within the PMS requires an even load distribution across all connected generators. Although manual load adjustment is possible, this function is limited to manual control mode and is not accessible in automatic mode. This limitation is one of the main motivations for the development of the tailored optimization model presented in this dissertation.

The specifications of the DF engines considered are listed below in Table 1.1:

Table 1.1 Specification of DF-8L 51/60 DF @ 100% load.

Engine Parameters	Specifications
Cylinder No (-)	8
Cylinder diameter (mm)	510
Stroke (mm)	600
Compression ratio (-)	13.3
Speed (rpm)	514
MCR power (kW)	8000
Firing order (-)	1-4-7-6-8-5-2-3
Mean effective pressure (bar)	19
Ignition pressure (bar)	190

This vessel provides a representative platform for evaluating real-time engine load optimization strategies for a variety of fuels and operating conditions. All optimization examples and model validations in this dissertation were derived from operational data collected aboard this vessel.

With the introduction of increasingly stringent regulations by the International Maritime Organization (IMO) such as MARPOL Annex VI, the Energy Efficiency Existing Ship Index (EEXI) and the Carbon Intensity Indicator (CII) the maritime industry is facing growing pressure to reduce emissions of CO₂, NOx and other harmful pollutants. This dissertation presents a practical and science-based solution to support compliance with these environmental targets.

From an operational and economic perspective, LNG carriers operate on long-term charter contracts, typically spanning 25 years, under consistent and predictable load patterns. This stability makes them particularly suitable for implementing intelligent, data-driven fuel-saving strategies.

The development of this research was directly influenced by the author's more than ten years of experience as chief engineer aboard LNG vessels with DFDE propulsion systems identical to those analyzed in this study. Through first-hand monitoring of engine room operations, the author observed recurring inefficiencies in load sharing. These findings formed the practical basis for the central investigation in this dissertation:

Can an intelligent, optimization-based load balancing algorithm improve fuel efficiency and reduce emissions compared to conventional PMS?

This real-world experience not only highlighted performance gaps but also served as a key motivation for the development and validation of a model that improves transparency, energy efficiency and long-term regulatory compliance over the entire lifecycle of an LNG carrier.

1.5. BOIL-OFF GAS MANAGEMENT AND DFDE ENGINE INTEGRATION

The LNG carrier described in the previous section is equipped with an advanced dieselelectric (DFDE) propulsion system that can utilize boil-off gas (BOG) as the primary fuel source. Understanding the general principles of BOG generation, handling, and conditioning is important to understand how the energy on board is managed and how optimization opportunities arise. This section describes the typical processes of BOG management on LNG vessels, focusing on how BOG is conditioned and integrated into DFDE systems, as is the case on the ship under consideration.

Over the last five decades, emissions of air pollutants from ships have increased significantly, with detrimental effects on both the marine ecosystem and human health [8]. To contribute to global efforts to reduce these harmful emissions, the International Maritime Organization (IMO) presented an initial strategy in April 2018 that aims to reduce total annual greenhouse gas (GHG) emissions by at least 50% by 2050 compared to 2008 levels [9].

Amid increasing environmental regulations, liquefied natural gas (LNG) has emerged as a promising alternative fuel for the maritime sector. Its use is particularly attractive as it virtually eliminates sulfur oxides (SOx) and particulate matter (PM) while significantly reducing emissions of nitrogen oxides (NOx) and carbon dioxide (CO₂) [10]. Typically, LNG engines running on the Otto cycle produce around 25 % less CO₂ and up to 85 % less NOx compared to conventional diesel engines [11]. This means they meet IMO Tier III standards and SOx restrictions in designated Emission Control Areas (ECAs).

In the marine sector, most LNG carriers use boil-off gas (BOG) from the cargo tanks for propulsion [12]. The dominance of steam propulsion systems, which are traditionally applied on the LNG carriers [13,14] is nowadays highly influenced by dual-fuel diesel engines (DFDE) [15,16] and their possible upgrades [17]. These dual-fuel diesel engines rely on a compressor system to supply vaporized LNG from the cargo tanks to the engine intake.

The transfer of heat from the surrounding environment into the LNG, even through insulated areas and containment tanks, causes the liquid to vaporize and form what is known as boil-off gas (BOG) [18,22]. The highest levels of BOG production typically occur during the transportation phase of the LNG cargo. The most important factors contributing to this include:

- Heat ingress into the tanks due to the temperature difference between the ambient conditions and the liquefied gas [18,23].
- Cooling of the cargo tanks during ballast voyages by spraying the remaining cargo with LNG to maintain an optimum internal temperature [18].
- Mechanical turbulence of the liquid caused by the ship's movement, especially in rough seas, increases the energy outflow and leads to greater BOG formation [18].

In order to keep the tanks at the intended pressure level, the resulting BOG must be extracted [21]. This is achieved by various systems on board:

• On ships without reliquification systems, the BOG is normally used as fuel for propulsion. Excess gas is either burned in a gas combustion unit (GCU) or used in

- boilers, depending on the system configuration, but this does not include energy recovery for pressure regulation [24].
- Conversely, ships equipped with reliquefication systems can recondense the BOG and return it to the cargo tanks in liquid form. However, this method requires a significant amount of energy to operate the reliquification plants [18,19,25].

In the case of medium-speed diesel-electric four-stroke propulsion systems, there has been a significant increase in newly built LNG vessels using dual-fuel diesel-electric (DFDE) power propulsion since 2003 [27]. This trend reflects a shift in LNG ship propulsion preferences towards DF engines that can run on both gaseous and liquid fuels [25–27].

A standard configuration for a diesel-electric drive system with dual-fuel engines (DF) is shown in Figure 1.3. In this arrangement, four DF engines are connected to generators that supply power to the entire vessel, including propulsion via electric motors and auxiliary loads (hotel) [20,26]. This arrangement, typical of modern LNG carriers, allows for flexible power distribution, operational redundancy and improved efficiency in different operating modes.

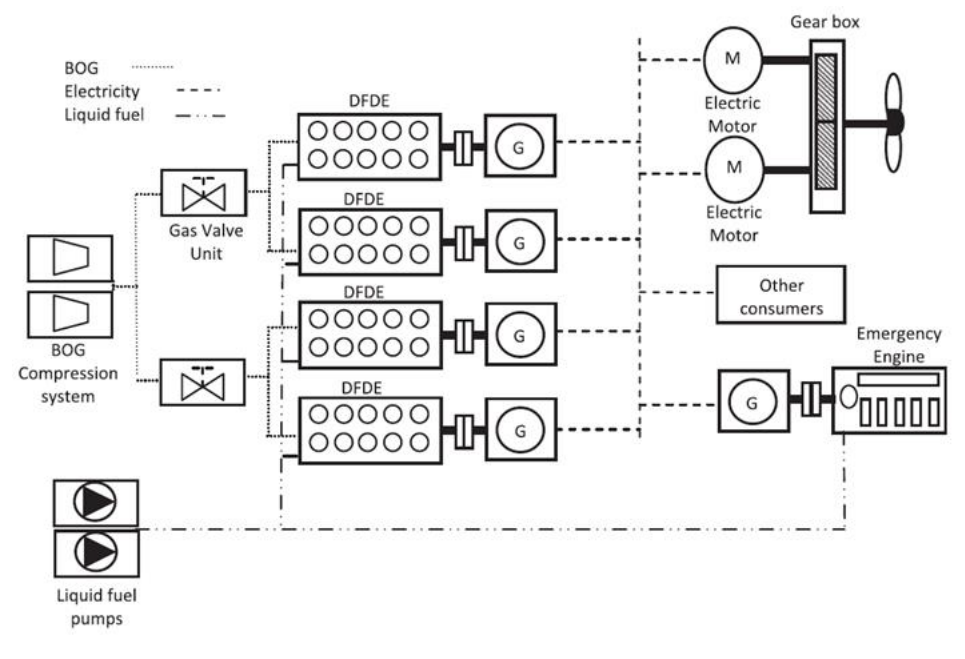


Figure 1.3 Configuration of diesel-electric propulsion using DF engines

Before BOG can be combusted in DF engines, it must undergo specific conditioning processes similar to that shown in Figure 1.4. Since DF engines are primarily designed to burn methane, other components of the natural gas (NG) must be removed to ensure proper combustion and prevent engine knocking [27,29]. This is done using a device called an oil mist separator, which separates methane from the other hydrocarbons in the NG [27,31].

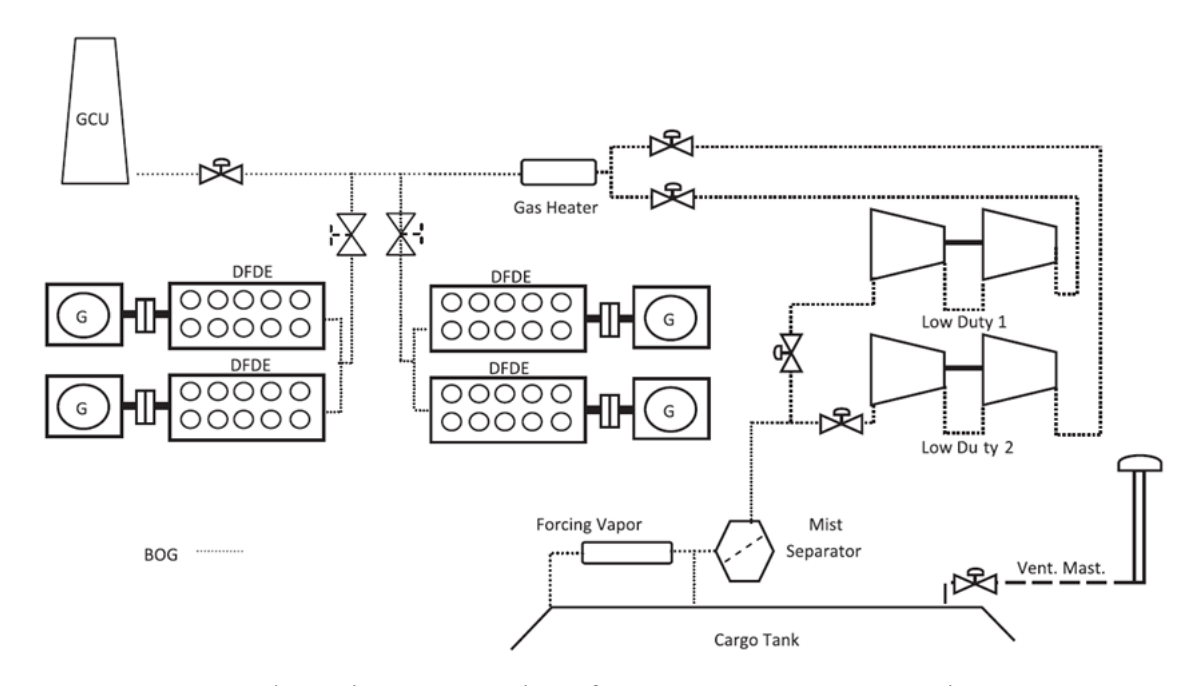


Figure 1.4 Schematic representation of a gas management system in a DFDE propulsion setup

After separation, the methane is drawn into low-duty compressors (LD compressors) that increase the gas pressure to 5–6 bar, which is suitable for engine operation [25,27,28,29,32].

Once the gas is pressurized, it is passed through a seawater-cooled heat exchanger to stabilize its temperature before it is delivered to the engines and GCU [30].

In summary, the management and utilization of boil-off gas is central to the energy strategy of DFDE-powered LNG vessels. Efficient BOG conditioning through separation, compression and temperature stabilization not only enables the safe and reliable operation of DF engines, but also plays a crucial role in overall energy efficiency and emissions control. These fundamental processes have a direct impact on engine performance, fuel consumption and exhaust emissions under different load conditions. Understanding this system architecture is crucial for evaluating and improving energy distribution strategies. The following sections focus on identifying the limitations of current energy management practices and developing an optimization model to minimize fuel consumption and environmental impact under real-world operating conditions.

2. LITERATURE REVIEW

A structured search process was used to compile a comprehensive literature review on the optimization of dual-fuel propulsion optimization and strategies for reducing emissions. The methodology of the literature search is described in the following section.

2.1. METHODOLOGY OF THE LITERATURE SEARCH

The literature search was carried out using a systematic search strategy in three large academic databases: Scopus, Web of Science, and Google Scholar. The aim was to find studies on the topics of fuel efficiency, emission reduction, and optimization of dual-fuel propulsion systems for ships.

Boolean operators and combinations of domain-specific keywords were used to achieve comprehensive results. The search syntax was adapted to the indexing format of each platform. For example:

For **Scopus** & **Google Scholar**: (Fuel OR gas OR petrol OR gasoline) AND (Consumption OR burning) AND (exhaust emissions OR emission reduction) AND (reduction OR decrease OR drop) AND (marine OR naval OR nautical OR vessel OR ship) AND (electric power plan OR power station OR electrical generating station) AND (dual-fuel OR combined fuel OR multi-fuel) AND (engine OR generator OR motor) AND (optimization OR optimization or fuel efficiency).

For **Web of science**: (((ALL=((Fuel OR gas OR petrol OR gasoline))) AND ALL=((Consumption OR burning))) AND ALL=((marine OR naval OR nautical OR vessel OR ship))) AND ALL=((electric power plan OR power station OR electrical generating station)).

The initial results included:

• Scopus: 41 references

• Web of Science: 143 references

• Google Scholar: Over 4800 filtered to review papers from 2015–2025

All results were manually screened to extract the most relevant studies based on the research focus on DFDE propulsion, real-time load optimization, and emissions compliance. Preference was given to peer-reviewed papers, recent conference proceedings, and studies with validated models.

2.2. LITERATURE REVIEW AND STATE-OF-THE-ART

This section provides an overview of key research related to the optimization of marine propulsion systems, focusing on both general strategies for improving energy efficiency and reducing emissions, as well as specific approaches for dual-fuel diesel-electric (DFDE) propulsion systems. The overview includes methods such as load balancing optimization, energy management algorithms, fuel consumption modelling and multi-criteria decision frameworks. Particular attention will be paid to studies that incorporate real-time operational data and take into account the regulatory requirements of MARPOL Annex VI, the Energy Efficiency Existing Ship Index (EEXI) and the Carbon Intensity Indicator (CII). By examining a wide range of optimization techniques for different ship types and propulsion configurations, this section highlights the current state of the art and identifies gaps that the present research aims to fill with a tailored, data-driven model for DFDE systems.

A previous research paper [4] analyzed in detail how different operating modes of ships affect the reduction of exhaust emissions and fuel consumption of LNG plants. This study analyses the dynamic interplay between power demand, specific fuel consumption and CO₂ and NO_x emissions under different operating scenarios characteristic of LNG tankers. The main objective is to identify the most efficient engine configuration for each operating mode, using data from simulators and test platforms, while complying with safety requirements and port regulations. An evaluation was carried out to assess the performance of the integrated PMS, particularly in relation to the manual allocation of engine load. The results of a detailed comparative analysis show that manual adjustment of engine loads provides better performance. In particular, the data shows that daily fuel consumption is lower when using marine diesel oil (MDO) or liquefied natural gas (LNG) when the load is manually optimised compared to the equal distribution forced by the PMS. For example, in a typical sailing scenario with a total power requirement of 17,700 kW over a 24-hour period, manual load distribution resulted in a reduction in fuel consumption of 4.09% for MDO and 3.34% for LNG. Given the considerable daily fuel consumption of such vessels, these improvements represent a significant annual saving.

In terms of NOx emissions, the analysis also showed that manual load sharing leads to lower emissions when the ship is operating on MDO compared to automatic load distribution managed by the PMS.

This research extends earlier work [3] that explored the capability of Liquefied Natural Gas (LNG) propulsion systems to lower fuel consumption by implementing controlled load

distribution among engines within a DFDE configuration. Based on cyclic data collection measured on board and using an optimization model, this study evaluates different load sharing strategies between optimization model output and automatic (equal) operation to determine their effectiveness in improving fuel efficiency. The analysis included scenarios with different fuel types, including Liquid Natural Gas (LNG), Marine Diesel Oil (MDO) and Heavy Fuel Oil (HFO), at different engine loads. The findings indicated that modifying load distribution in accordance with the optimization model led to moderate improvements in fuel efficiency across nearly all load ranges, when compared to traditional uniform load-sharing approaches managed by energy management systems.

Although the model presented in [3] effectively demonstrated fuel savings through optimised load distribution, the subsequent study in [4] extended the scope of the model to include exhaust emissions, in particular nitrogen oxides (NOx) and carbon dioxide (CO₂), in response to stricter environmental regulations. The inclusion of emissions in the optimization framework enables a more comprehensive strategy for the sustainable propulsion of LNG-fuelled ships. This research highlights the effectiveness of an optimization model tailored to load distribution between DFDE engines in LNG ship propulsion systems, with a focus on minimising both fuel consumption and exhaust emissions, particularly nitrogen oxides (NO_x). Expanding on earlier research [3], which focussed solely on fuel consumption, the improved model presented in [4] integrates emission-related parameters and thus corresponds to the maritime industry's evolving focus on comprehensive sustainability. By optimising engine load allocation using weighted criteria for fuel consumption and emissions, the model achieves a significant reduction in NO_x emissions while improving fuel efficiency in line with current environmental regulations.

Recent studies have increasingly focussed on improving marine engine performance and reducing emissions, mainly in response to stringent environmental regulations and the growing need for improved fuel efficiency. For example, [33] presents a robust approach to optimise both the design and operating parameters of diesel-electric propulsion systems on board ships, with the primary aim of increasing energy efficiency and reducing fuel consumption. In the study, a genetic algorithm is used to identify the most effective configuration and operating strategy. Variables such as the number and type of motors, their power and speed as well as the optimum distribution of the load across the motors are considered.

The study evaluates various propulsion system configurations, including both AC and DC systems, to identify the most fuel-efficient configuration under both design and non-design

conditions. The study focuses on a pleasure craft with a target speed of 17 knots and investigates engine selection and optimal operating points in a speed range of 10 to 17 knots. The optimization algorithm identifies the most efficient engine operating parameters at reduced speeds and determines the appropriate number and specifications of diesel generators. Two different energy management strategies are compared: one with even load sharing and one that allows uneven load distribution between the generators. The results emphasise the advantages of variable speed operation over fixed speed operation, including enhanced engine performance, reduced fuel usage, and minimized disruptions caused by frequent generator switching. In summary, the study finds that diesel-electric propulsion systems, especially those incorporating variable speed operation and adaptable load management, offer better fuel efficiency and operational performance at lower cruising speeds.

Reference [34] provides an overview of various optimization-based strategies for the management of power and energy systems on board ships. These approaches aim to reduce fuel consumption, minimise environmental impact, limit capital investment, optimise the weight and dimensions of onboard equipment and extend the operational life of the vessel. The study examines techniques used to improve the efficiency of power and energy management systems. Similarly, Carlsen in [35] applies several optimization algorithms in different scenarios using the Metso DNA platform, an integrated automation system. The study shows that the Metso DNA system with four diesel generators achieves an average energy saving of 2.36% under different load conditions. In contrast, the use of a simple simulator results in savings of only 0.1675% at lower loads and 2.5248% at higher loads when comparing configurations with unbalanced loads to those with evenly distributed loads.

In [36], an optimization strategy for an all-electric cruise ferry is presented with the aim of reducing operating costs and greenhouse gas (GHG) emissions while improving the Energy Efficiency Operational Indicator (EEOI). The study evaluates several diesel generator load scenarios and shows a cost reduction of approximately 2.88% through propulsion optimization alone and 2.66% when propulsion control is combined with an EEOI constraint. In contrast to these approaches, our model proposed in this study uses real-time operational data and enables the dynamic prioritisation of emission reduction over fuel efficiency through the use of adjustable weighting factors. In this way, the model can maintain robust performance under different and variable ship operating conditions. By treating emissions as a central optimization parameter rather than a secondary constraint, the proposed system provides an integrated and effective solution compared to conventional methods. While various optimization strategies have been explored for power and energy management on ships, few have successfully

combined real operational data with load balancing optimization tailored to DFDE configurations. This research advances the field by presenting a real-time, data-driven optimization model developed specifically for DFDE propulsion systems that has been proven to improve fuel efficiency and reduce emissions under real-world operating conditions. In [37], a control strategy for limiting fuel consumption and emissions for an all-electric propulsion system with two fuel types is presented. The results show that cost efficiency often collides with environmental objectives. In particular, when the EEOI restrictions are cancelled at high load, the system achieves a reduction in operating costs of almost 11%.

In [38], the researchers propose an advanced approach for power management of electric marine power systems that include all-electric propulsion, onboard energy storage and shore power interfaces. This approach uses a fuzzy logic-enriched particle swarm optimization algorithm to lower costs, reduce greenhouse gas emissions and ensure compliance with technical and operational limits. Simulation results show that this algorithm outperforms conventional methods in terms of both cost savings and emissions performance.

In [39], the author provides a general overview of fuel efficiency considerations for diesel engine-powered gensets. The study includes measurements of fuel consumption in different operating scenarios and presents an optimization technique based on genetic algorithms to improve system efficiency. This method shows potential fuel savings of up to 3.1%. Similarly, the researchers in [40] apply two optimization strategies: Gradient search and genetic algorithms to minimise fuel consumption. For a given generator configuration, the gradient search results in a modest saving of 0.1%, while the genetic algorithm achieves savings of up to 3%.

The study in [41] presents an optimization model to be used in the early stages of ship design to support the selection of the most suitable diesel engine configuration within a diesel-electric (DE) propulsion system. This model evaluates both the operating costs, taking into account potential NO_x taxation, and the initial capital investment. It emphasises that higher initial costs may be justified by long-term fuel savings, so it makes economic sense to consider capital and operating expenditures together. Similarly, [42] examines several strategies to reduce fuel consumption, including weather routing, the optimal alignment of diesel generators (DG) and the integration of weather routing into the ship's PMS, which applies to both identical and non-identical engine types. The study also considers the role of energy storage solutions, such as battery systems. When optimising load distribution, the implementation of these strategies results in up to 5% fuel savings.

In [43], an energy management strategy based on dynamic programming is presented for a complex marine energy system with electric shaft machines. The study considers both propulsion engines running on heavy fuel oil and generator engines running on light fuel oil. Despite the contradictory goals of minimising operating costs while simultaneously reducing greenhouse gas emissions, the model shows that effective operational optimization is possible. The implementation of a combination of strategies leads to fuel savings of up to 3.8%. In [44], a comprehensive approach is proposed to identify the optimal system configuration from both economic and environmental perspectives. By applying the whale optimization algorithm to control energy consumption on board ships, the study finds a reduction in fuel consumption and emissions of between 4.04% and 8.86%. Likewise, [45] presents a method for optimizing engine load distribution using mixed-integer linear programming, which was tested using a case study on a cruise ship. The results indicate that fuel savings of around 3% are possible, which contributes to a corresponding reduction in pollutant emissions.

In addition, [46] investigates the efficient use of generators with a focus on minimising greenhouse gas emissions. The results show that emission levels vary depending on electricity demand and operating conditions and that the implementation of a suitable load balancing strategy can lead to an emission reduction of up to 22%.

There are numerous studies on the optimization of DFDE engines, such as [47–52]. However, no approach similar to the one presented in this research has been identified in the available literature that considers the optimization of DFDE power plants and the reduction of fuel consumption and exhaust gas emissions through the load sharing between engines. Consequently, this research examines the potential for reducing fuel consumption and exhaust emissions through a case study involving DFDE engines installed on an LNG-powered vessel.

To summarise, the literature reviewed shows significant advances in dual-fuel engine technology, emissions legislation and ship energy management strategies. However, current PMS on LNG ships are generally based on fixed or uniform load distribution algorithms that do not dynamically adapt to operational or environmental priorities. While various studies address the optimization of fuel consumption or emissions, few integrate both in a real-time, data-driven framework applicable to DFDE propulsion systems. Furthermore, existing models often lack validation against full-scale ship data. These gaps highlight the need for a comprehensive, adaptive model to optimise engine utilisation while minimising fuel consumption and pollutant emissions, and at the same time integrating with existing PMS systems. This dissertation addresses this need by developing and validating a novel optimization approach that incorporates multiple fuel types, real-world operational data and

multi-objective	e criteria to	improve the	efficiency a	and environm	ental footprint	of DFDE m	arine
power plants.							

3. RESEARCH METHODOLOGY AND MODEL DEVELOPMENT

The research methodology uses a multi-pronged approach to develop and validate an

optimization model for the load sharing of engines in LNG propulsion systems. First, a

comprehensive literature review was conducted to establish a baseline of current practice and

identify gaps in fuel efficiency and emissions management. Extensive data collection was then

carried out on LNG vessels and real-time operational data on fuel consumption, engine load

and emissions were recorded under different conditions and fuel types. This empirical data was

used to develop a robust optimization model, which was tested using MATLAB simulations to

evaluate different load balancing strategies compared to conventional PMS. Validation of the

model included a real-world implementation on test vessels to compare simulated predictions

with actual performance, ensuring the practical applicability and effectiveness of the model in

reducing fuel consumption and emissions. This methodology not only supports theoretical

advances in energy optimization on ships but also underlines the commitment to empirical

validation and practical implementation.

3.1. PRELIMINARY ANALYSIS USING SHIP SIMULATOR DATA

The LNG vessels and their equipment considered in this study have different power

consumption requirements depending on the vessel's mode of operation (loading/unloading in

port, anchoring, loaded or ballast condition at sea, maneuvering, etc.). Under these conditions,

the ship power plant must be able to handle many combinations of energy demands with high

efficiency. To determine the required number of engines in the grid, both the economic (fuel

consumption) and environmental (exhaust emissions) efficiency of the engine should be

considered.

For each of the above ship operating situations, the PMS itself performs its function, but

based on the author's experience with this type of marine LNG systems, in most cases PMS is

not necessarily the optimal economic and environmental solution.

In a preliminary study [1,2] that preceded the hypothesis, exhaust gas data was recorded

on a ship simulator for comparison: nitrogen oxides (NOx), carbon dioxide (CO₂) and specific

fuel oil consumption (SFOC).

Simulator – General characteristics of the ship:

length: 299.9 m,

breadth: 45.8 m,

24

- design draft: 11.5 m,
- speed service approx.: 19.5 knots,
- cargo Tank capacity: 170,200 m³.

Simulator – General characteristics of the engines:

- manufacturer: MAN B&W,
- type: 8L51/60DF,
- type: Four-stroke, in-line, dual fuel, turbocharged,
- rated power: 8,000 kW (MCR) on LNG, 8,000 kW (MCR) on MDO,
- speed: 514 rpm,
- cylinder bore: 510 mm,
- piston stroke: 600 mm,
- no. of cylinders: 8.

Measurements were made on three different types of propulsion fuel:

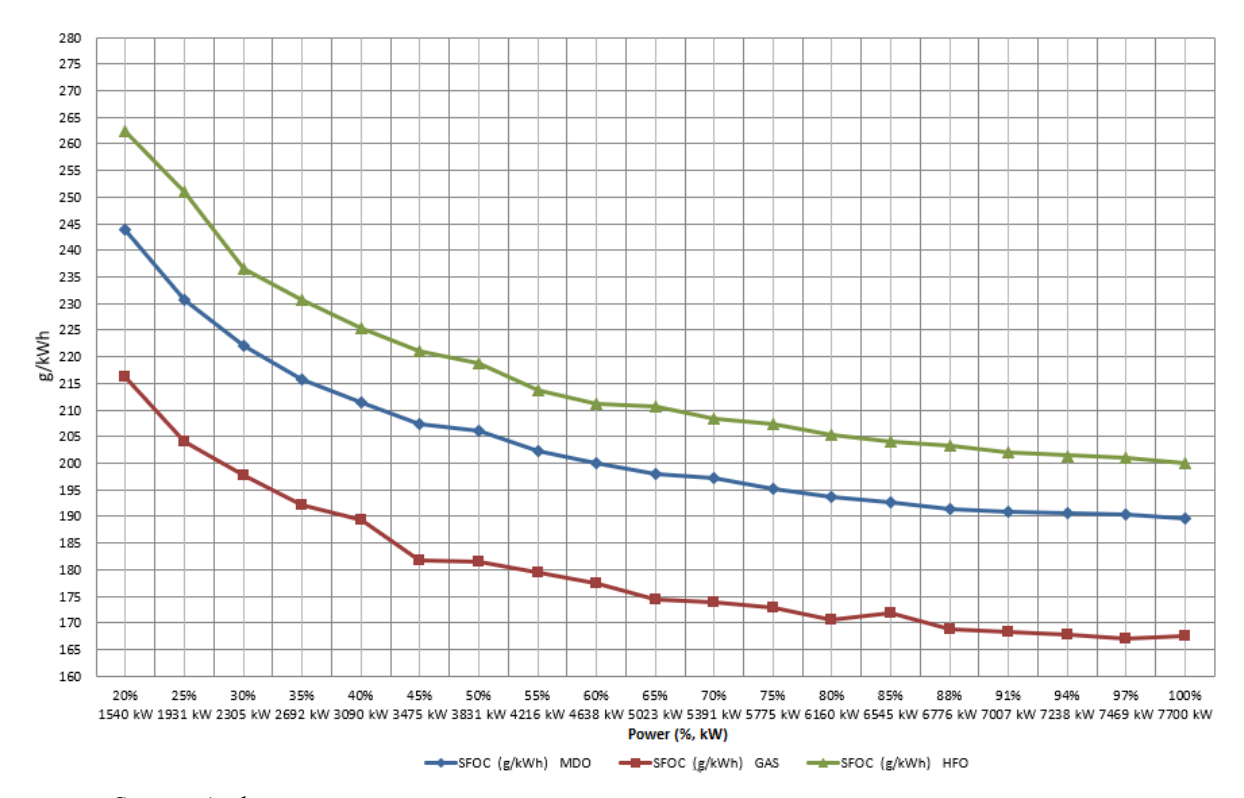
- HFO Heavy fuel oil,
- MDO Marine diesel oil and,
- LNG Liquefied natural gases.

Figure 3.1 shows SFOC, expressed in g/kWh at different engine loads and for three different types of fuel (HFO, MDO and LNG) taken on ship simulator.

To facilitate comparison of measuring units with other fuels, LNG consumption was recalculated and the final value was given in g/kWh. In calculation, data on gas density and lower calorific value are taken from LNG specification as shown below:

- Standard density of the gas 0.7740 kg/m³
- NCV (Net Calorific Value) natural gas (volume) 37874 kJ/m³

It can be seen that LNG has the lowest SFOC, followed by MDO, and that the specific fuel consumption is highest when the engine uses HFO. The graph shows that for all three fuel types, the SFOC is higher at lower engine loads and gradually decreases in parallel as the engine load increases.

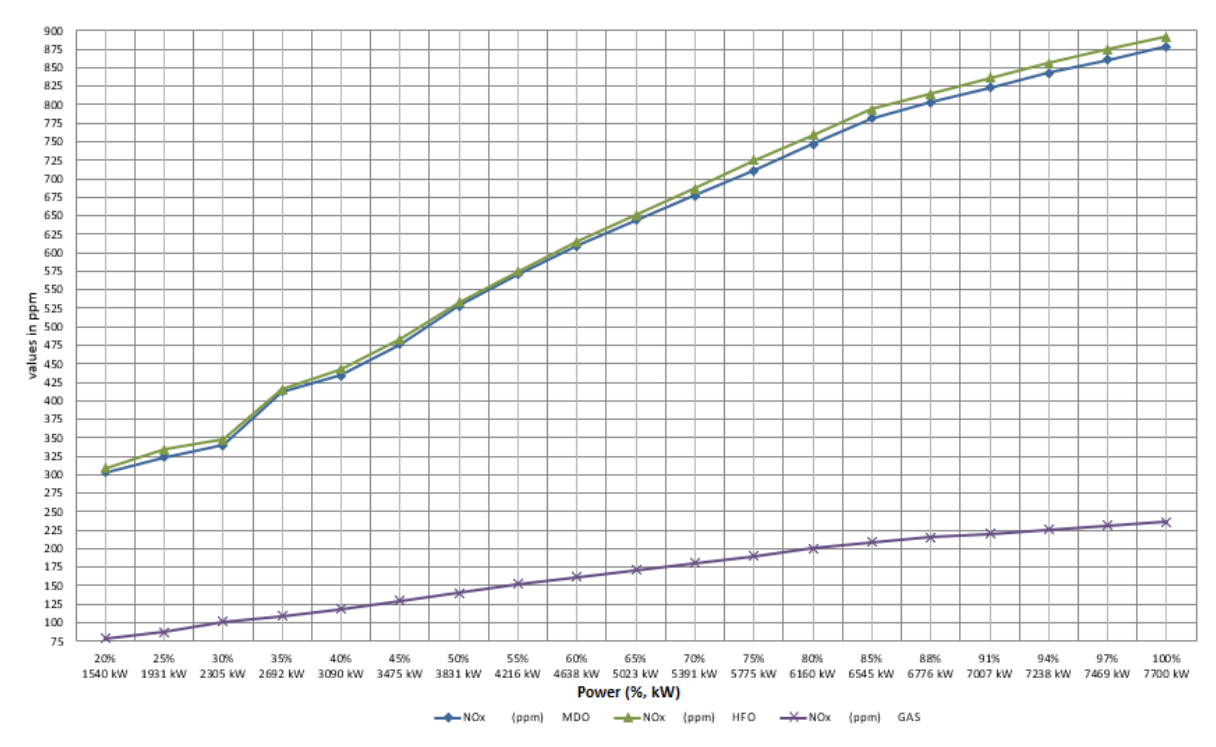


Source: Author

Figure 3.1 Specific Fuel Oil Consumption (SFOC) as a function of engine load for HFO, MDO, and LNG, recorded during simulator tests

Figure 3.2 shows the NOx (ppm) emissions at various engine loads and when running the engine on three types of fuel (HFO, MDO and LNG) recorded on the simulator.

As can be seen from the graph, NOx emissions are lower at lower engine loads and increase with engine load for all three considered fuel types. There are significant differences when the engine is running on LNG. NOx emissions are significantly lower than when the engine operates on liquid fuels (HFO and MDO). It is also noted that they increase slightly in relation to the engine load. NOx emissions when the engine is operated with HFO and MDO are slightly increased at all loads when HFO is used compared to MDO, and this ratio is constant. This trend in NOx emissions can be explained by the fact that the formation of NOx in a diesel engine depends on the combination of high temperatures, the availability of oxygen and nitrogen, and the duration of combustion. Since the formation of NOx is strongly dependent on the combustion temperature, the rate of formation in exhaust gases increases at higher temperatures [53, 54].



Source: Author

Figure 3.2 Nitrogen oxide (NO_x) emissions, measured in ppm, as a function of engine load during simulator operation with HFO, MDO and LNG

Results from Figure 3.3 show that CO₂ emissions (expressed in %) increase steadily in parallel with the engine load. It is also observed that the CO₂ content is consistently slightly lower in all operating modes when the engine is running on LNG than with the other two liquid fuels, and that this difference is much more significant at some engine operating points. The biggest difference in CO₂ content is when the engine is running with a load of 30%. The CO₂ content for LNG is then 2.6%, for MDO 3.0% and for HFO the CO₂ content is even higher and is 3.1%. Since the amount of CO₂ emitted is directly proportional to the amount of fuel consumed and energy efficiency, a reduction in CO₂ emissions can be achieved by reducing SFOC [55]. According to the results in Figure 3.1, the lowest SFOC values are obtained when the engine is running on gas fuel, which could lead to conclusion that CO₂ content curve should have same pattern.

Martinić et al [1] performed a comparative analysis of simulator and test bed data in terms of exhaust emissions (CO₂ and NOx) and SFOC, which determined highest deviations in CO₂ results.

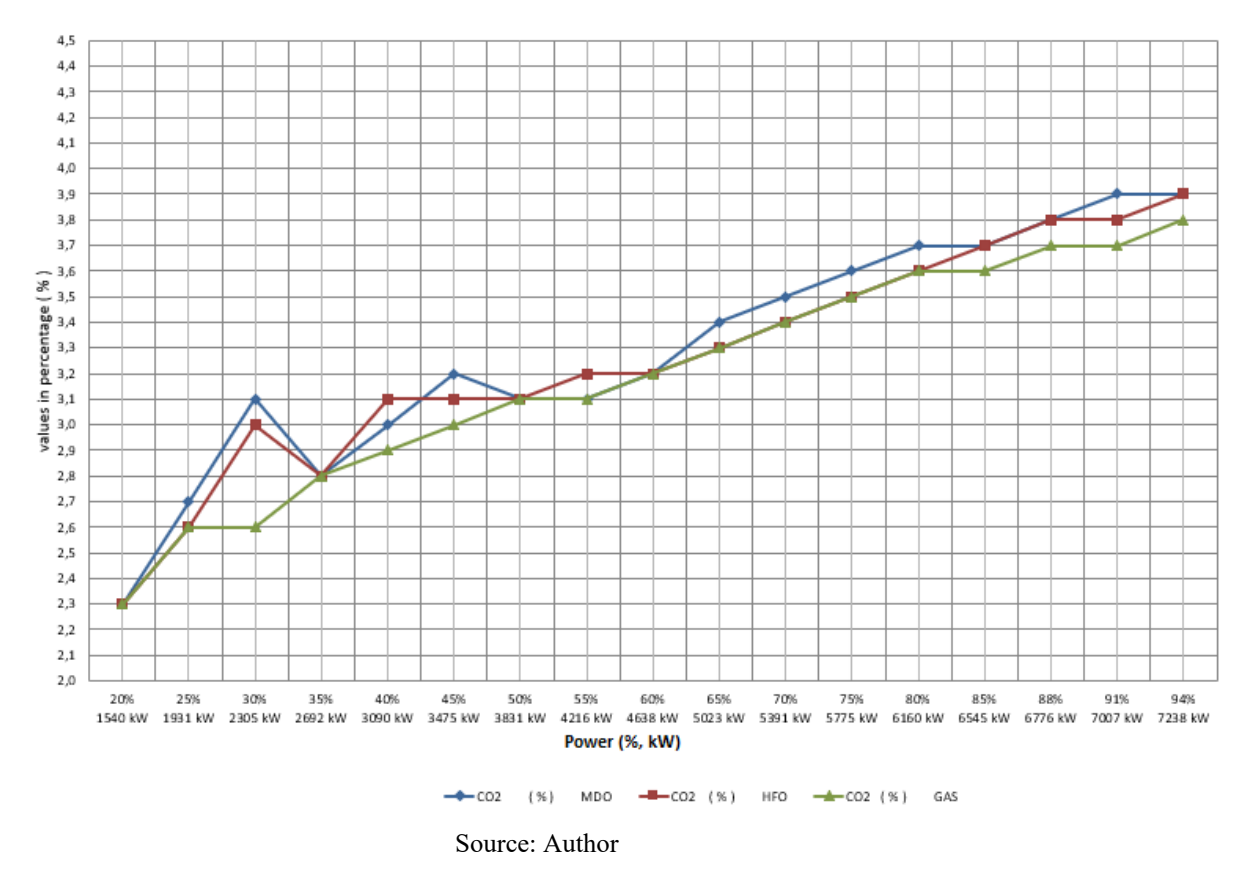


Figure 3.3 Carbon dioxide (CO₂) emissions, expressed as a percentage depending on the engine load, based on simulator tests with HFO, MDO and LNG

Considering the above results from the fuel consumption and NO_x emissions measurements performed in the simulator, LNG is the first choice in fuel selection, both from an economic and environmental point of view.

Table 3.1 shows each operating mode together with the corresponding power output, analyzing two different engine configurations. The first configuration reflects the default load distribution via the PMS, where power is automatically distributed evenly across all active engines without considering optimal engine performance, fuel efficiency or emission levels. The second configuration bypasses the PMS and allows manual load adjustment between the engines. In this configuration, the engines are operated at their most efficient load points, while the remaining power requirement is covered by an additional engine running at a lower load level.

Table 3.1 Different engine load distribution

LOAD	Configuration	SFOC (g/kWh)			Consumption MT/day			NOx (ppm)		
		GAS	MDO	HFO	GAS	MDO	<i>HFO</i>	GAS	MDO	HFO
10000 kW	2 Eng. equally sharing load (2 x 5000kW)	2*175,7	2*198,8	2*210,4	42,16	47,71	50,49	344	1290	1304
	2 engine adjusted load (1x6500kW / 1x3500kW)	1*170 1*184	1*192,2 1*207,5	1*204 1*220,2	41,97	47,41	50,31	338	1262	1276
15300 kW	3 Eng. equally sharing load (3 x 5100kW)	3*175,7	3*198,8	3*210,4	64,5	72,99	77,25	516	1935	1956
	3 engine adjusted load (2x6500kW / 1x2300kW)	2*170 1*198	2*192,2 1*222,3	2*204 1*239	63,96	72,23	76,83	513	1922	1950
22000 kW	4 Eng. equally sharing load (4 x 5500kW)	4*173,7	4*196,4	4*208,2	91,71	103,7	109,9	740	2784	2820
	4 engine adjusted load (3x6500kW / 1x2500kW)	3*170 1*194	3*192,2 1*218,7	3*204 1*234,5	91,2	103,1	109,5	728	2726	2766

Source: Author

For all three load scenarios shown in Table 3.1 and for the three fuel types, the second configuration, in which the engine loads are manually adjusted, shows a slight advantage in terms of fuel efficiency. The results show that the daily fuel consumption, measured in tons per day (MT/day), is slightly lower in this manually optimized configuration than in the baseline scenario, in which the load is evenly distributed by the PMS. In terms of NOx emissions, the manually adjusted strategy, where one engine is operated close to its optimal load (about 85% of MCR) while the remaining load is allocated to another engine with lower output, results in lower emission levels. These results suggest that this approach is more environmentally friendly than a uniform load distribution.

Table 3.2 Overall result differences

LOAD	Configuration		mption differe percentage (%)		Difference in percentage (%) NOx			
		GAS	MDO	HFO	GAS	MDO	HFO	
10000 kW	2 Eng. equally sharing load (2 x 5000kW)	0,45	0,62	0,35	1,74	2,17	2,14	
	2 engine adjusted load (1x6500kW / 1x3500kW)	/	/	/	/	/	/	
15300 kW	3 Eng. equally sharing load (3 x 5100kW)	0,83	1,04	0,54	0,58	0,67	0,3	
	3 engine adjusted load (2x6500kW / 1x2300kW)	/	/	/	/	/	/	
22000 kW	4 Eng. equally sharing load (4 x 5500kW)	0,55	0,57	0,36	1,62	2,08	1,91	
	4 engine adjusted load (3x6500kW / 1x2500kW)	/	/	/	/	/	/	

Source: Author

Table 3.2 shows the difference in the results in percentages. In all three sections, the lower values are considered as reference values. It can be seen that fuel consumption (MT/day) and NOx emissions (ppm) increase slightly for all three fuel types and for all loads considered, clearly indicating that the second configuration/option, where the load is manually adjusted between the engines, offers more economic and environmental benefits than the first configuration/option, where the load is evenly distributed between the engines according to the PMS.

The results of the simulator-based analysis provided convincing initial evidence that strategic load sharing, especially through manual tuning, can lead to noticeable improvements in fuel efficiency and emissions reduction. These results confirmed the basic idea that uniform load sharing systems, as implemented by standard PMS, may not be optimal under real-world operating conditions.

Encouraged by the trends observed in the simulator, which clearly showed lower SFOC and reduced NOx and CO₂ emissions when the engines were operated close to their optimal load points, the research moved on to the next critical phase, namely the acquisition of real-time measurements on an operating LNG vessel. This progress was important to validate the simulator's trends under dynamic, real-world conditions, including changing sea conditions, port protocols and aging equipment.

Therefore, we set out to collect real data on board to quantify the potential benefits and test the scalability of the load optimization concept in an authentic environment. These measurements formed the empirical basis for the development of a MATLAB-based optimization model, which was calibrated, validated and tested using real data from the ship in different operating modes.

3.2. EMISSION MEASUREMENTS IN REAL CONDITIONS OF SHIP EXPLOITATION

The measurements were carried out under real operating conditions of the ship and in different operating modes, using all three fuel types: LNG, HFO and MDO in accordance with the requirements in Annex 4 of the NOx Technical Code 2008 [56].

These measurements covered engine loads ranging from 20% to 90%, with data collected in 10% increments. The analysis of the collected data showed that an optimized distribution of the load on the Dual-Fuel Diesel-Electric systems is required to reduce fuel consumption and exhaust emissions. To increase the credibility of the results, additional measurements were

taken at intermediate points between the original data values, resulting in a 5% refinement of the engine load data set, which was then used for model calibration. In this process, the automatic load sharing was disabled, and the load was manually increased in 5% increments until the target value was reached. Once the predetermined load was reached, it was maintained for at least 10 minutes. Data recording only began after all engine operating parameters had stabilized, in accordance with the procedures described in sections 6.4.9.2 and 6.4.9.3 of the NOx Technical Code 2008 [54] as shown as an example in Figure 3.4 taken during measurements on an LNG ship.



Figure 3.4. Example of an emission measurement while the engine is running on LNG

The fuel consumption data were collected using a "145 PROFLOW Series 'J' Vane meter" mass flow meter, which had a valid calibration with an accuracy of $\pm 0.2\%$ at the time of measurement.

When evaluating the performance characteristics of different fuel types, it is important to understand that the specific fuel oil consumption (SFOC) is not a fixed value, but varies considerably depending on the engine load. Specific fuel oil consumption (SFOC) varies significantly with engine load and typically shows its optimum efficiency at 80–85% of MCR [57, 58]. This behaviour is consistent with that of diesel engines running on HFO or MDO, where low loads result in poor combustion and higher consumption. Dual-fuel engines fuelled with LNG show similar but sometimes flatter trends and benefit from lean combustion and lower thermal losses [59]. Accurate modelling of this non-linear relationship is essential for a realistic fuel and emissions analysis [60, 61].

The characteristic parabolic SFOC trend over the engine load can be explained by several thermodynamic and mechanical factors. At low load, combustion is less complete due to lower temperatures and pressures in the cylinder, resulting in higher unburnt fuel losses and poor combustion efficiency. In this range, frictional losses and auxiliary loads, which remain relatively constant, consume a higher proportion of engine power and increase the SFOC. In addition, turbocharger performance is suboptimal due to reduced exhaust energy, resulting in insufficient air supply and less efficient fuel-air mixing [62,].

When the load increases towards the optimal range of 80–85% MCR, the engine operates at its highest thermal and mechanical efficiency. The turbochargers operate effectively, combustion becomes more complete, and the relative influence of fixed losses decreases, leading to a minimization of SFOC.

Beyond this point, the SFOC rises again due to the increased thermal load and requires conservative combustion strategies to avoid knocking and overheating. The timing of fuel injection can be adjusted to reduce peak pressure, which slightly reduces efficiency. Additional cooling and lubrication requirements at high loads also increase parasitic losses, all of which contribute to the increase in SFOC. These combined effects underline the importance of modelling SFOC as a non-linear function of load, especially when comparing different fuels or performing performance optimization.

While the parabolic SFOC trend can generally be observed in all marine 4 stroke engines, there are important differences between diesel (HFO/MDO) and gas (LNG) operation. In dual-fuel engines, LNG combustion occurs in a lean premix mode, which offers better combustion stability at low and medium loads due to lower cylinder temperatures and cleaner combustion characteristics. This results in a flatter SFOC curve where efficiency remains relatively high over a wider load range [62].

However, at high loads, dual-fuel engines running on LNG are subject to knock restrictions that force earlier derating or conservative tuning strategies that reduce thermal efficiency. In addition, the excess air ratio must be maintained to avoid pre-ignition, further limiting optimization. Although LNG generally leads to lower absolute SFOC values, especially under clean conditions, its efficiency behavior across the load differs from that of diesel fuels and needs to be analyzed separately in optimization models.

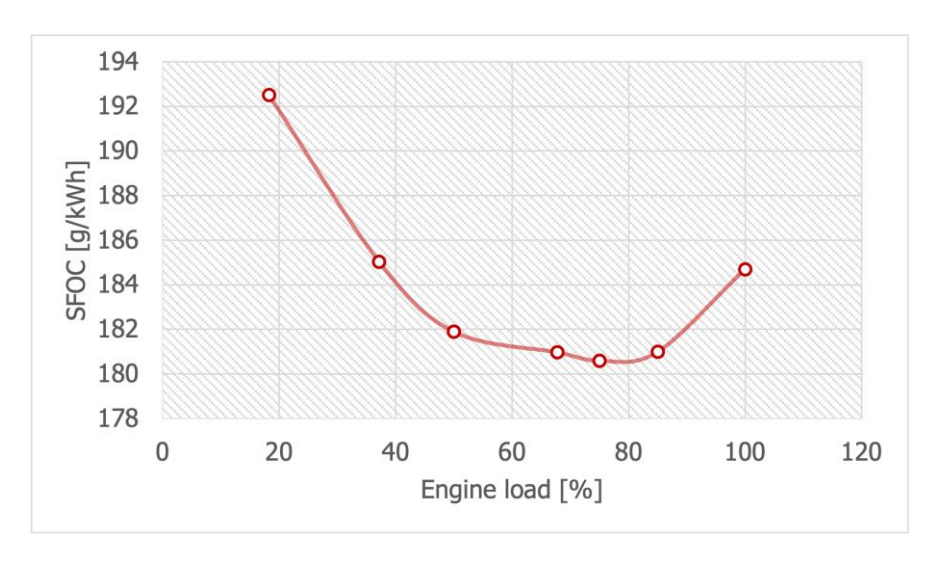


Figure 3.5 Specific fuel oil consumption (SFOC) of a diesel engine over the engine load.

The figure 3.5 shows a characteristic parabolic SFOC trend curve for a marine diesel engine running on conventional fuels such as HFO. At low load, combustion is inefficient due to lower temperatures in the cylinder and incomplete fuel oxidation, resulting in higher SFOC values. As the load increases, combustion efficiency improves, the turbochargers operate more effectively and friction losses decrease proportionally, so that the minimum SFOC value is around 75–85% of the engine load. Beyond this point, thermal loads and conservative injection timing at high load increase cooling losses and reduce combustion efficiency, so that the SFOC value increases again [62].

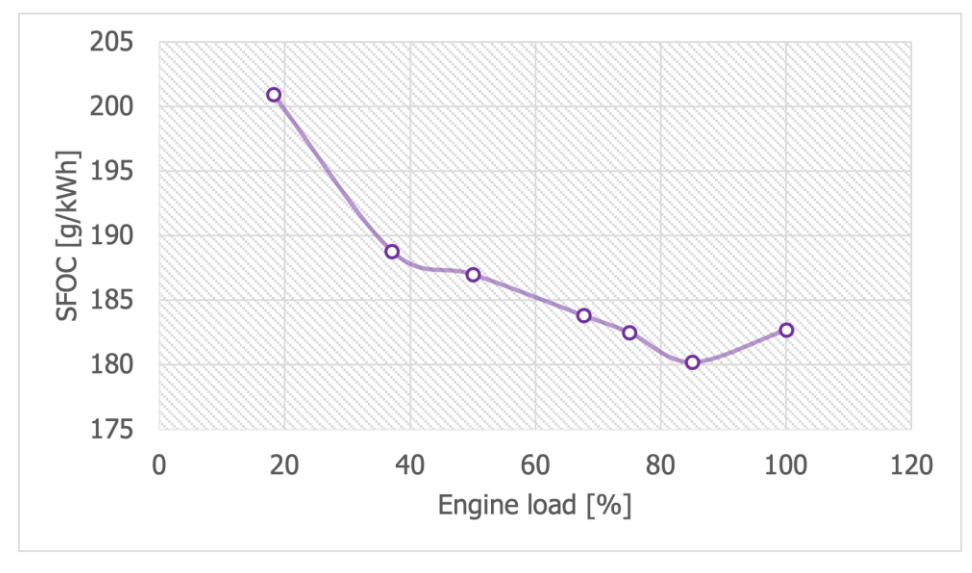


Figure 3.6 Specific fuel oil consumption (SFOC) for a dual-fuel engine in diesel mode.

This curve in Figure 3.6 is similar to that of a conventional diesel engine, but shows slightly higher SFOC values, especially at low load. Dual-fuel engines running in diesel mode may be less well optimized for full-time diesel operation due to compromises in injector design and combustion chamber geometry. As with conventional diesel engines, the SFOC minimum is near 80–85% load, but the overall fuel efficiency is somewhat lower due to system complexity and conservative tuning [62].

Figure 3.7 graphically presents the recorded data for SFOC for all three fuel types and as a function of the engine load.

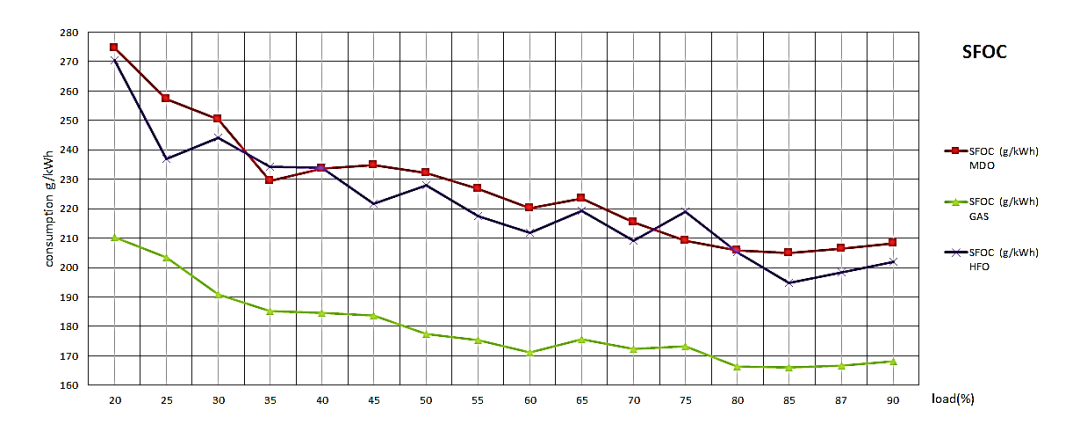


Figure 3.7 Fuel consumption data for three different types of fuel depending on the engine load

The exhaust gas measurements were carried out with a "Testo 350 Maritime" analyzer, the same device that was previously used for the measurements on the test bench of the ship under consideration, as shown in Figure 3.8.



Figure 3.8 Exhaust gas analyzer "Testo 350 Maritime", used for measurements on an LNG ship

Figure 3.9 graphically presents the recorded CO₂ emission data for all three fuel types as a function of engine load.

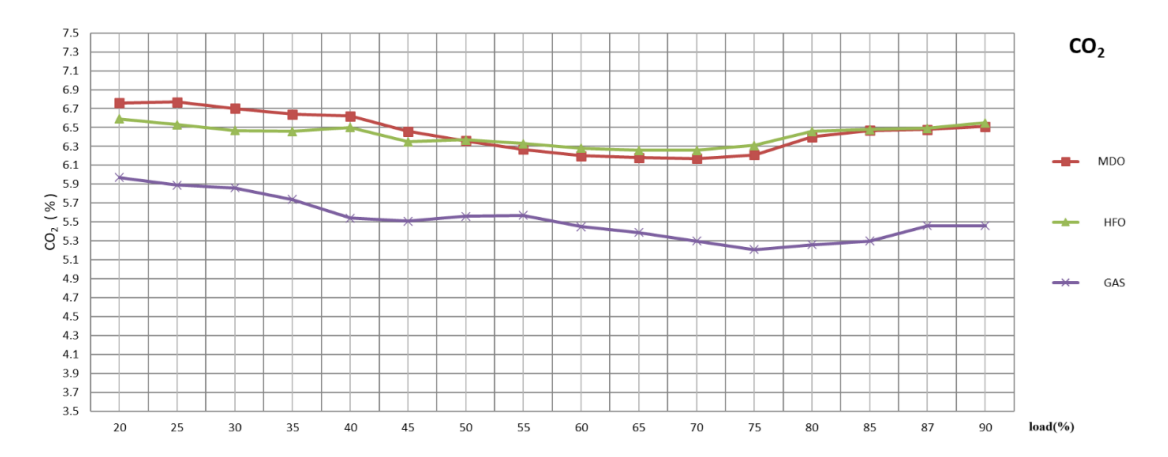


Figure 3.9 CO₂ emissions for three types of fuel depend on the engine load

Figure 3.10 illustrates the measured NO_x emission data for all three fuel types, presented as a function of engine load.

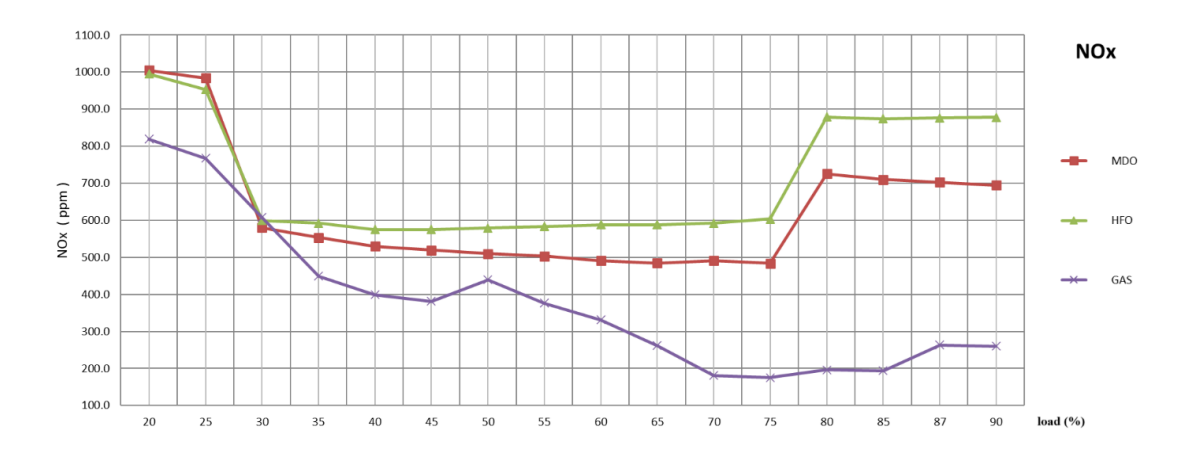


Figure 3.10 NOx emissions for three types of fuel depending on the engine load

For all measurements, care was taken to ensure that the accuracy of the devices was within the maximum tolerance limits specified in section 1.3.1 of Annex 4 of the 2008 Technical Code. In addition, the positioning of the emission probes was carefully checked. Wherever possible, the probes were placed at a distance of at least 0.5 metres or three times the diameter of the exhaust pipe, whichever was greater, in front of the exhaust outlet. The placement was also chosen so that the exhaust temperatures at the probe reached at least 343 K (70 °C), which meets the test cycle requirements described in Section 3.2 of the 2008 Technical Code [54]. This arrangement is shown in Figure 3.11, which was taken during the actual data collection phase for this study.



Figure 3.11 Position of the sampling probes during recording under real operating conditions.

The engine's operating parameters, including NOx and CO₂ emissions and specific fuel oil consumption (SFOC), were monitored and analyzed across the entire load spectrum from 20% to 90%, using discrete data points. This data set served as the basis for the development of an optimization model to calculate the optimal utilization of each diesel generator based on the required electrical output of the marine power plant. The aim was to improve energy efficiency by reducing fuel consumption and minimizing emissions of harmful gases such as CO₂ and NOx. The results of the study confirmed the initial hypothesis that the existing PMS logic for individual engine control on board an LNG vessel can be improved. The analysis of real operating data also provided a basis for defining directions for future research.

3.2.1. Comparison of generator systems with constant and variable speed

In DFDE systems, the specific fuel oil consumption (SFOC) profile of engines driving synchronous generators at constant speed exhibits a pronounced parabolic characteristic. At fixed speed (typically 514 rpm for 60 Hz systems), these engines exhibit poor efficiency at low loads due to incomplete combustion and sub-optimal turbocharger performance. The SFOC reaches a minimum in the range of 75–85% of maximum continuous power (MCR). After that,

the efficiency drops again due to the thermal load and conservative combustion tuning. This inherent inefficiency at non-optimal load points makes such systems suitable for load redistribution strategies such as those presented in this study.

Conversely, variable speed generator systems, allow the speed to be matched to the actual load, flattening the SFOC curve and improving fuel efficiency over a wider operating range. These systems reduce SFOC losses at low loads and provide greater flexibility, but at the cost of greater system complexity and the need for advanced electronic control. Although not the focus of this thesis, such architecture represents a logical future direction for marine propulsion and the optimization strategies developed here could be extended to variable speed configurations.

A recent experimental study [63] highlights the efficiency advantage of variable-speed generator systems. At around 65 % engine load, the specific fuel oil consumption (SFOC) for variable-speed engines ranged between 195 – 198 g/kWh, whereas fixed-speed engines operated at 204 – 214 g/kWh. At low load (~25 %), the difference widened further: 214 – 226 g/kWh for variable-speed compared to 238 – 270 g/kWh for fixed-speed units. These empirical results underscore how variable-speed operation substantially lowers SFOC across a broad range of engine loads.

3.3. OPTIMIZATION MODEL

3.3.1. Overview of the development of the optimization model

The development of the optimization model in this dissertation took place in two distinct phases, reflecting the progressive nature of the research and its focus on evolving environmental and operational priorities in the maritime industry.

The first version of the model was developed with the primary goal of minimizing the overall fuel consumption for LNG ship propulsion systems. This was achieved by analysing real, onboard measurement data and interpolating specific fuel oil consumption (SFOC) curves to determine the most fuel-efficient engine load configurations.

Building on the foundations and results of this model, a second, improved version was developed that incorporated exhaust emission parameters in particular nitrogen oxides (NOx) and carbon dioxide (CO₂) into the optimization framework. This multi-criteria model allows for flexible prioritization of fuel consumption and environmental impact through the use of weighting coefficients and is better suited for modern regulatory requirements in maritime transport such as MARPOL Annex VI, EEXI and CII.

Both model versions are described in detail in the following sections. First, the methodology of the pure fuel optimization model is presented, followed by the structure and implementation of the extended model that includes emissions. Examples and results from each model are presented to illustrate their development and application in real-world scenarios.

3.3.2. Initial Model: Fuel Consumption Optimization Only

The optimization model was developed based on on-board fuel consumption measurements collected during operation with different types of fuel. As the data was collected at discrete intervals, namely 5% load increments, interpolation was required to generate continuous input values for the model. This interpolation allows the model to determine the optimal load distribution between the generators with greater accuracy. Without interpolation, the model would be limited to assigning load shares only in fixed 5% increments, which reduces the accuracy of the optimization.

Interpolation is performed in MATLAB using spline interpolation as explained in [64]. For a given set of n data points (x_i, y_i) where i = 1, 2, ..., n, spline interpolation in MATLAB aims to find a polynomial function S(x) such that:

$$S(x_1) = y$$
 for $i = 1, 2, ..., n$, (1)

Interpolated function S(x) can be mathematically represented as follows:

$$\begin{cases}
S_1(x) & \text{if} \quad x_1 \leq x \leq x_2 \\
S_2(x) & \text{if} \quad x_2 \leq x \leq x_3 \\
& \cdot & , \\
S_{n-1}(x) & \text{if} \quad x_{n-1} \leq x \leq x_n
\end{cases} \tag{2}$$

where:

$$S_{i}(x) = a_{i}(x - x_{i})^{3} + b_{i}(x - x_{i})^{2} + c_{i}(x - x_{i}) + d_{i} \quad \text{for} \quad i = 1, 2, ..., n - 1$$
(3)

MATLAB selects the coefficients a_i , b_i , c_i and d_i such that S(x) interpolates data points and satisfies the continuity of the first and second derivatives at each point x_i .

The fuel consumption data used for the interpolation was initially collected at discrete load points and a mathematical spline interpolation technique was applied in MATLAB to generate smooth, continuous curves for all three fuel types. The resulting interpolated data sets are shown in Figure 3.12 for HFO, Figure 3.13 for MDO and Figure 3.14 for LNG.

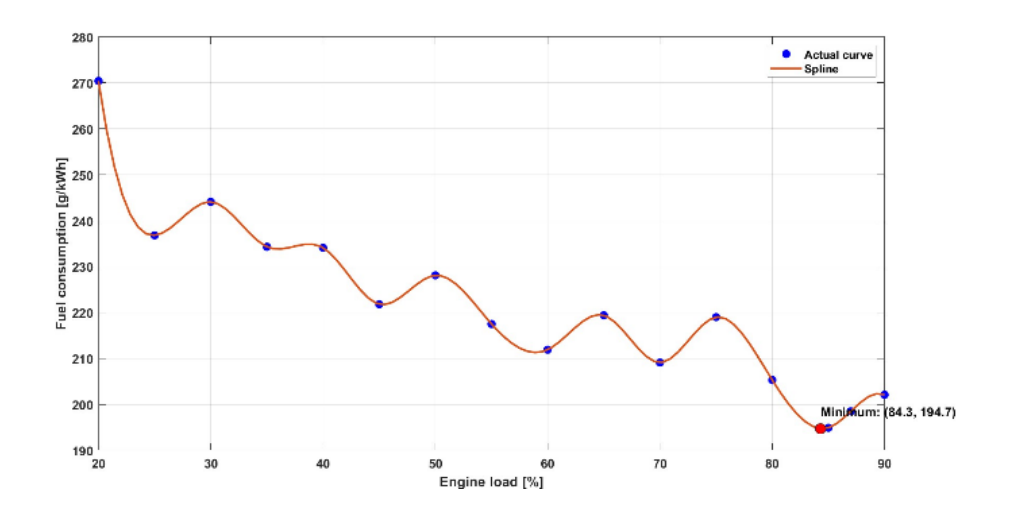


Figure 3.12 SFOC on HFO.

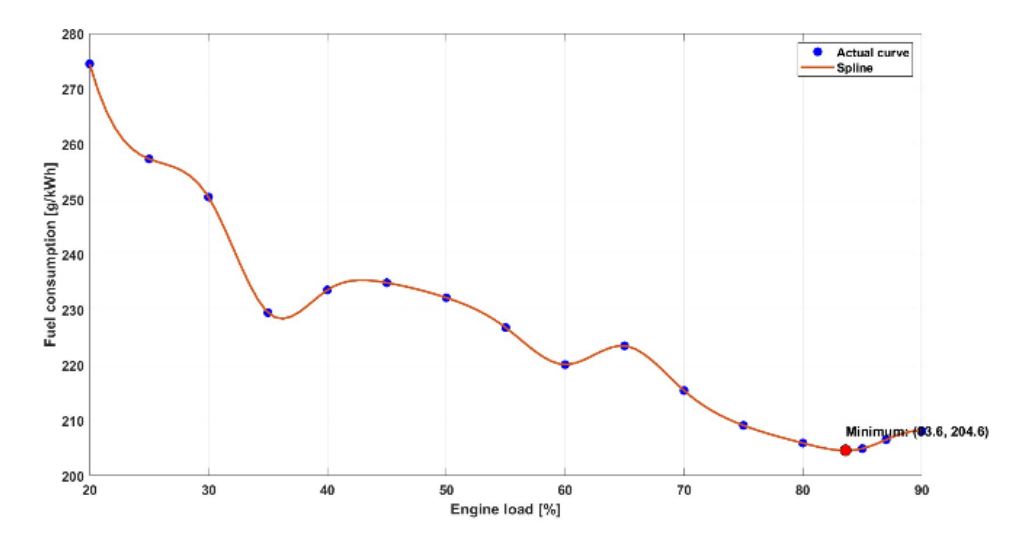


Figure 3.13 SFOC on MDO.

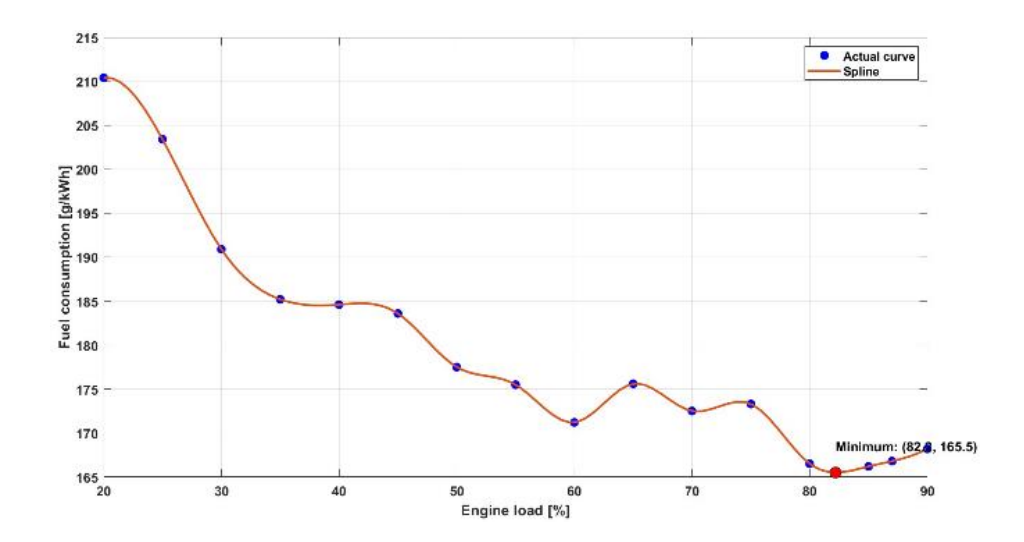


Figure 3.14 SFOC on LNG.

As soon as the SFOC values are interpolated, they can be integrated into the optimization model. This model, implemented in MATLAB, follows the workflow shown in Figure 3.15. The objective function evaluates the overall fuel consumption using the interpolated SFOC curves for the selected fuel type with the aim of minimizing fuel consumption while meeting the required power output. The model is subject to the following constraints:

• The output power of a diesel generator set is limited by its specifications as presented in Table 1.1, (see Section 1.4) meaning that each generator can only be assigned a load in the range between 20% and 90% of the specified power of the generator. This constraint is modeled by bounding the load percentage per engine with lower-bound variable *lb* and upper-bound variable *ub*.

- The load demand is limited so that it does not exceed the total rated output of all generators connected to the grid.
- Restricting the choice of fuel ensures that the generators are only operated with one type of fuel at any one time.

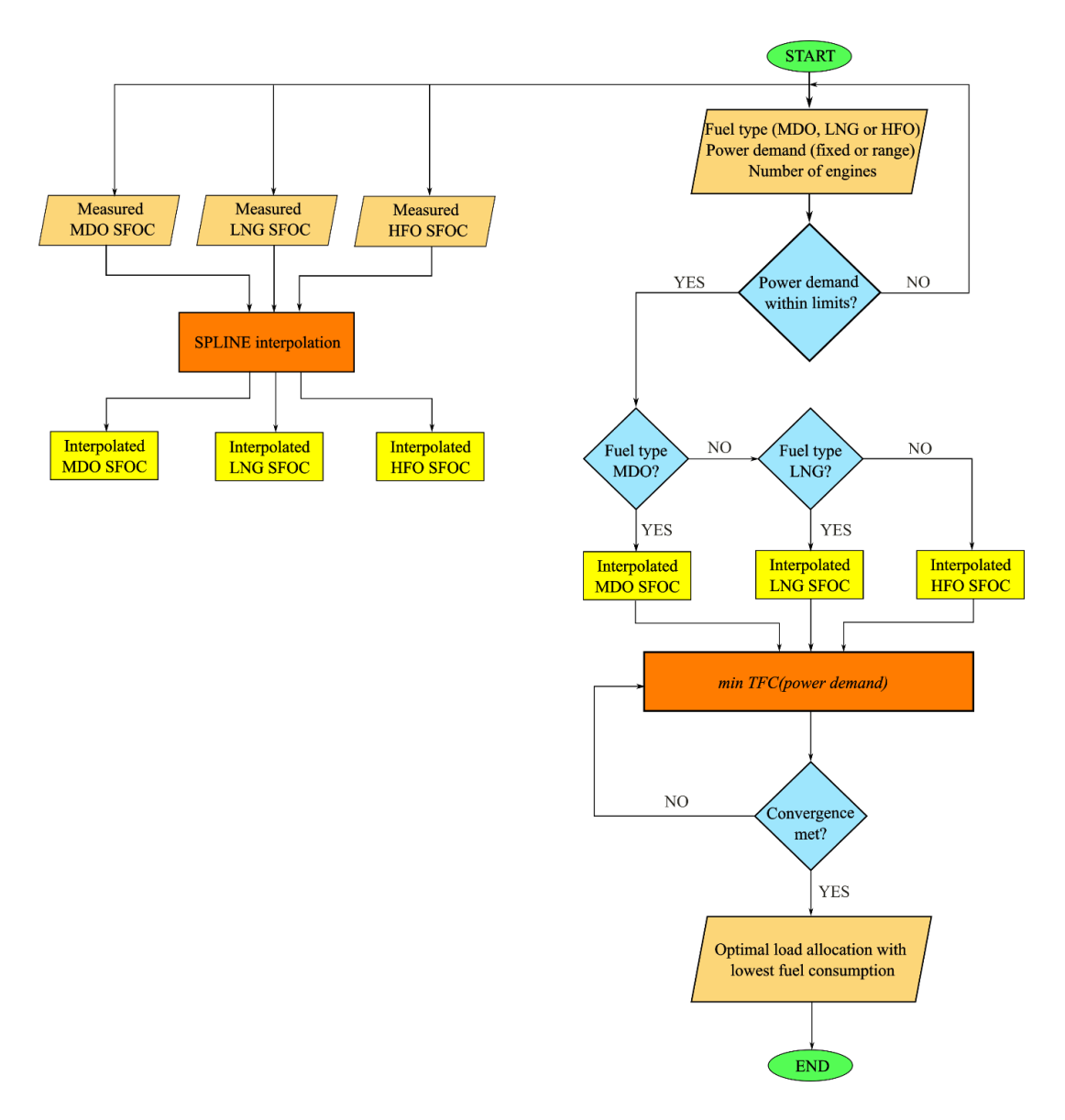


Figure 3.15 Optimization model flow chart.

The optimization process is carried out using the *fmincon* function and aims to minimize the total fuel consumption (TFC) while complying with the defined mathematical constraints:

minTFC(powerdemand) such that
$$\begin{cases} lb \leq \text{powerdemand} \leq ub \\ lb = 20(\%) \\ ub = 90(\%) \end{cases}$$
, (4)

The algorithm starts with an initial estimate of the load distribution and iteratively adjusts this allocation to minimize the total fuel consumption (TFC) while complying with the predefined constraints and boundary conditions. The process continues until a convergent solution is reached. The final output consists of the optimal load allocation values corresponding to a given power demand and engine configuration. The model not only calculates optimal allocations for a given power level but is also capable of evaluating load distributions over a range of power requirements. In both cases, the total fuel consumption is given for both the optimized allocation and for a baseline scenario with uniform load sharing, allowing for direct comparison.

The proposed optimization model is intended for practical integration into existing energy management systems on board LNG ships. Its implementation by ship engineers and operators can be done in the following steps:

- Data collection: continuous monitoring and recording of engine performance and fuel consumption data.
- Integration of the model: incorporating the optimization model into the ship's energy management software to dynamically adjust the load distribution.
- Real-time adjustment: using the results of the model to adjust the engine load in real time to the operating conditions and target fuel efficiency.
- Validation: regular validation of the model's recommendations against empirical performance data to ensure accuracy and effectiveness.

This approach provides a practical and actionable framework for reducing fuel consumption and emissions when operating LNG vessels.

3.3.3. Enhanced Model: Multi-Criteria Optimization (Fuel and Emissions)

The refined model follows the workflow shown in Figure 3.16, contains the same three fuel types as the previous version Heavy Fuel Oil (HFO), Marine Diesel Oil (MDO) and Liquefied Natural Gas (LNG), with all relevant operational data organized in a specific input file. The optimization process uses spline interpolation in MATLAB, as described in [64] and detailed in Section 3.3.2, to standardize the data and construct cost functions based on specific fuel oil consumption and NOx emissions. The entire optimization process, including data processing and comparison of the results, is summarized in Figure 3.16.

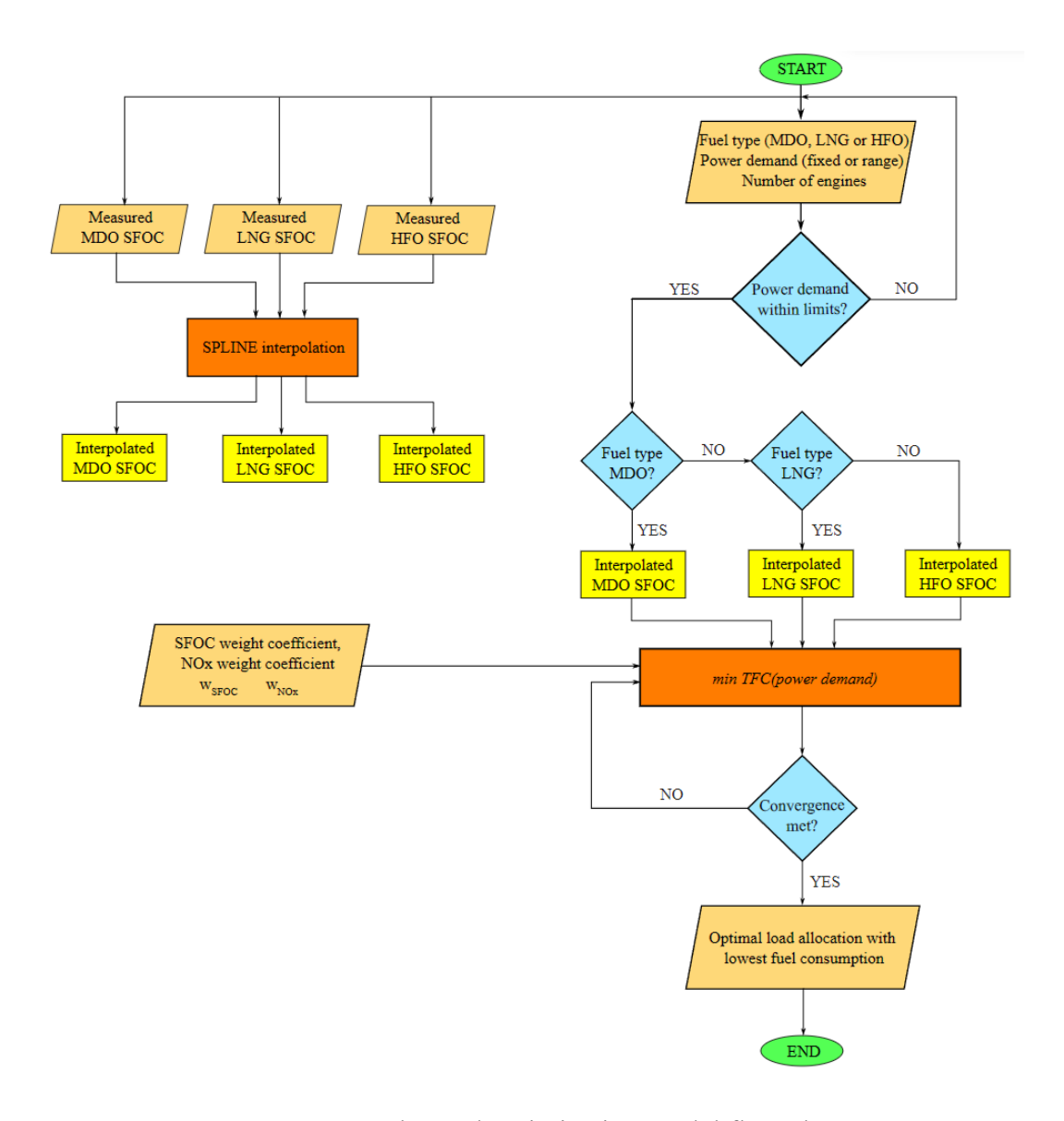


Figure 3.16 Enhanced optimization model flow chart

The objective function applies weighting factors to represent the relative importance of each parameter, with normalization based on the maximum operating values for each engine. As in the fuel-only model, optimization is performed using the *fmincon* function, now applied to the new weighted objective function. The model also includes a penalty function to ensure that the combined motor power is precisely matched to the required power demand. The results of the optimized load distribution are compared with those of a scenario with uniform load distribution. The performance of the model is visualized using bar charts showing fuel consumption and emission figures under different operating strategies. This visualization provides meaningful insights into improving the sustainability and efficiency of marine engine operation. This model proposes a weight coefficient for fuel consumption (wf_{FC}) and NOx

 (wf_{NOx}) , thus incorporating them into the previously developed optimization model. These weights are used to prioritize fuel consumption and emissions in the optimization as follows:

$$[w_{SFOC}, w_{NOx}]$$
 such that
$$\begin{cases} 0 < w_{SFOC} < 1\\ 0 < w_{NOx} < 1\\ w_{SFOC} + w_{NOx} = 1 \end{cases}$$
 (5)

The normalization process is used to adjust the weighting factors so that each contributes proportionally to the overall objective function. Without normalization, factors with larger raw values could have a disproportionate influence on the result, regardless of their relative importance.

The objective function can be described as follows:

$$TFC = Fuel\ consumption(power\ demand) \cdot w_{SFOC}$$

$$+ NOx\ emission(power\ demand) \cdot w_{NOx}$$
 (6)

The enhanced model uses the same base optimization structure and constraints as the fuelonly model (see Eq. 4), with additional weighted emission terms described above.

Similar to the fuel-only model, the process starts with an initial estimate of the load distribution, which is then iteratively refined to minimize the total fuel consumption (TFC) function while respecting all specified constraints and limits. This optimization continues until a stable solution is reached. The end result is an optimized load configuration that matches the required power, the number of active engines and the assigned weighting factors for SFOC and NO_x. In addition to optimizing for a single power level, the model is also designed to determine the ideal load distribution across a range of power requirements. In each case, it compares the optimized configuration with a baseline scenario with evenly distributed loads and gives the total fuel consumption for both approaches.

4. RESULTS AND DISCUSSION OF THE OPTIMIZATION MODEL

This chapter presents the results obtained by applying the optimization model to real ship operating data. The following sections describes the input parameters and calculation methods used to simulate the engine performance under different load and fuel conditions.

4.1. OVERVIEW OF THE APPLICATION OF THE MODEL AND THE ANALYTICAL APPROACH

The optimization model developed in the previous chapter was applied to real operating data of LNG ship systems to evaluate its effectiveness in reducing fuel consumption and exhaust emissions. The simulations were carried out for different operating modes of ships including port operations, ballast voyages, loaded voyages and cargo handling using different fuel types (LNG, MDO and HFO).

The model was configured to accept key input parameters such as the total power requirement, the selected fuel type and user-defined weighting factors for fuel consumption (wf_{FC}) and nitrogen oxide emissions (wf_{NOx}) .

In order to accurately simulate the performance of an engine under different operating conditions, it is necessary to determine the performance of each engine based on its percentage utilization in relation to the Maximum Continuous Rating (MCR).

In this study, the engine load is determined based on the effective power output of MAN 8L51/60DF engines measured under actual operating conditions. For generator driven systems, which are typical for DFDE LNG carriers, the engine load is calculated based on the real-time electrical power of the generator. This power is derived using the standard three-phase power equation:

$$P = \sqrt{3} \cdot U \cdot I \cdot cos(\phi) \tag{7}$$

where is:

P - Real power (kW)

U - Line voltage (V)

I - Line current (A)

 $cos(\phi)$ - Power factor

After the calculation, this power is compared with the maximum continuous rating (MCR) of the engine, which is specified as 8000 kW at 514 rpm for the MAN 8L51/60DF engine. The percentage load is thus defined as:

$$Load(\%) = \left(\frac{P_{actual}}{P_{MCR}}\right) \times 100 \tag{8}$$

This method of determining the engine load via the generator output is both practical and accurate, as the electrical power produced by the generator is directly proportional to the mechanical power supplied by the engine. As marine diesel generators are rigidly coupled to their engines and have minimal mechanical losses, measurements of actual power (derived from voltage, current and power factor) provide a reliable representation of the effective engine load. This approach is widely used in energy management systems and complies with the standards set by classification societies and engine manufacturers. It thus provides the basis for linking fuel consumption and emission measurements to discrete load levels (e.g. 10%, 15%, etc.), which is crucial for the development and validation of load-dependent optimization models.

If, for example, a generator output of 4000 kW is measured, the engine operates at 50% load. This process is continuously controlled by the engine's control and automation system (e.g. MAN SaCoS), which ensures real-time monitoring and accurate load determination.

In propulsion systems where the engines are mechanically connected to the propeller shaft (and not to a generator), the engine load is determined using the braking power calculated from the torque and the engine speed, as expressed by the equation:

$$P = \frac{2\pi \cdot T \cdot n}{60,000} \tag{9}$$

where is:

P = Brake power (kW)

T = Torque (Nm), measured via a torsiometer

n =Engine speed (rpm)

This method is applicable when torsiometers are installed on the shaft and is typical for direct drive propulsion applications.

These two methods the measurement of electrical power in generator systems and the calculation of mechanical torque in drive systems allow the practical and accurate determination of motor load. This information is crucial for modelling optimization measures, fuel calculation, emission monitoring and general performance evaluation of marine power plants.

On this basis, optimized engine load distributions were created using interpolated power data. All simulations and calculations were performed in MATLAB.

Visualizations such as bar graphs and trend lines were created to compare the optimized results with the baseline performance under the standard PMS, which distributes the loads evenly across the engines. These comparisons provided a clear basis for evaluating the benefits of the optimization model under practical operating conditions.

The results presented in the following sections quantify the fuel savings and emissions reductions for a range of realistic scenarios and fuel types, confirming the performance and practical relevance of the model.

4.2. INITIAL OPTIMIZATION MODEL – FUEL CONSUMPTION ONLY

The initial version of the optimization model was developed to minimize fuel consumption without considering emissions. It was tested across various power demands and fuel types to evaluate potential fuel savings compared to the standard equal-load distribution used by PMS.

4.2.1. Heavy Fuel Oil (HFO) Optimization Example

Figure 4.1 shows the fuel consumption for HFO in a power plant operating in the range of 25,000 to 29,000 kW, distributed over five engines representing the high load range for normal ship operation.

The graph compares two load distribution strategies:

- 1. Consumption at the same load (red bars): The total power is distributed evenly across all engines.
- 2. Optimized consumption (blue bars): The optimization model allocates power based on the most efficient engine load to minimize fuel consumption.

The x-axis represents the required power, which ranges from 25,000 kW to 29,000 kW in 500 kW increments, while the y-axis shows the total fuel consumption in kilograms per hour (kg/h). The fuel flow measurements were performed using a "145 PROFLOW Series 'J' Vane

Meter" mass flow meter, which was properly calibrated and operated with a measurement accuracy of $\pm 0.2\%$.

The graph shows that an optimized load distribution at almost all power levels consistently results in lower fuel consumption than a uniform distribution. The only exception is 27,500 kW, where both methods result in the same consumption. This underlines the ability of the optimization model to reduce fuel consumption, which translates into both economic and environmental benefits.

For example, at 25,000 kW, a uniform load results in a fuel consumption of 5,484 kg/h, while the optimized configuration consumes only 5,260 kg/h, a reduction of 4.25%. At 29,000 kW, fuel consumption in the optimized scenario drops from 6,307 kg/h to 5,996 kg/h, which corresponds to a saving of 5.18%. These results underline the effectiveness of the model in improving fuel efficiency, particularly at higher power levels, and provide useful guidance for operational and cost optimization.

The optimization approach shows improved fuel efficiency, especially at higher power requirements. This is an important finding with practical implications for operational planning and cost control.

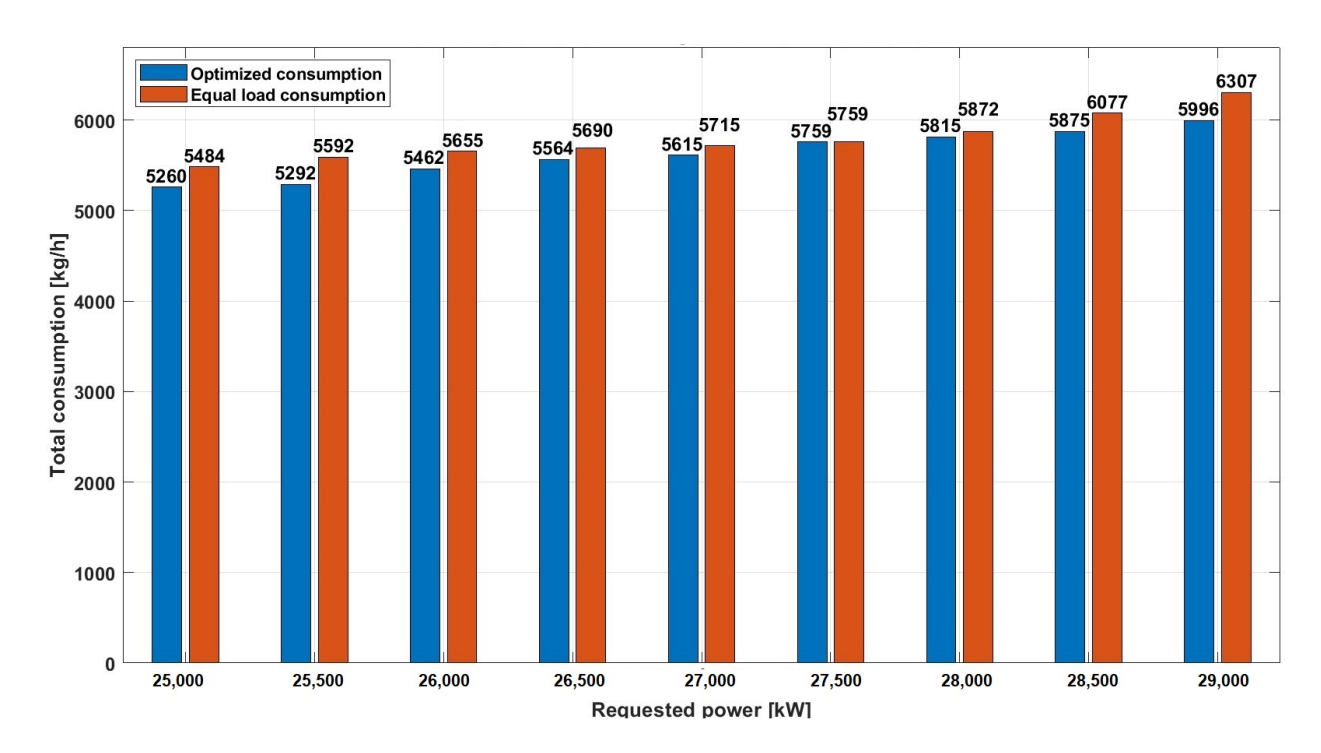


Figure 4.1 Comparative analysis of HFO consumption for the power range 25,000–29,000 kW.

The 3D bar chart in Figure 4.2 visualizes the percentage load distribution across five engines within a power plant, corresponding to a total power requirement of 25,000 kW to 29,000 kW. This visualization shows how the total load is distributed across the individual engines at different power levels. Each color-coded segment represents the proportion of the total load allocated to a specific engine for each power demand scenario.

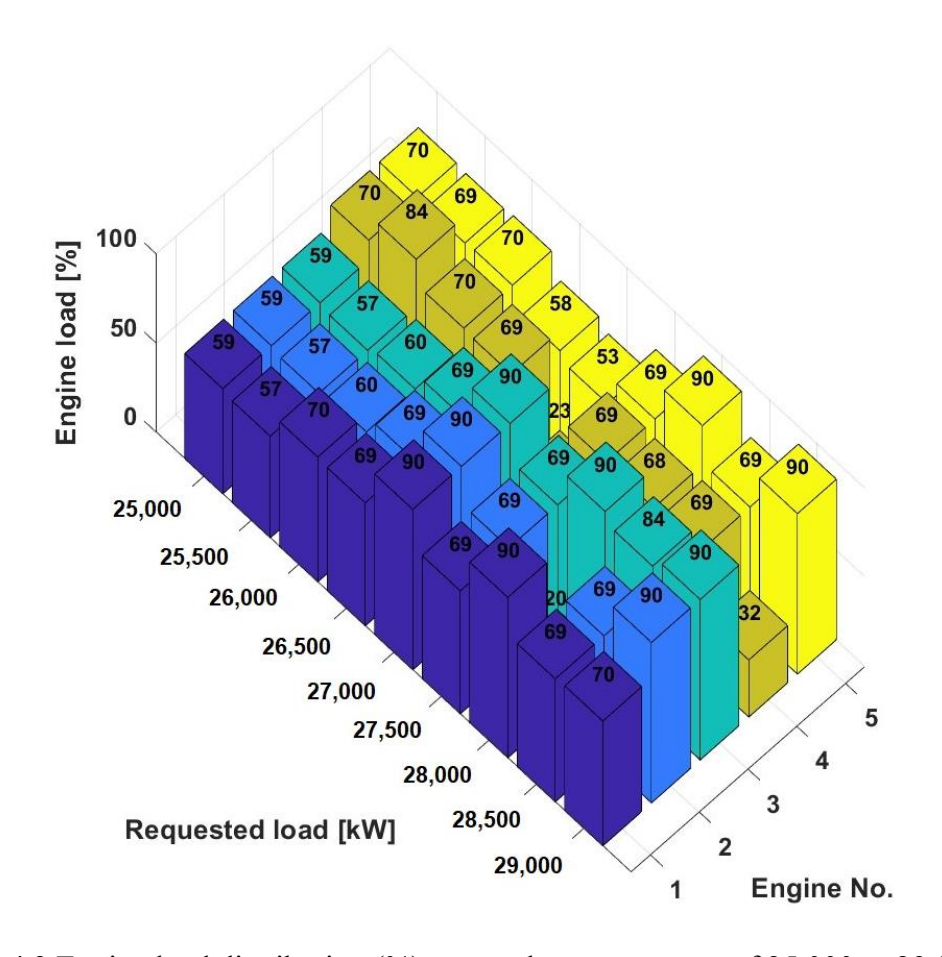


Figure 4.2 Engine load distribution (%) across the power range of 25,000 to 29,000 kW

Figures 4.3 and 4.4 show bar charts illustrating a comparative analysis of fuel consumption for two different load distribution strategies, a uniform distribution and the configuration recommended by the optimization model at a fixed total power demand. Two specific load cases were selected for this comparison, representing the most common operating conditions in normal ship operation:

- Load of 10,000 kW with two engines in use, used mostly for port operation (loading unloading cargo).
- Load of 23,000 kW with four engines in use, used mostly for sea going (laden, ballast).

In the visualizations, the left-hand diagram shows the number of active engines together with the percentage load assigned to each, while the right-hand diagram compares the total fuel

consumption (kg/h) under two different load distribution approaches: optimized and uniform distribution.

As shown in Figure 4.3, the optimized load configuration results in a fuel consumption of 2,119 kg/h for a power demand of 10,000 kW covered by two engines. In contrast, the uniform distribution approach consumes 2,193 kg/h, which corresponds to an increase of 3.37%. This shows that the optimized strategy delivers the same power more efficiently and reduces fuel consumption under these specific operating conditions.

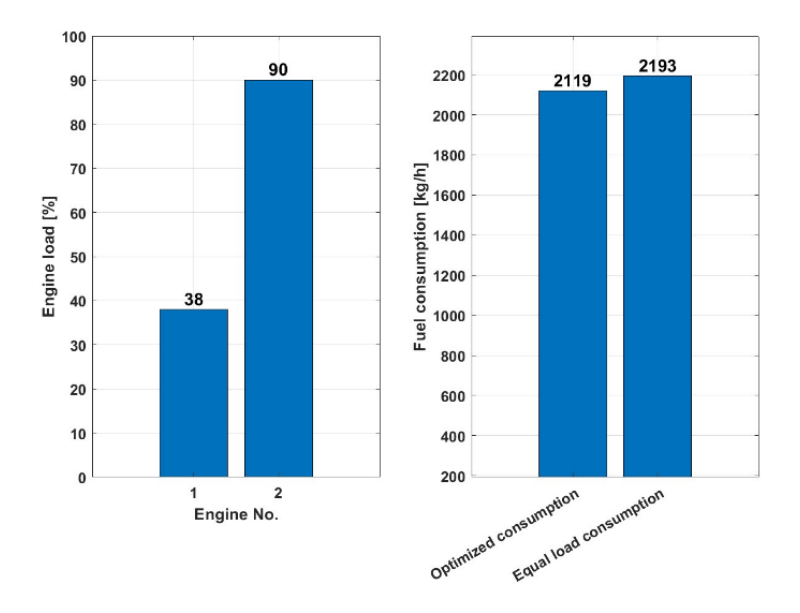


Figure 4.3 Load distribution between the engines and HFO consumption at 10,000 kW load demand

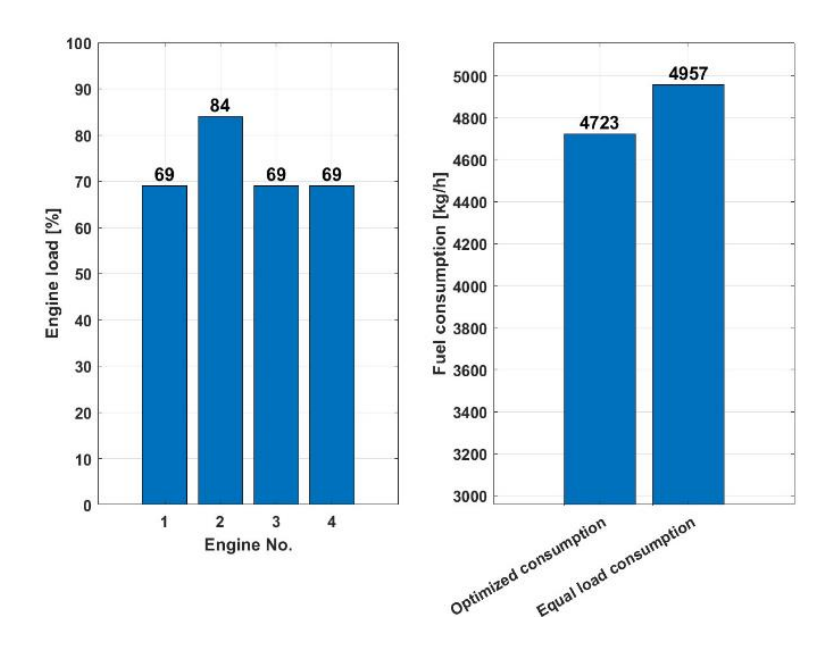


Figure 4.4 Load distribution between the engines and HFO consumption at 23,000 kW load demand

Figure 4.4 shows that with a total load of 23,000 kW distributed over four engines, the optimized load configuration results in a fuel consumption of 4,723 kg/h. In comparison, the equal load distribution leads to a higher consumption of 4,957 kg/h, which corresponds to an increase of 4.72%. This clearly shows that the optimized strategy achieves the same performance more efficiently and with less fuel.

These diagrams provide a comparative assessment of two approaches to load balancing the engines with different energy requirements in the energy system of an LNG vessel. In both low and high-power scenarios, the optimized distribution method consistently proves to be more fuel efficient than the uniform load distribution, highlighting its practical advantage in improving overall energy efficiency.

4.2.2. Marine Diesel Oil (MDO) Optimization Example

Figure 4.5 shows a comparison between two fuel consumption strategies, expressed in kilograms per hour (kg/h) at different power requirements in kilowatts (kW). The red bars show the fuel consumption with an even load distribution, in which the PMS distributes the power evenly to all active engines. The blue bars, on the other hand, represent the optimized fuel consumption calculated on the basis of the load distribution recommended by the optimization model.

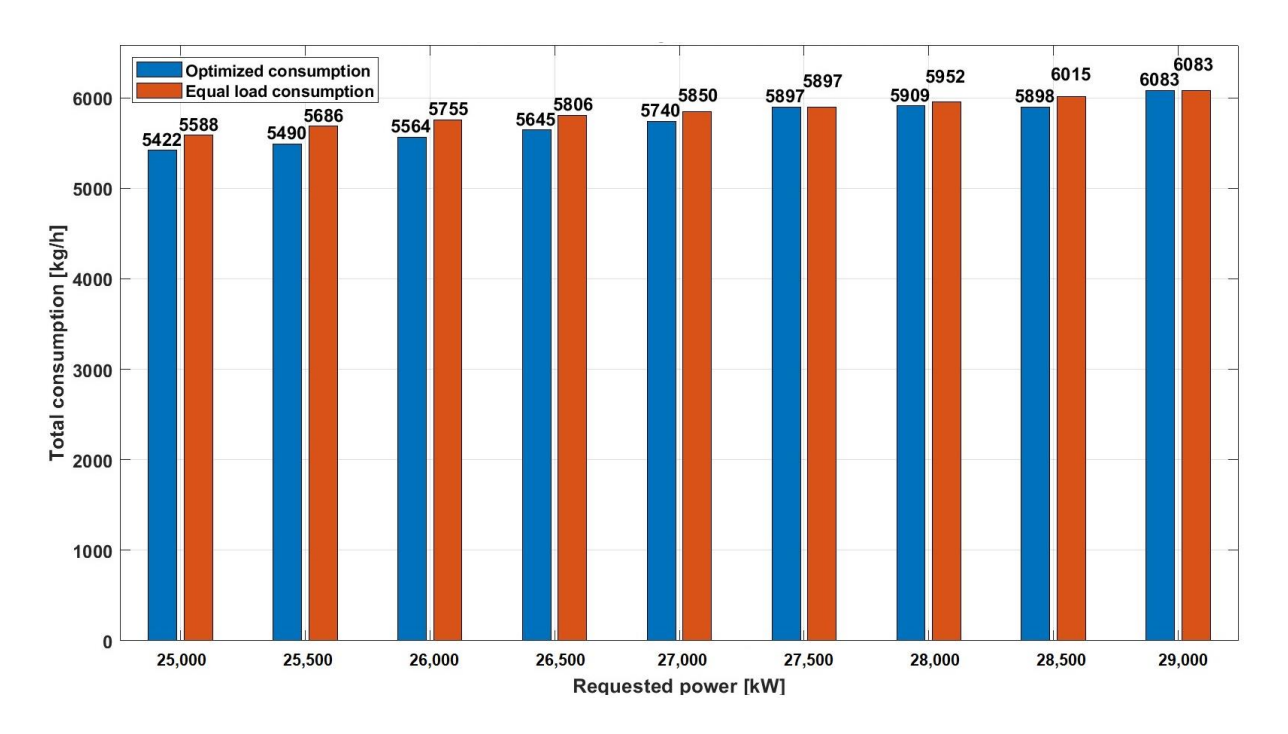


Figure 4.5 Comparative analysis of MDO consumption for the power range 25,000–29,000 kW

At all power levels examined, the optimized fuel consumption remains consistently lower than that of the same load distribution. This confirms that the optimization model, similar to the previous HFO case, also improves fuel efficiency when operating with MDO, resulting in lower fuel consumption for the same power.

The difference in fuel consumption between the two load distribution strategies varies across the power levels analyzed. At 25,500 kW, for example, the optimized approach leads to a saving of 196 kg/h, which corresponds to a reduction of 3.57% compared to a uniform load distribution. At higher outputs, such as 28,500 kW, the savings fall to 117 kg/h, which still represents an improvement of 1.98%. It is noteworthy that at two particular load points, 27,500 kW and 29,000 kW, no significant difference in fuel consumption is observed between the two strategies. In line with the earlier comparison with HFO, this analysis confirms that the optimization model improves fuel efficiency at different loads even when using MDO fuel.

In addition, the 3D bar chart in Figure 4.6 shows the percentage distribution of the load across five engines in a power plant for a power range of 25,000 kW to 29,000 kW to illustrate how the load is distributed across the individual engines at different requested total outputs.

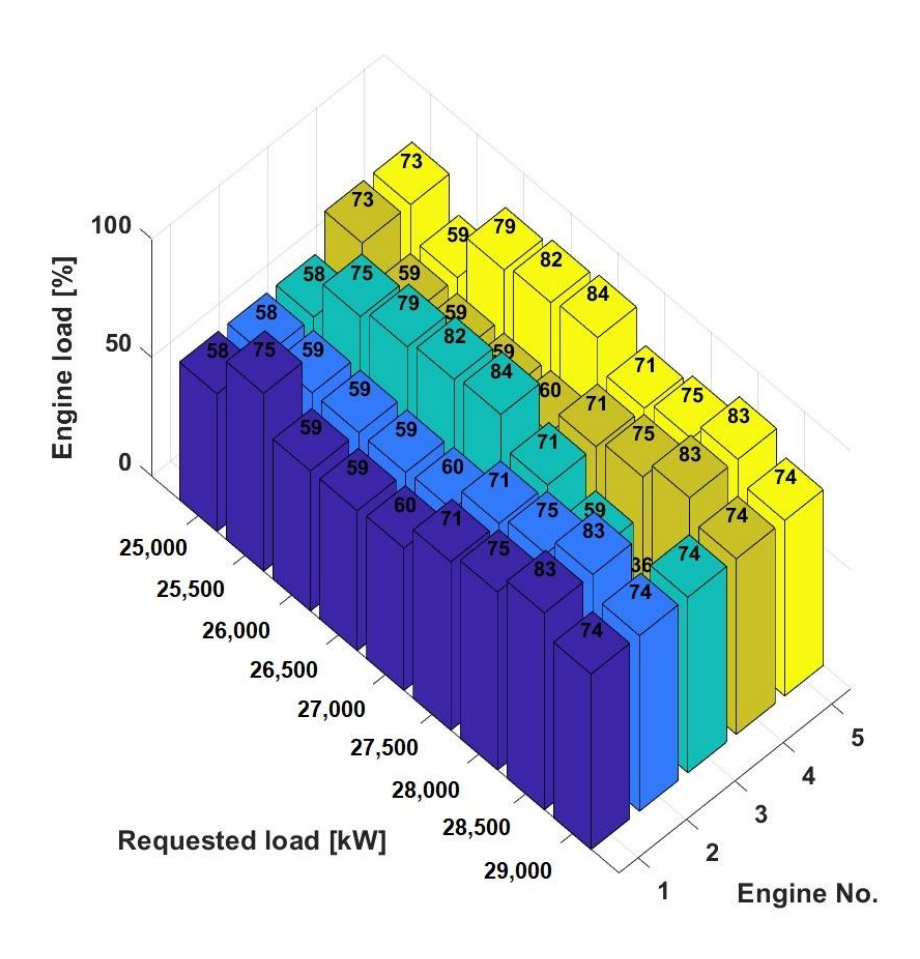


Figure 4.6 Load distribution (%) by engines for the power range 25,000–29,000 kW

A comparative analysis was carried out regarding the fixed power demand of the LNG plant at two levels: 10,000 kW and 23,000 kW. As can be seen in Figure 4.7, the optimized load distribution results in a fuel consumption of 2,152 kg/h when operating at 10,000 kW with two engines. In contrast, the scenario with even load distribution results in a slightly higher consumption of 2,235 kg/h. This shows that the uniform distribution approach consumes 3.85% more fuel than the optimized configuration, which underlines the improved efficiency achieved through load optimization.

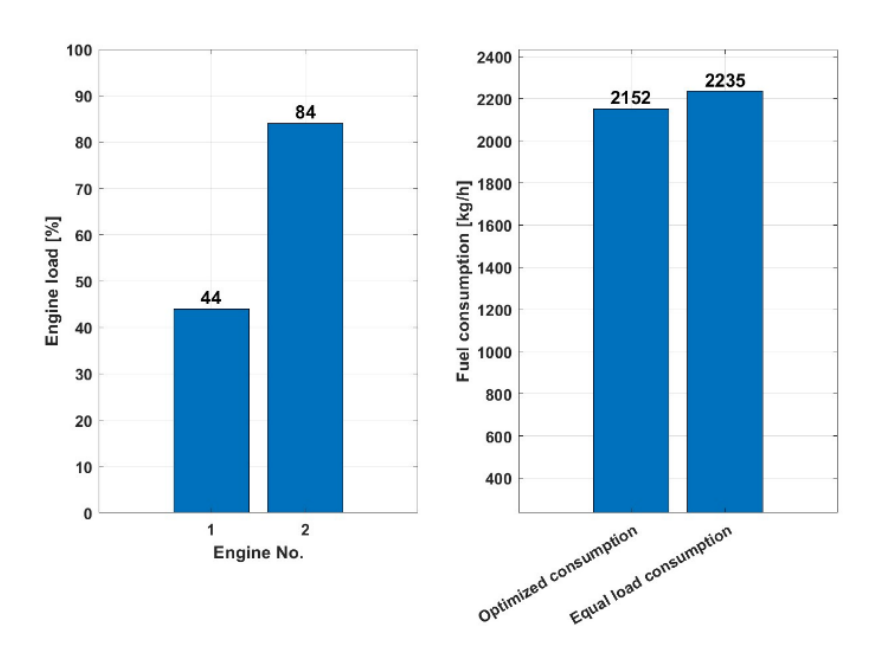


Figure 4.7 Load distribution across the engines and corresponding MDO consumption for a power requirement of 10,000 kW

Figure 4.8 shows that with a total power requirement of 23,000 kW and four engines, the optimized load distribution results in a fuel consumption of 4,811 kg/h. In comparison, the scenario with the equal load distribution consumes slightly more, namely 4,839 kg/h, which corresponds to an increase of 0.58%. This shows that the optimized configuration is more fuel-efficient at this power level and achieves the same power with lower fuel consumption.

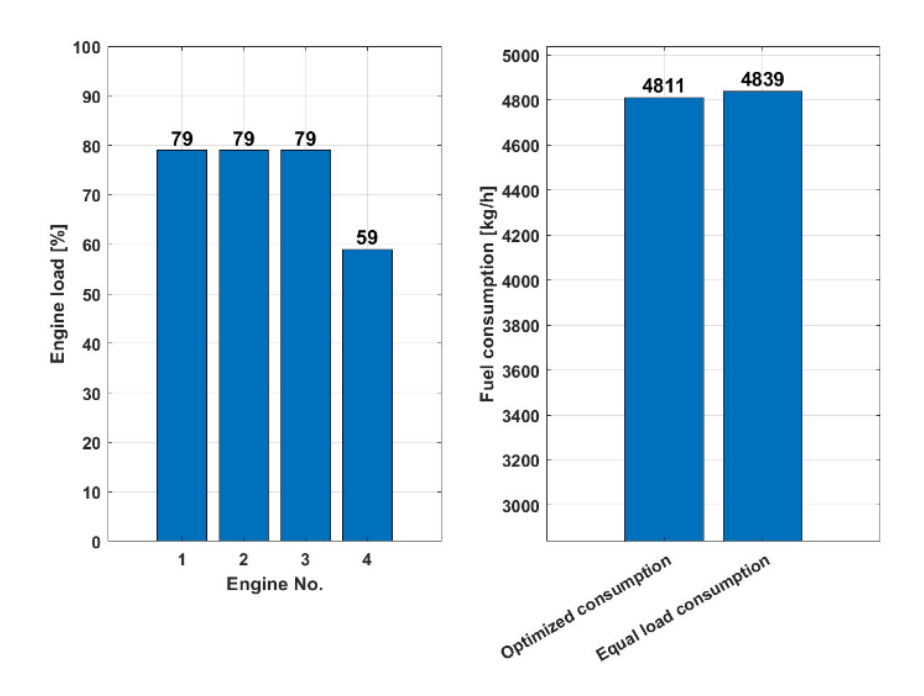


Figure 4.8 Load distribution across the engines and corresponding MDO consumption for a power requirement of 23,000 kW

As in the previous analysis with HFO, the diagrams with MDO fuel also confirm that optimized load distribution offers higher fuel efficiency compared to uniform load distribution. In both scenarios studied, with power requirements of 10,000 kW and 23,000 kW, the optimized configuration consistently consumes less fuel to deliver the same power, demonstrating its superiority in terms of operating efficiency.

4.2.3. Liquefied Natural Gas (LNG) Optimization Example

A comparative consumption analysis was also conducted for LNG fuel over the same power range as the previous HFO and MDO assessments to evaluate the effectiveness of the optimization model for this fuel type. To ensure consistency and comparability across fuel types, the LNG consumption values were recalculated and expressed in grams per kilowatthour (g/kWh). The gas density and net calorific value used for this conversion are taken from the LNG specifications given below:

- Standard density of gas is 0.7740 kg/m³.
- NCV (net calorific value) of natural gas (volume) 37.874 MJ/m³.

The fuel flow measurements were performed with a "Promass 80" mass flow meter, which was certified at the time of testing and operated within a measurement tolerance of $\pm 0.1\%$.

Similar to the previous comparative evaluations with HFO and MDO, the performance of the optimization model was also evaluated with LNG fuel under different load conditions and two different load distribution strategies.

As shown in Figure 4.9, the greatest fuel savings are achieved through optimized load distribution at the lower (25,000–26,000 kW) and upper (28,000–29,000 kW) end of the power range. In the medium power range (around 27,000 kW), both load distribution methods lead to comparable fuel consumption.

The clearest difference can be observed at a demand of 29,000 kW, where the optimized scenario records a fuel consumption of 4,869 kg/h - 2.94 % less than the 5,017 kg/h consumed with the equal load distribution.

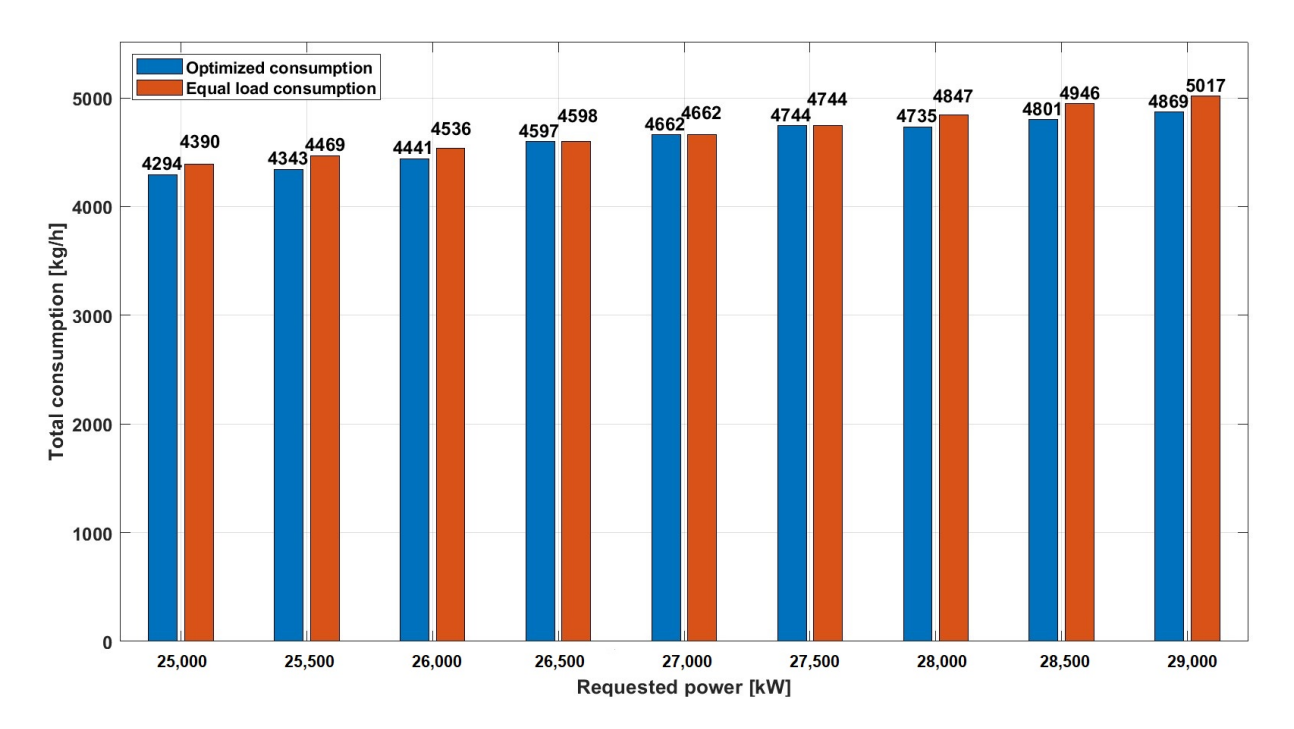


Figure 4.9 Comparative analysis of LNG consumption for the power range 25,000–29,000 kW

The 3D bar chart below illustrates the percentage load distribution across the individual engines in the power range from 25,000 to 29,000 kW when running on LNG fuel (Figure 4.10).

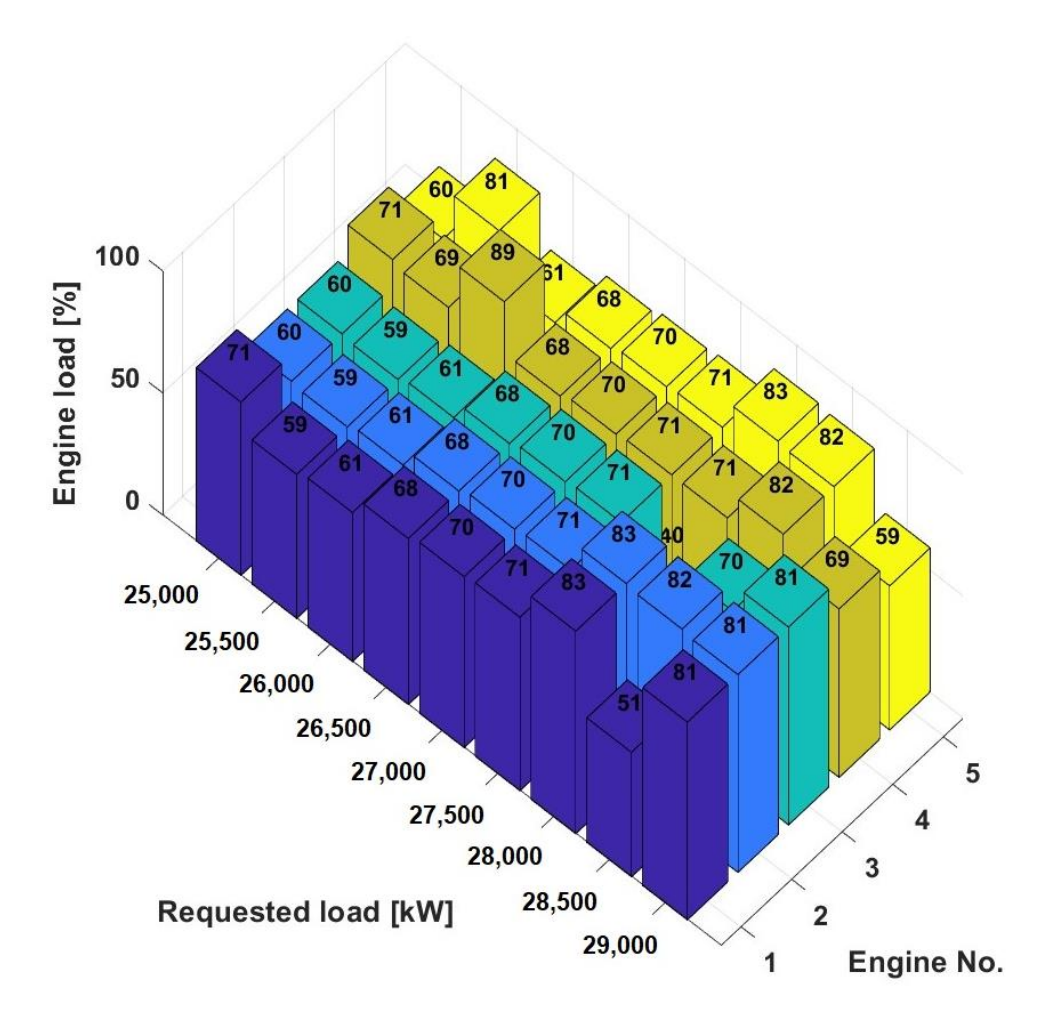


Figure 4.10 Engine load distribution (%) over the power range of 25,000–29,000 kW

In order to perform a comparative assessment of fuel consumption for a fixed power demand using LNG fuel in line with the previous analyses with HFO and MDO, the same load levels of 10,000 kW and 23,000 kW were selected for the assessment.

As can be seen in Figure 4.11, the optimized load distribution with a load of 10,000 kW and two engines in operation results in a fuel consumption of 1,721 kg/h. In contrast, the scenario with the equal load distribution results in a slightly higher consumption of 1,756 kg/h. This shows that the optimized configuration achieves the same output with approx. 2% less fuel, which demonstrates its superior efficiency for this operating condition.

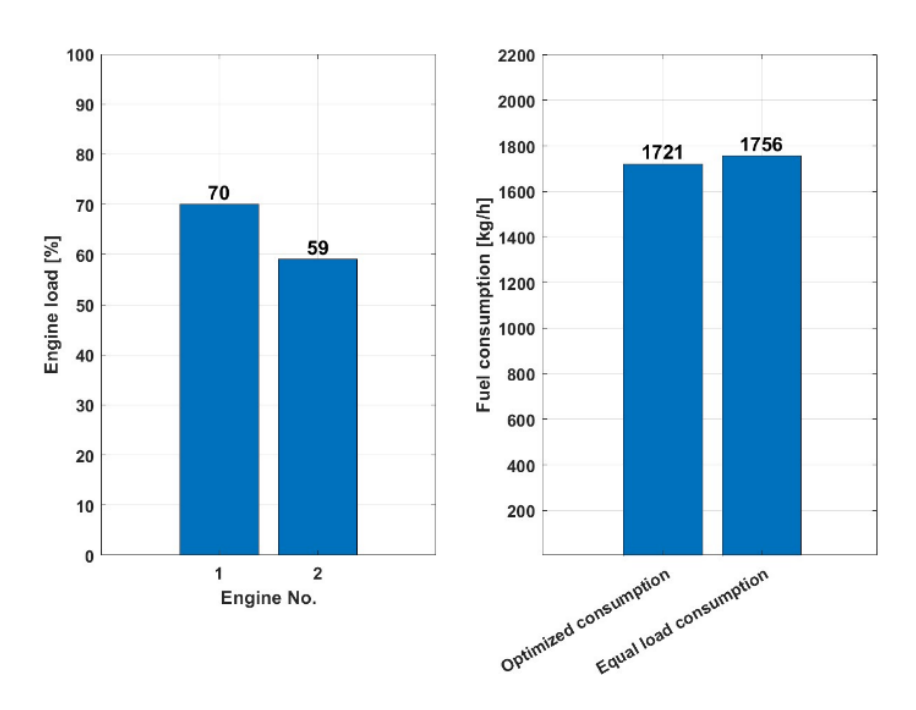


Figure 4.11 Load distribution across the engines and corresponding LNG consumption for a power requirement of 10,000 kW

Figure 4.12 shows that the optimized load distribution leads to a fuel consumption of 3,872 kg/h with a power requirement of 23,000 kW and four engines in operation. In comparison, the configuration with the equal load distribution consumes slightly more, namely 3,988 kg/h. This reflects a 2.90% reduction in fuel consumption with the optimized strategy and confirms greater efficiency in meeting the same power requirement.

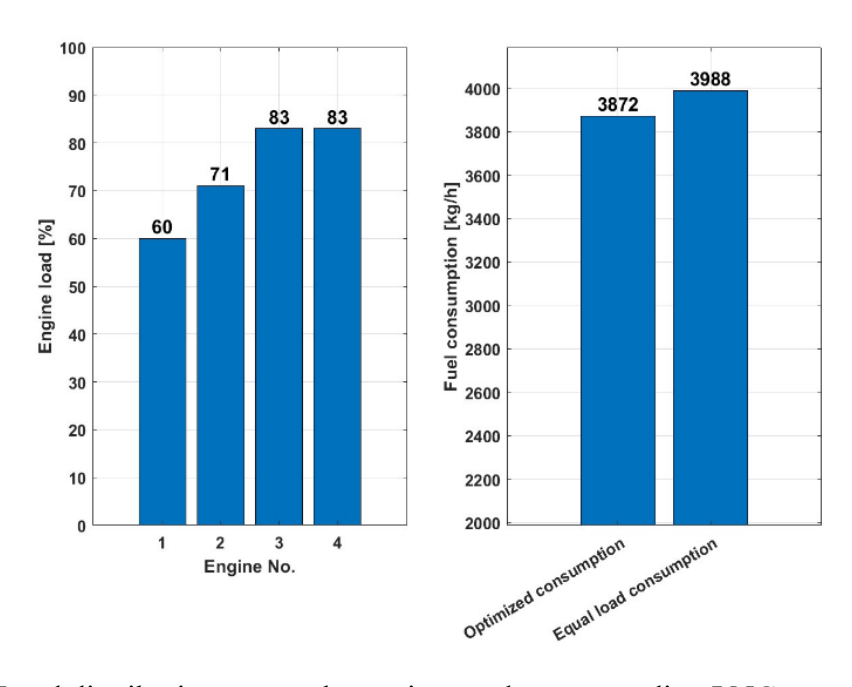


Figure 4.12 Load distribution across the engines and corresponding LNG consumption for a power requirement of 23,000 kW

As with the earlier analyses with HFO and MDO, the graphs for LNG fuel consumption clearly show that the optimized load sharing strategy is consistently more fuel efficient for both power levels investigated (10,000 kW and 23,000 kW). It achieves the same performance with lower fuel consumption and thus confirms the effectiveness of the optimization approach with different fuel types.

In summary, the optimization model shows remarkable improvements in fuel efficiency for all three fuel types HFO, MDO and LNG. The results consistently indicate that the optimized load distribution of the engine outperforms the standard uniform distribution controlled by the PMS. Among the fuels analyzed, HFO shows the greatest relative fuel savings, while MDO and LNG also show considerable, albeit slightly smaller, improvements. These results underpin the effectiveness of the proposed optimization model for different fuel types and show its great potential for improving fuel efficiency and thus reducing NOx and CO₂ emissions. The comparative evaluation of the scenarios before and after optimization for each fuel type confirms the robustness of the model and its practical applicability under real operating conditions.

4.3. ENHANCED OPTIMIZATION MODEL (FUEL AND EMISSIONS)

The following case studies present the results of the optimization model applied to a total power demand of 20,000 kW - a typical operating load during a sea voyage with four engines and different fuel types. The main objective of the model is to minimize fuel consumption and reduce greenhouse gas emissions, in particular CO_2 and NOx, through strategic allocation of engine loads. To balance the trade-off between fuel efficiency and emissions, the model contains weighting factors for fuel consumption (wf_{FC}) and nitrogen oxide emissions (wf_{NOx}), which were set at 0.6 and 0.4 respectively for all fuel types. These weightings reflect a slightly higher priority for energy efficiency, which is in line with the IMO's decarbonization targets and the economic incentives for operators.

4.3.1. Liquefied Natural Gas (LNG) Optimization Example

Figure 4.13 shows that the optimized fuel consumption is 3,498 kg/h, compared to 3,512.21 kg/h with the equal load distribution. Although the difference of 14.21 kg/h may seem modest, it underlines the effectiveness of the optimization model, especially when the relatively high

weighting of fuel consumption ($wf_{FC} = 0.6$) is taken into account. This result emphasizes the importance that the model places on fuel efficiency as a key priority in load distribution.

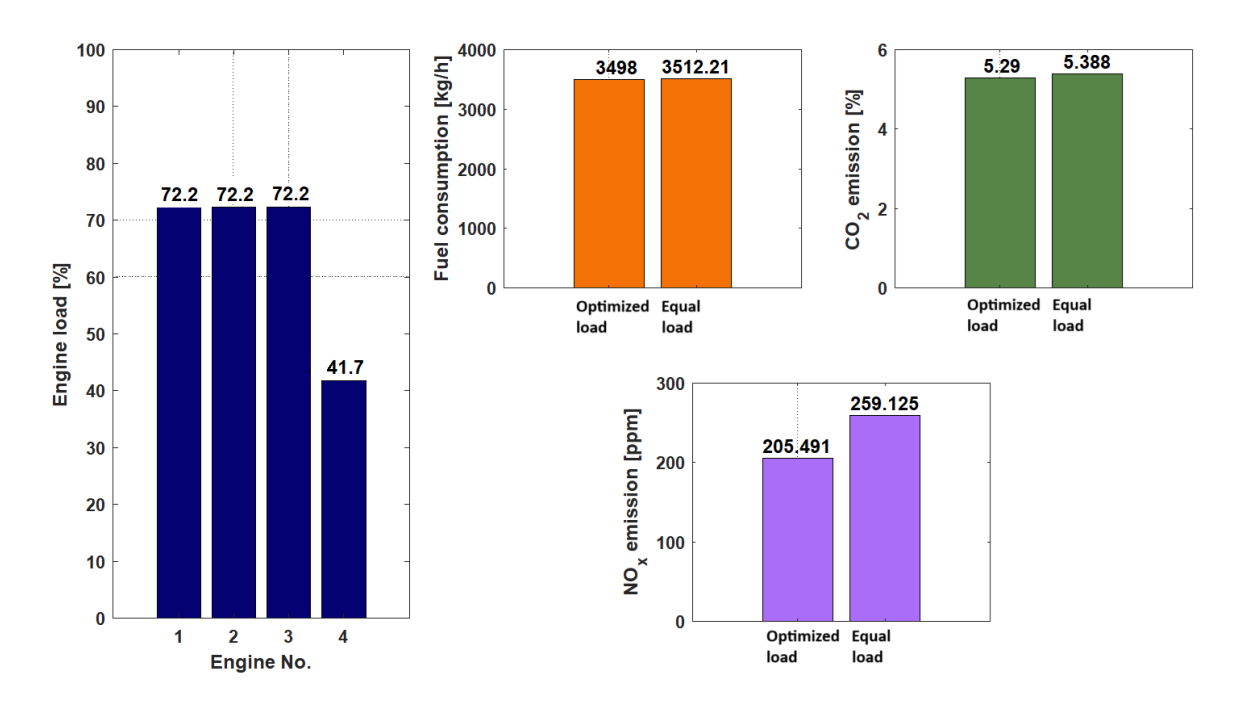


Figure 4.13 Optimization example for LNG with a power requirement of 20,000 kW using four engines

With the optimized load distribution, CO₂ emissions were 5.290%, compared with 5.388% under equal load distribution. This corresponds to a reduction of 0.098 percentage points, or about 1.82% relative to the equal load baseline. Although this reduction is modest, it is in line with the priority the model gives to fuel consumption over emissions, as reflected by the weighting factor for NOx ($wf_{NOx} = 0.4$).

The greatest effect of the optimization can be observed in NOx emissions. Under the optimized scenario, NOx levels dropped to 205,491 ppm, compared to 259,125 ppm under a uniform load distribution, a remarkable reduction of 20.69%. This result confirms the effectiveness of the model in reducing NOx emissions, although emissions are secondary to fuel consumption. Overall, the optimization strategy made a significant contribution to more environmentally friendly ship operation.

Overall, the optimization model achieves a balanced result by prioritizing fuel consumption while significantly reducing NOx emissions. Although the improvement in fuel efficiency is modest, the considerable reduction in NOx emissions emphasizes the model's ability to improve environmental performance without compromising operational efficiency.

In summary, the optimized load distribution supports more efficient and environmentally sustainable operation with LNG and demonstrates the effectiveness of the model in balancing fuel consumption and emissions control, particularly in terms of NO_x reduction.

4.3.2. Marine Diesel Oil (MDO) Optimization Example

Figure 4.14 shows that the optimized fuel consumption is 4,354.1 kg/h, while the fuel consumption with the equal load distribution is 4,470.2 kg/h. This represents an increase in consumption of 2.66% for the uniform load sharing scenario and clearly shows that the optimized load sharing provides greater fuel efficiency for a total power requirement of 20,000 kW by achieving the same power with lower fuel consumption.

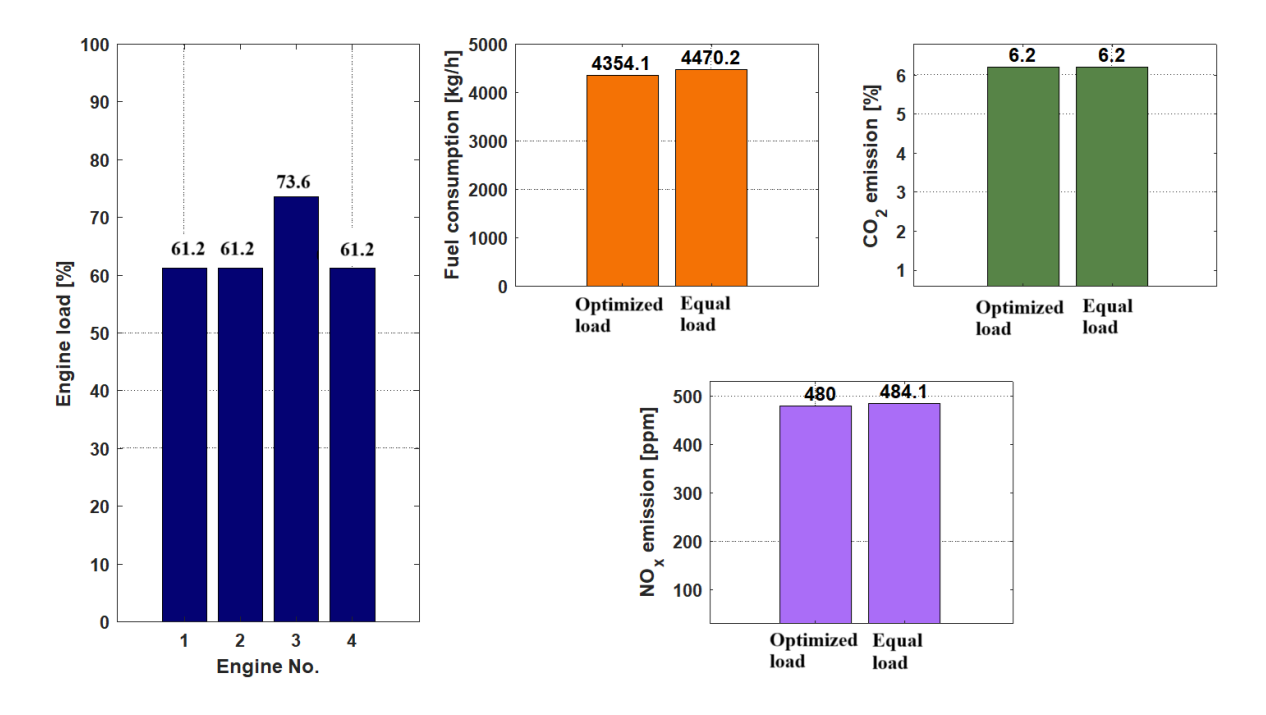


Figure 4.14 Optimization example for MDO with a power requirement of 20,000 kW using four engines

The CO₂ emission share remains constant at 6.2% in both load distribution scenarios. However, there is a slight improvement in NOx emissions. The optimized load distribution leads to a reduction to 480 ppm, compared to 484.1 ppm with the equal load distribution, which corresponds to a decrease of around 0.85%.

In summary, the optimized load scenario reduced fuel consumption by 2.66% and NO_x emissions by 0.85%, consistent with previous results for LNG, which not only improves fuel

efficiency but also supports greener operations. These results confirm the effectiveness of the model in achieving a balanced approach to fuel savings and emissions reduction.

4.3.3. Heavy Fuel Oil (HFO) Optimization Example

Figure 4.15 shows that the optimized fuel consumption is 4,282.2 kg/h, while the uniform load distribution results in a consumption of 4,386.9 kg/h. This corresponds to an increase in fuel consumption of 2.44% with uniform load distribution. These results confirm that the optimized load sharing for a total power requirement of 20,000 kW is more fuel efficient as it achieves the required power with lower fuel consumption.

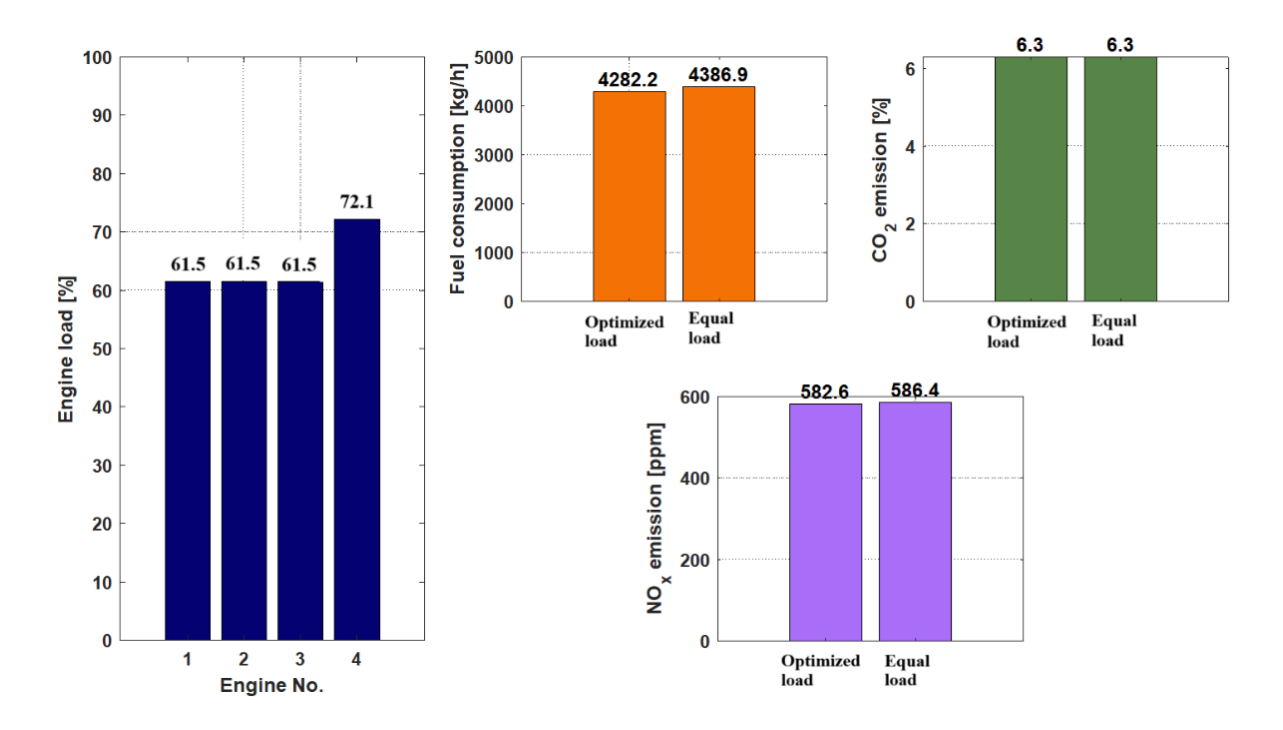


Figure 4.15 Optimization example for HFO with a power requirement of 20,000 kW using four engines

As can be seen from the diagram, the percentage of CO_2 emissions in this case remains constant at 6.3% (as in the case of HFO), but in contrast to the previously considered fuel (LNG).

With the optimized load distribution, NOx emissions are reduced to 582.6 ppm, compared to 586.4 ppm in the scenario with the equal load distribution. Even though the weighting factor for NO_x ($wf_{NOx} = 0.4$) indicates that emission reduction was a secondary objective compared to fuel consumption, the model still achieved a measurable improvement in environmental performance.

In summary, the optimized load configuration not only improves fuel efficiency but also contributes to a cleaner operating profile, as observed with LNG. These results confirm the model's ability to effectively balance fuel consumption and emissions control under realistic operating conditions.

4.3.4. Heavy Fuel Oil (HFO) Optimization Example across a wide load range

Figure 4.16 shows the fuel consumption for heavy fuel oil (HFO) in a power plant operated with five engines in the power range of 24,000 kW to 26,000 kW, a load range that frequently occurs in typical ship operation. The diagram compares the fuel consumption in kilograms per hour (kg/h) under two load distribution scenarios:

- Equal load distribution (light orange bars): Represents a scenario where the power is distributed evenly across all engines by the PMS.
- Optimized load distribution (dark orange bars): Represents a scenario where load is allocated based on the recommendations of an optimization model to improve fuel efficiency.

In this analysis, the optimization model used the following weighting factors for all fuel types: a weighting factor for fuel consumption (wf_{FC}) of 0.4 and a weighting factor for nitrogen oxide emissions (wf_{NOx}) of 0.6. These values show that emission reduction is given a higher priority, while fuel efficiency is still taken into account.

The x-axis represents the requested power, which ranges from 24,000 kW to 26,000 kW in 500 kW increments, while the y-axis shows the corresponding total fuel consumption in kilograms per hour (kg/h).

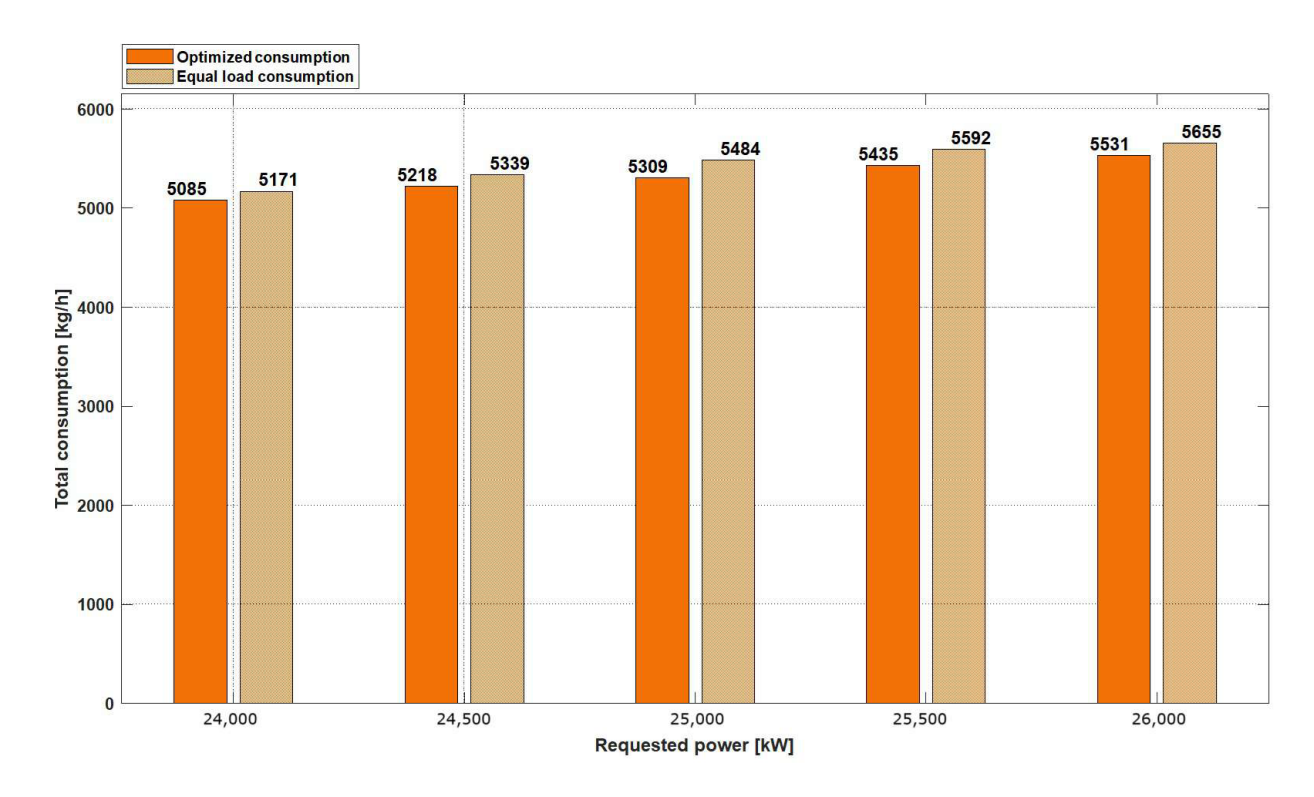


Figure 4.16 Fuel consumption for the power range 24,000–26,000 kW

The graph shows that the optimized load distribution consistently leads to lower fuel consumption across the entire observed power range compared to a uniform load distribution. This underlines the effectiveness of the optimization model in improving fuel efficiency, which can translate into both economic savings and reduced environmental impact.

For example, at an output of 24,000kW, the fuel consumption with uniform load distribution is 5171 kg/h, while the optimized configuration achieves a lower consumption of around 5085 kg/h, which corresponds to a reduction in fuel consumption of 1.66%.

With an output of 26,000 kW, the fuel consumption with the equal load distribution is 5655 kg/h, while the optimized load distribution achieves a lower consumption of 5531 kg/h. This corresponds to a reduction of around 2.19%, which further underlines the consistent fuel savings achieved by the optimization over the entire power range investigated.

The results indicate that the optimization model achieves an increasingly better fuel economy with increasing energy demand and thus provides valuable insights for improving operational planning and cost management in marine energy systems.

Figure 4.17 shows a comparison of CO₂ emissions at different power demand levels (24,000 kW to 26,000 kW) under optimized and uniform load distribution scenarios. The graph shows that the percentage share of CO₂ emissions is constant at 6.3 % across all observed power levels, regardless of the load distribution strategy used. This result is consistent with the

weighting factor of zero assigned to CO₂ in the optimization model, which means that CO₂ emissions were not directly considered in the optimization process. As a result, the focus on parameters such as fuel consumption and NOx emissions had no impact on the CO₂ emission values, which remained stable throughout.

In accordance with IMO regulations and guidelines, CO₂ emissions as reflected in CII, EEPI, cbDIST, clDIST [65], EEXI [66] and EEOI [67] are generally calculated assuming complete combustion of the fuel. However, since complete combustion rarely occurs under real operating conditions, this assumption was not taken into account in the present analysis.

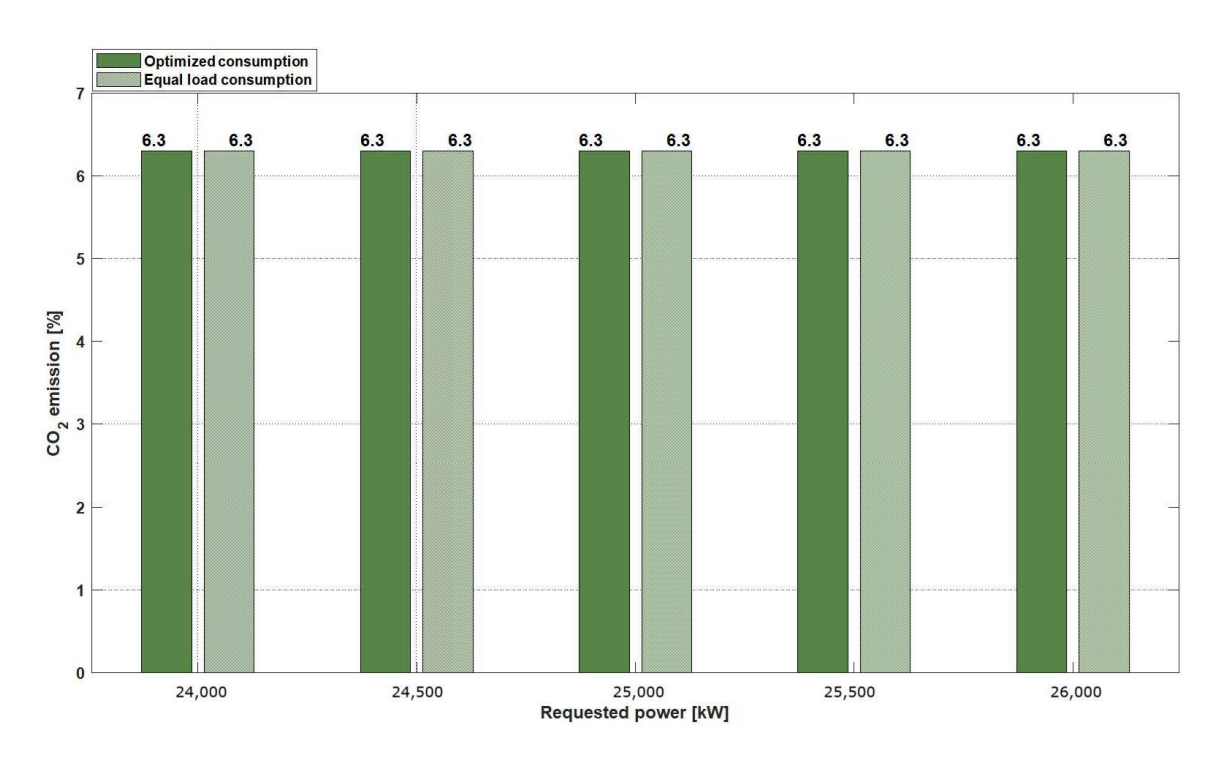


Figure 4.17 CO₂ emission share for the power range of 24,000–26,000 kW

Figure 4.18 shows a comparison of NOx emissions (in ppm) for different power requirements in the range from 24,000 kW to 26,000 kW under optimized and uniform load distribution strategies. The data shows that the scenario with optimized load distribution results in consistently lower NOx emissions for all power levels investigated. At 24,000 kW, for example, the optimized configuration results in 583.4 ppm NO_x, while the uniform load distribution results in a slightly higher emission value of 586.7 ppm. At the upper end of the power range, at 26,000 kW, NO_x emissions fall to 577.2 ppm in the optimized scenario, compared to 591.8 ppm in the uniform load sharing scenario, which corresponds to a reduction of 2.52%. These results demonstrate the effectiveness of the optimization model in minimizing NOx emissions, particularly at higher operating loads.

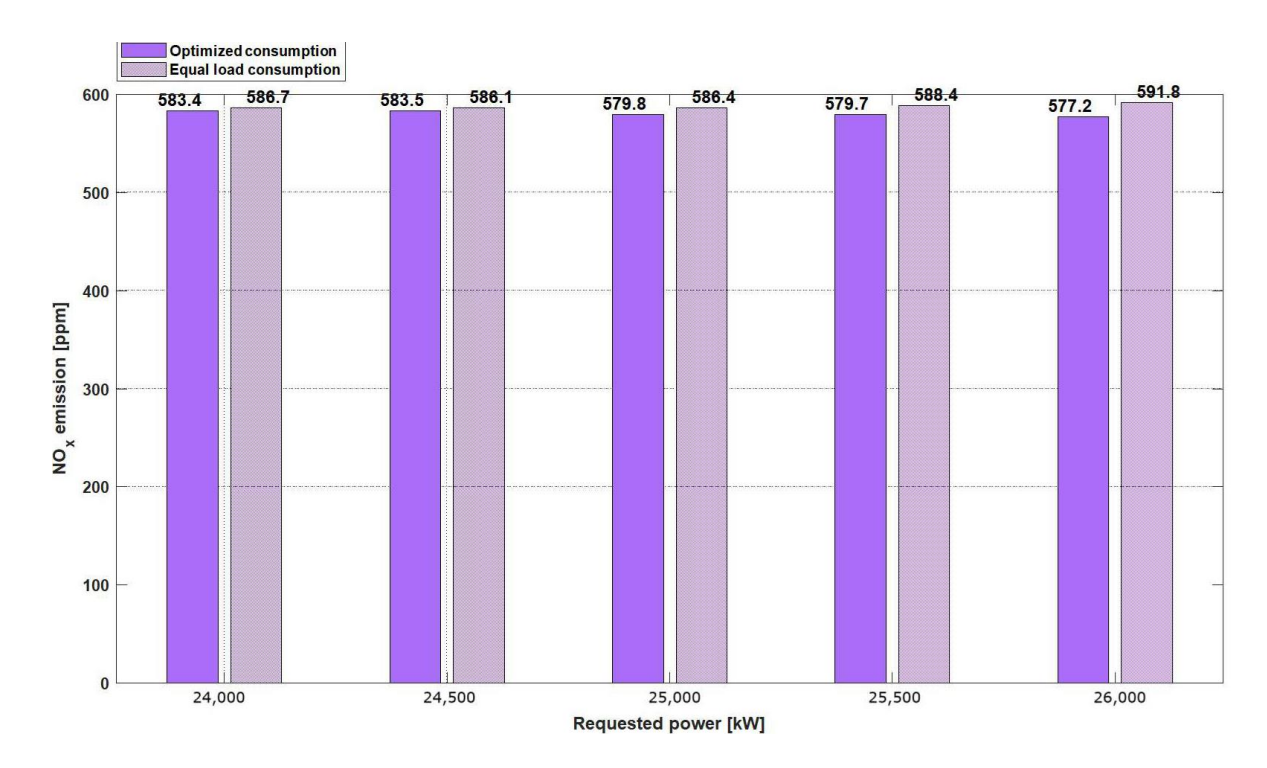


Figure 4.18 Share of NOx emissions for the power range 24,000–26,000 kW

Although the observed reductions in NOx emissions are relatively modest, they underline the effectiveness of the optimization model in targeted emission control, especially under the influence of the weighting factor (wf_{NOx}) assigned to NOx emissions. Although the absolute differences are not significant, the consistent downward trend across all power levels shows that the load optimization strategy reliably contributes to NOx reduction. This trend highlights the model's ability to improve environmental performance through strategic load balancing and emphasizes its value in supporting cleaner and more sustainable ship operations.

The 3D bar chart in Figure 4.19 illustrates the percentage load distribution across five engines in a power plant operating in a power range from 24,000 kW to 26,000 kW. This visual representation effectively conveys how the total load demand is distributed across the individual engines at different power levels. Each color-coded segment within the bars corresponds to the proportion of the total load allocated to a specific engine, providing a clear overview of how the optimization model balances motor loads in response to different power requirements.

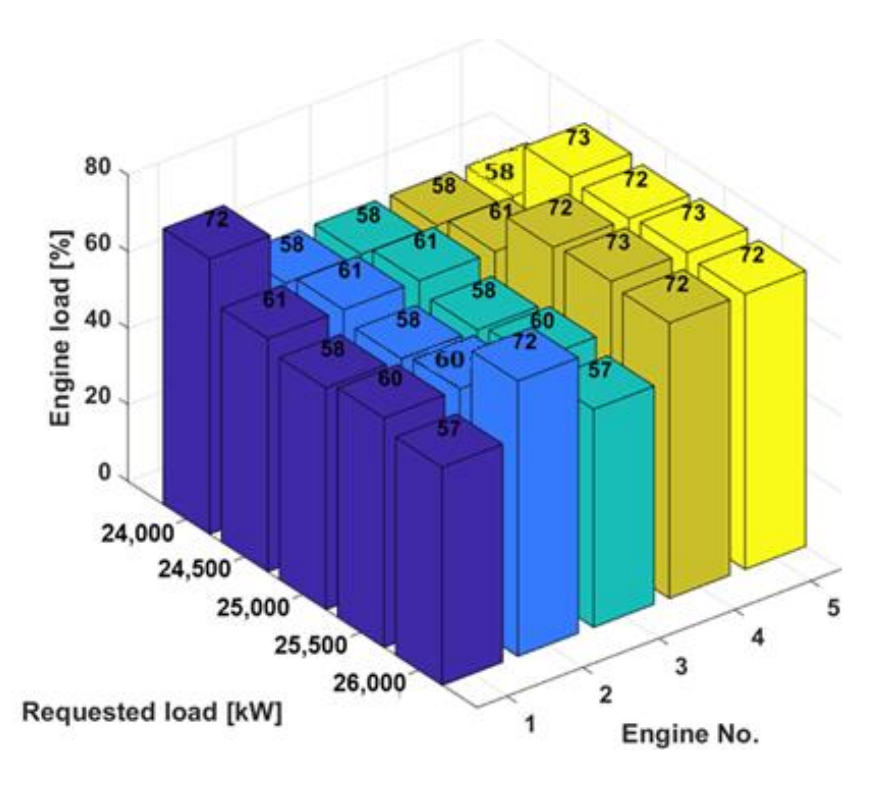


Figure 4.19 Percentage load distribution across the engines for the power range of 24,000–26,000 kW

4.3.5. Overview of the tested operating scenarios

The examples presented illustrate the effectiveness of the optimization model in controlling the distribution of load between DFDE engines in LNG-powered marine propulsion systems with the primary aim of minimizing fuel consumption and exhaust emissions, especially NOx. By fine-tuning load sharing between multiple engines based on weighted fuel efficiency and emission criteria, the model enables a notable reduction in NOx emissions and delivers moderate improvements in fuel consumption while ensuring compliance with relevant environmental regulations.

The results indicate that optimizing the load distribution of engines brings considerable benefits for both the environment and operation. In certain scenarios, NOx emissions could be reduced by up to 23%, while fuel consumption could be reduced evenly, if only slightly, across all load levels. This method has proven to be effective in improving fuel efficiency and reducing emissions under real-world conditions, as confirmed by on-board validation tests.

The flexibility of the model, as evidenced by its performance with different fuel types and load conditions, emphasizes its suitability for different marine propulsion systems. Furthermore, this study highlights the value of integrating emission parameters such as CO₂

and NOx into optimization frameworks that promote broader strategies to improve engine efficiency and mitigate the environmental impact of maritime operations.

The multi-criteria optimization model validated in this study demonstrates its ability to support different operational approaches and environmental regulations by allowing adjustments to the weighting factors for fuel consumption and emissions. This flexibility strengthens the robustness of the model and emphasizes its ability to adapt to specific regulatory frameworks and operational requirements. By allowing fine-tuning of these parameters, the model can produce customized solutions that effectively balance fuel efficiency and emissions reduction, underlining its practical relevance for real-world maritime applications.

4.4. EXAMPLE OF MODEL VALIDATION WITH CONSUMPTION AND EMISSION ANALYSIS BASED ON WEIGHT FACTORS FOR HFO AT HIGH LOAD DEMAND

Figures 4.20, 4.21, and 4.22 show the effects of varying the weighting factors for fuel consumption (wf_{FC}) and NOx emissions (wf_{NOx}) on the results of the optimization model in terms of fuel consumption, CO₂ emissions and NOx values at a high-power requirement of 25,000 kW. This power level was chosen to ensure that all five engines were operated with HFO in order to test the model under realistic conditions at high load. The results confirm the model's ability to adapt effectively to changing priorities. With increasing weighting of fuel consumption and NOx emissions, there is a clear linear decrease in fuel consumption (and therefore CO₂ emissions) and NOx emissions. This confirms the effectiveness of the model in achieving a balance between operational efficiency and environmental performance. The range of weighting factors from 0.1 to 0.9 supports the principle of joint prioritization and allows for flexible trade-offs between minimizing fuel consumption and reducing NOx emissions, ensuring that neither objective is neglected. This underlines the robustness of the model and its suitability for dynamic, targeted optimization in maritime applications.

In addition, the application of weighting factors in the range of 0.1 to 0.9 corresponds to the principle of distributed prioritization and ensures that no single objective has a disproportionate influence on the optimization result. By maintaining a moderate sum of weights across all targets, the model supports a balanced assessment where each criterion, such as fuel consumption and emissions, contributes proportionally to the overall result. This strategy

increases the flexibility of the model in different operating scenarios while ensuring consistency and comparability of results across different optimization settings.

Figure 4.20 illustrates the correlation between the weighting factor for fuel consumption (wf_{FC}) and total fuel consumption in kilograms per hour (kg/h), with wf_{FC} values between 0.1 and 0.9. The data shows a clear downward trend in fuel consumption as the weighting factor for fuel efficiency increases. The greatest reduction occurs between wf_{FC} values of 0.1 and 0.2, suggesting that even small increases in fuel efficiency weighting led to significant improvements at lower weighting. As the weighting factor approaches 0.9, the fuel reduction decreases, suggesting that the benefit of further prioritization diminishes.

Overall, this trend highlights the ability of the optimization model to improve fuel efficiency when fuel consumption is given a higher operational priority.

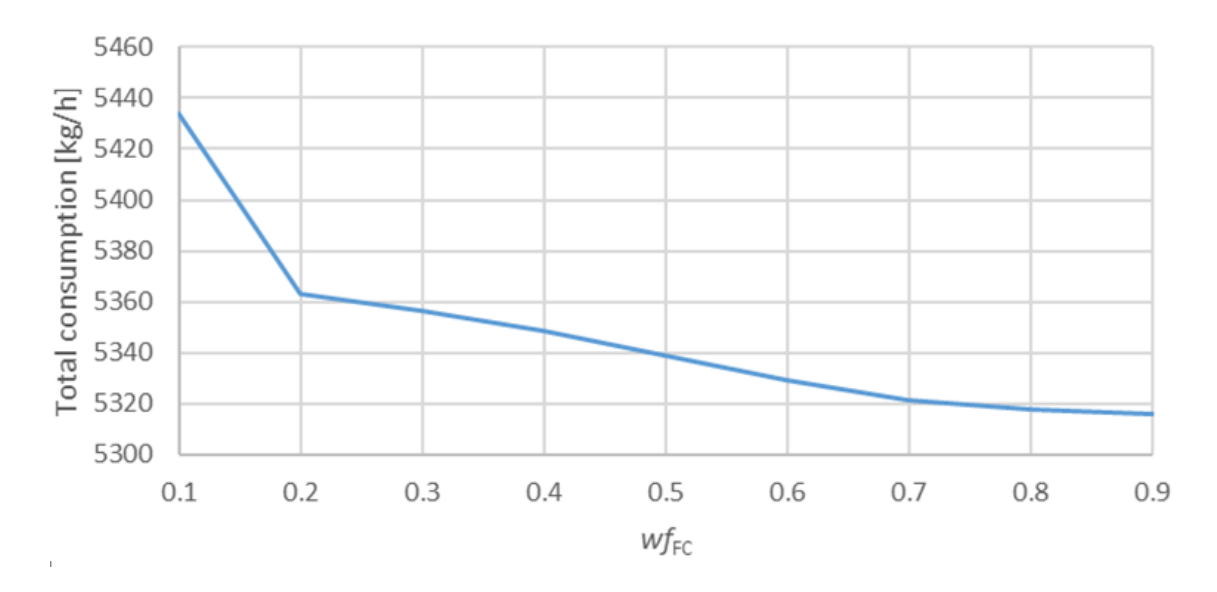


Figure 4.20 Fuel consumption as a function of weighting factors for fuel optimization

Figure 4.21 illustrates the trend in CO₂ emissions (expressed as a percentage) in relation to the weighting factor for fuel consumption (wf_{FC}).

A consistent downward pattern can be seen, indicating that CO_2 emissions decrease with increasing wf_{FC} and correspondingly reduced fuel consumption.

The strongest decrease occurs between $wf_{FC} = 0.1$ and $wf_{FC} = 0.2$, after which the decrease gradually decreases.

Considering that CO₂ emissions are directly proportional to fuel consumption, the observed reduction confirms that the optimization model not only improves energy efficiency but also reduces environmental impact, thereby supporting both sustainability goals and regulatory requirements

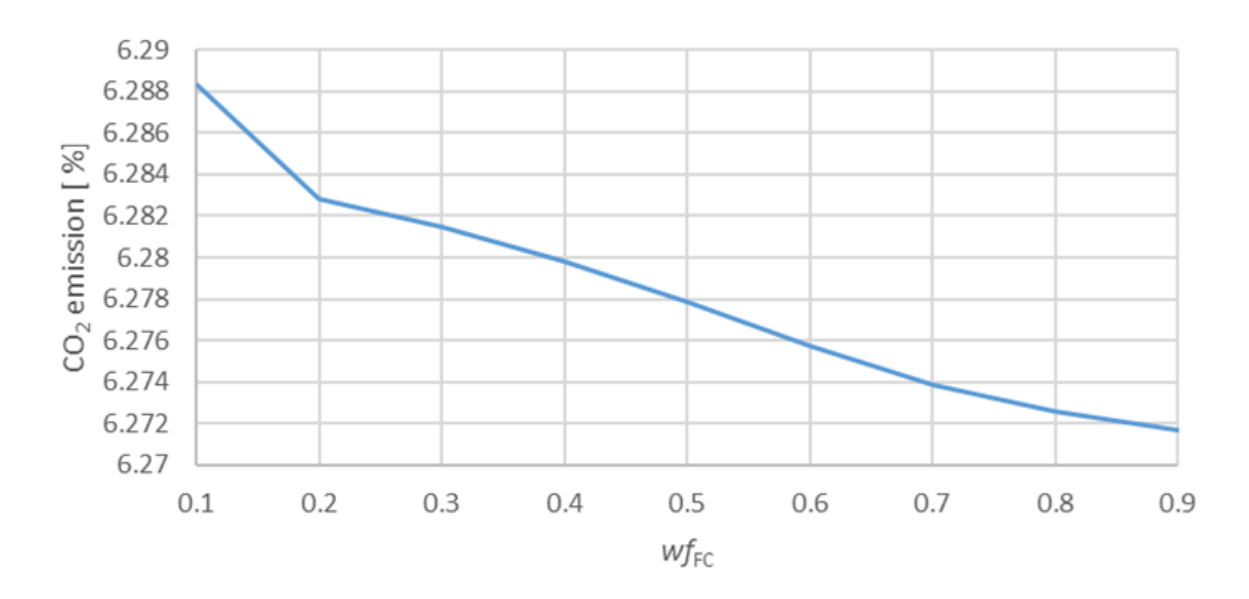


Figure 4.21 CO₂ emissions based on the fuel weighting factors

Figures 4.20 and 4.21 show comparable downward trends that emphasize the close correlation between fuel consumption and CO₂ emissions. The results clearly show that increasing the weighting factor for fuel consumption (*wf*_{FC}) within the optimization model not only increases operational efficiency but also contributes to a moderate reduction in greenhouse gas emissions, particularly CO₂. This dual benefit is critical to meeting energy efficiency targets and environmental regulations and confirms the effectiveness of the model in minimizing both fuel consumption and associated emissions.

Figure 4.22 shows the correlation between the NOx emission weighting factor (wf_{NOx}) and the corresponding NOx emissions, expressed in parts per million (ppm). The values of the weighting factor range from 0.1 to 0. 9.

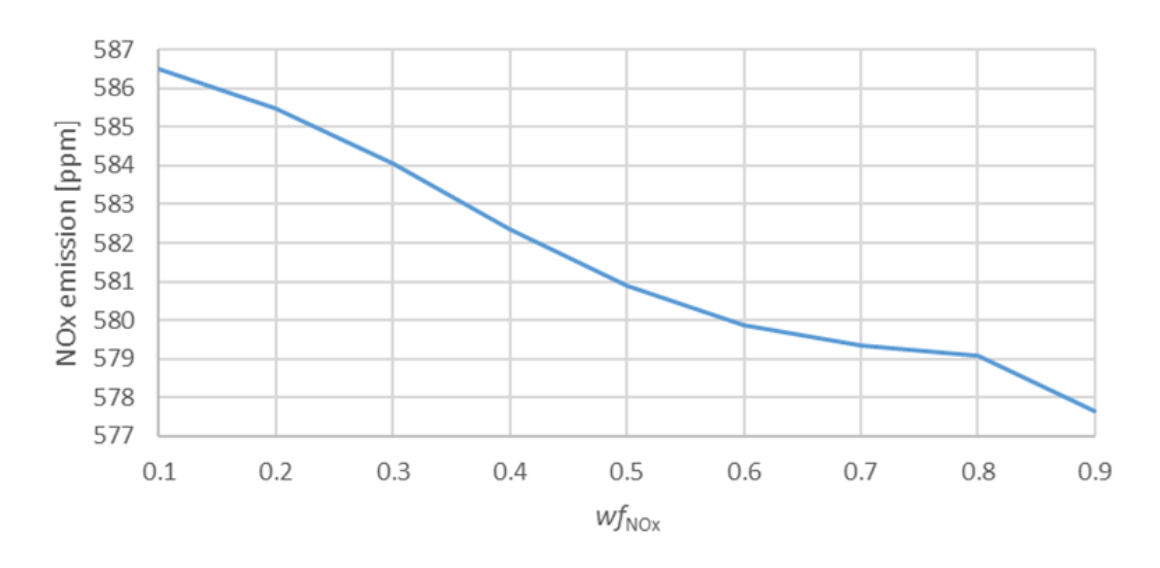


Figure 4.22 NOx emissions based on the weighting factors

As the weighting factor for NOx (wf_{NOx}) increases, a steady decrease in NOx emissions is observed, demonstrating the effectiveness of the optimization model in prioritizing and reducing NOx emissions.

Initially, there is a steeper decline between wf_{NOx} values of 0.1 to 0.3, with emissions falling from around 587 ppm to 583 ppm. This is followed by a more gradual decline between 0.3 and 0.7, reaching around 579 ppm. From 0.7 to 0.9, the trend steepens again, and emissions continue to fall to 577 ppm.

These results emphasize the ability of the model to support multiple environmental goals while reducing NOx emissions alongside fuel consumption and CO₂ emissions.

4.5. VALIDATION OF THE OPTIMIZATION MODEL WITH LNG ACROSS THE DIFFERENT OPERATING MODES

To ensure the practical reliability of the optimization model developed, validation was carried out with real operating data from various operating modes of ship operation. While the fuel consumption was validated in all tested modes including loaded passage, ballast passage, cargo loading and unloading the validation of emissions was carried out exclusively during the cargo loading mode.

This operating mode was selected for emissions validation because the ship's engines operate at the lowest power, a condition under which emissions behavior is particularly sensitive to changes in load distribution. Therefore, it represents a critical test case to evaluate the model's potential to reduce harmful exhaust emissions under the most emission-intensive conditions.

Emissions were not validated separately under higher load conditions for two main reasons. Firstly, it is well documented from a technical point of view that reducing fuel consumption at medium and high loads, where combustion is more efficient, leads directly to lower emissions, particularly of CO₂ and NOx. Secondly, and equally important, were the technical and logistical constraints associated with relocating and reconnecting emissions measurement equipment. This process is complex and time-consuming and requires careful coordination, access to the system and adherence to safety protocols. Although the vessel is operated under a long-term charter contract and follows a generally predictable voyage pattern, making it ideal for modelling long-term performance, this operational predictability does not necessarily imply technical flexibility. In practice, frequent time constraints in ports, tight

schedules and unplanned operational changes often limit the ability to perform such specialized measurement tasks across multiple engine configurations and voyage phases.

Therefore, emissions validation strategically focused on the most operationally sensitive mode, while consumption validation for all modes confirmed the robustness of the model. This approach ensured that the model was both technically sound and practically aligned with the realities of commercial LNG ship operations.

Based on this validation framework, the analysis of fuel savings and emission reductions was carried out exclusively with liquefied natural gas (LNG) as the primary fuel. This choice was based on the operational profile of the selected case study vessel, which uses LNG almost exclusively during all phases of the voyage due to a long-term charter contract that requires consistent fuel efficiency and emission compliance.

Although the engine is technically capable of running on heavy fuel oil (HFO) and marine diesel oil (MDO), these fuels are only used in exceptional circumstances. HFO is used automatically in the event of malfunctions in the gas combustion system to ensure uninterrupted propulsion, while MDO is primarily used for system flushing during extended maintenance work. In both cases, these fuels are used at specific engine loads and outside of typical operating cycles, making them unsuitable for consistent model validation.

For this reason, the validation was performed in full for all operating modes of the vessel with LNG, reflecting the standard energy profile of the vessel. Supplementary results for MDO and HFO were only evaluated at selected loads to investigate the comparable emission and fuel consumption characteristics. This approach ensures that the model remains both operationally relevant and methodologically sound without compromising the integrity of the validation process.

For this case study analysis, an LNG vessel with the specifications listed in Table 1.1 (see Section 1.4) was considered. This vessel was selected for the case study because it operates under a long-term charter contract (25 years) and is therefore ideally suited to evaluate the effectiveness of the mathematical model in reducing fuel consumption and emissions over longer periods of time. LNG ships, especially those with long-term charter contracts, operate in predictable patterns, making them ideal for implementing fuel saving and emission reduction strategies. In addition, the ship has well-defined time frames for a voyage that must be adhered to in terms of a binding long-term charter contract and therefore lends itself to simulating long-term savings given the ship's constant routine.

A voyage of a considered ship that includes the loading of the cargo, the loaded passage, the unloading of the cargo and the return to the same port (ballast passage) to load the cargo again. The duration of a typical voyage is 26 days as follows:

- Load port 1.5 days
- Loaded passage 10 days
- Discharge port 1.5 days
- Ballast passage 13 days

The analysis examines the fuel consumption and exhaust emissions across all real operating intervals of the ship, based on equal power distribution between the engines according to the PMS. The simulation model is then applied under identical load conditions to compare fuel consumption and emissions between the two approaches. To validate the model, a real-time redistribution of the engine load is performed according to the optimization model. This allows the identification of deviations between the simulated results and the actual performance after load redistribution.

The following weighting factors were applied in the optimization model for the reduction of fuel consumption (wf_{FC}) and NOx (wf_{NOx}) and for all operating modes considered: wf_{FC} at 0.5 and wf_{NOx} at 0.5.

The measurements were carried out with a "Promass 80" mass flow meter (Figure 4.23), which had a valid calibration certificate at the time of data acquisition and operated within a tolerance of $\pm 0.1\%$.



Figure 4.23 "Promass 80" mass flow meter

In DFDE engines, a small amount of pilot fuel is supplied via secondary fuel lines in addition to the primary fuel lines. This pilot fuel is essential for ignition when the engine is operating in LNG-air mixture mode [68] or distillate [69] mode to ensure proper nozzle cooling. The 'micro-pilot' injection system consumes less than 1% of the total fuel oil consumption and is therefore not included in the fuel oil consumption (FOC) calculation for the considered fuel type. The performance and efficiency of DFDE engines are well documented in the existing literature [70–78].

4.5.1. Loaded passage optimization example (24,000 kW)

Loaded conditions refer to a voyage in which the propulsion power plant operates at a higher load while the ship is fully loaded, as shown in Figure 4.24.

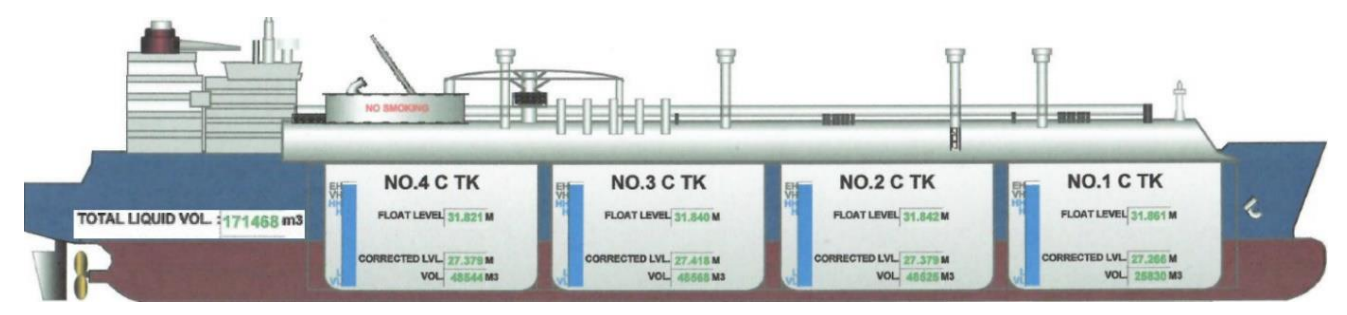


Figure 4.24 IAS representation of cargo Tank conditions

A typical example of a loaded passage is a power demand of 24,000 kW with four engines running in the network. Figure 4.25 shows the Integrated Automation System (IAS) representation of the engine load distribution under the PMS, which ensures an even power distribution among the engines. At this load, each engine operates at approximately 77% capacity. The calculated total fuel consumption for all engines in the network is 4084.8 kg/h, which is consistent with the results of the optimization model.

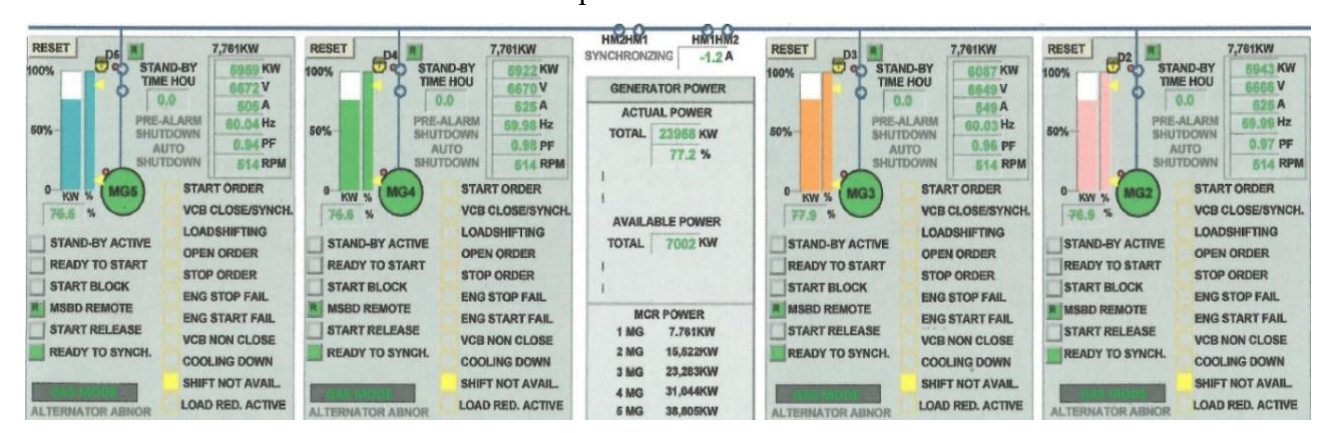


Figure 4.25 IAS representation of load distributions according to the PMS

In order to compare the consumption data obtained with the optimized consumption, a manual redistribution of the motor load in the network was carried out according to the optimization model at the same load of 24,000 kW.

The screenshot of IAS in Figure 4.26. shows that two engines are operating with a load of 84% of the load, while the other two engines are operating with a slightly lower load of 72%. This redistribution is in line with the recommendations of the optimization model and enables a more efficient allocation of energy while ensuring operational stability.

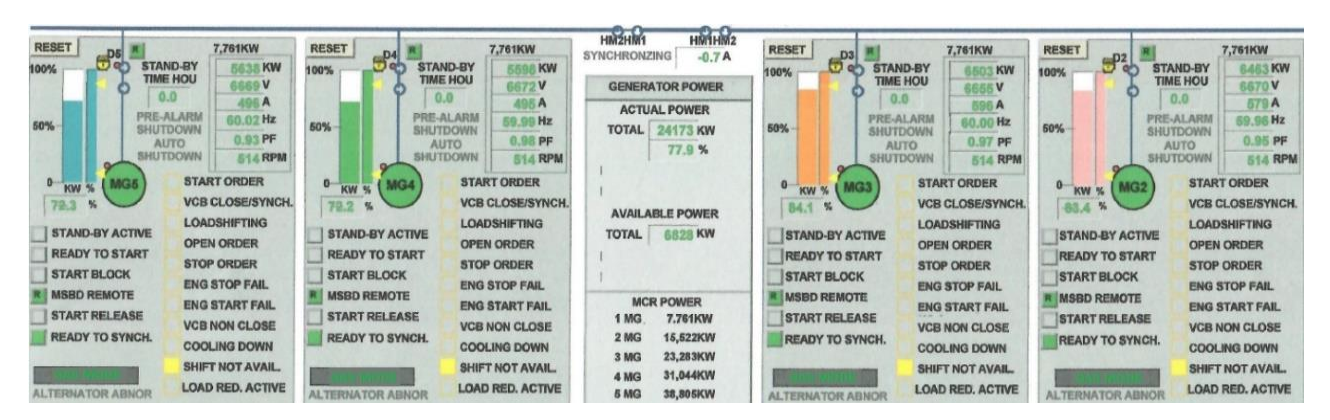


Figure 4.26 IAS representation of load distributions according to the optimization model

Figure 4.27 shows an optimization example for LNG with a total power requirement of 24,000 kW, distributed across four engines. The diagram on the left shows the number of engines in operation and their respective percentage utilization. The three other diagrams provide a comparative analysis of the key performance indicators between two engine load distribution scenarios: optimized and equal load. In particular, they show the differences in fuel consumption (kg/h), CO₂ emissions (%) and NOx emissions (ppm) and illustrate the efficiency gains achieved by the optimized load distribution.

With this optimized load distribution, the calculated fuel consumption is 4054.4 kg/h, which corresponds to a reduction of 30.4 kg/h or 0.74% compared to the conventional equal load distribution under the PMS with the same total power requirement. Converted into tons, this reduction equates to a fuel saving of approximately 7.3 MT over the course of a 10-day loaded passage, demonstrating the tangible benefits of the optimization model in improving energy efficiency.

As the graph shows, the percentage share of CO₂ emissions remains constant at 5.2 % in both scenarios. This shows that the optimization model achieves fuel savings without changing the proportional share of CO₂ emissions in the exhaust gas.

With the optimized load distribution, NOx emissions fall to 171.8 ppm, compared to 192.2 ppm in the scenario with the same load distribution. This corresponds to a reduction of 11.87 % and shows that the greatest effect of the optimization in this ship regime can be observed in NOx emissions. The results show that the optimization of loading effectively reduces NOx emissions and thus contributes to a more environmentally sustainable ship operation without compromising performance.

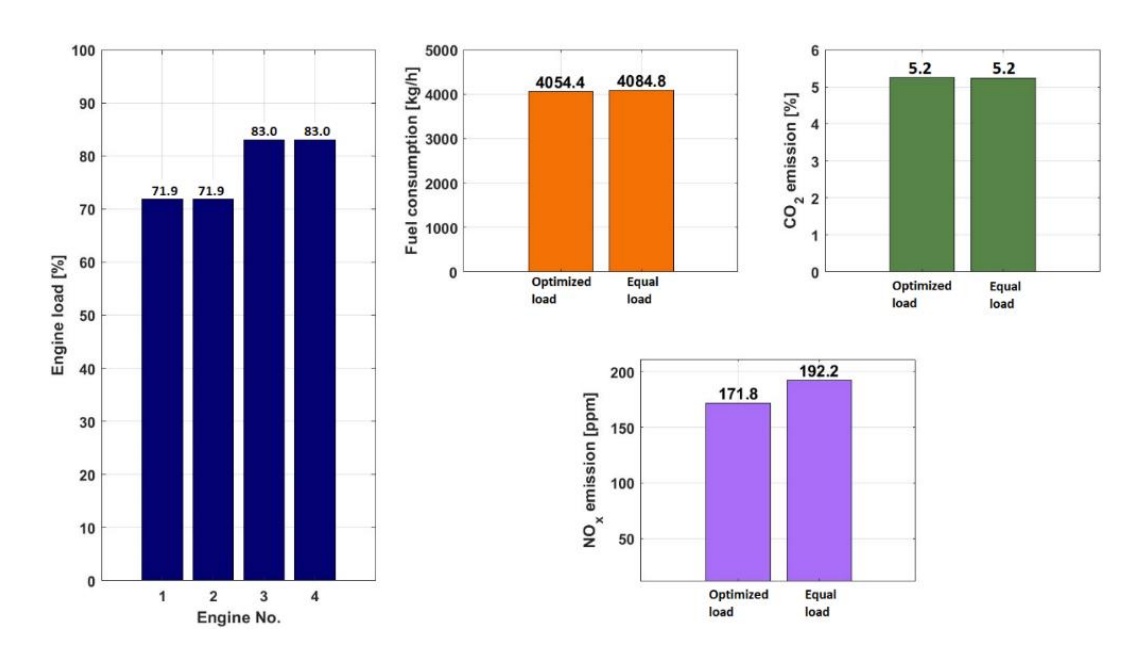


Figure 4.27 Optimization example for LNG at 24,000 kW on four engines.

4.5.2. Ballast passage optimization example (17,500 kW)

A ballast passage refers to a voyage in which the ship sails with a moderate load on the propulsion system and no cargo on board, as shown in Figure 4.28.

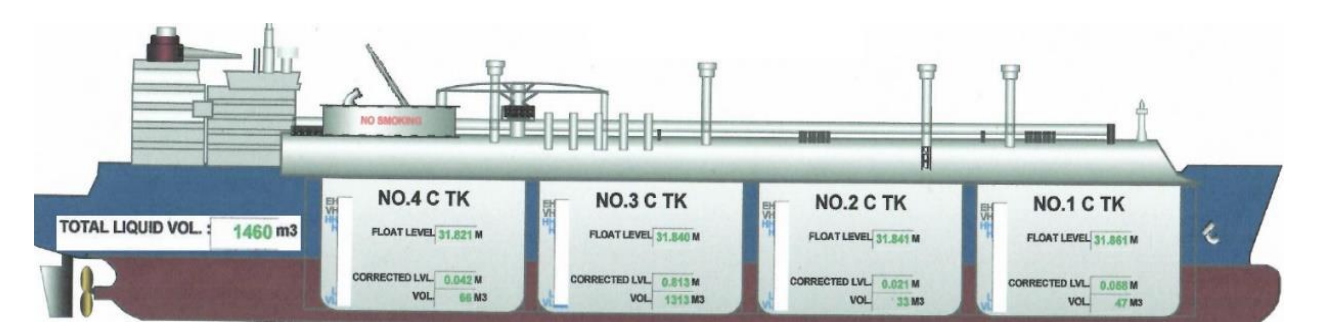


Figure 4.28 IAS representation of cargo Tank conditions

In a typical ballast passage, the propulsion power plant operates with a load of approx. 17,500 kW, with three engines running in the network. Figure 4.29 shows a screenshot of the load distribution of the IAS engines under the PMS, where the power is evenly distributed among the engines. Under these conditions, each engine operates at approximately 75% of the load. The calculated total fuel consumption for all engines in the network is 3021 kg/h, which is consistent with the results predicted by the optimization model.

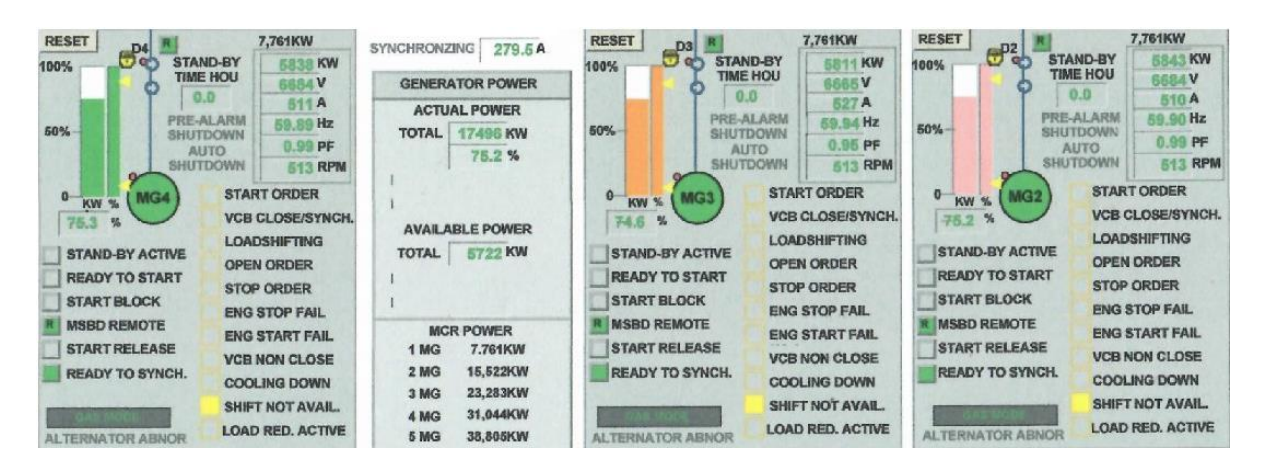


Figure 4.29 IAS representation of load distributions according to the PMS

In order to compare the fuel consumption data determined under standard conditions with the optimized scenario, a manual redistribution of the engine load was carried out in accordance with the optimization model, maintaining the same total load of 17,500 kW.

The IAS screenshot in Figure 4.30 illustrates the optimized load distribution, where one engine operates at 81.9% load, while the other two engines run at a lower load of 71.8%. This redistribution is in line with the recommendations of the optimization model and ensures a more efficient distribution of power with stable operation.

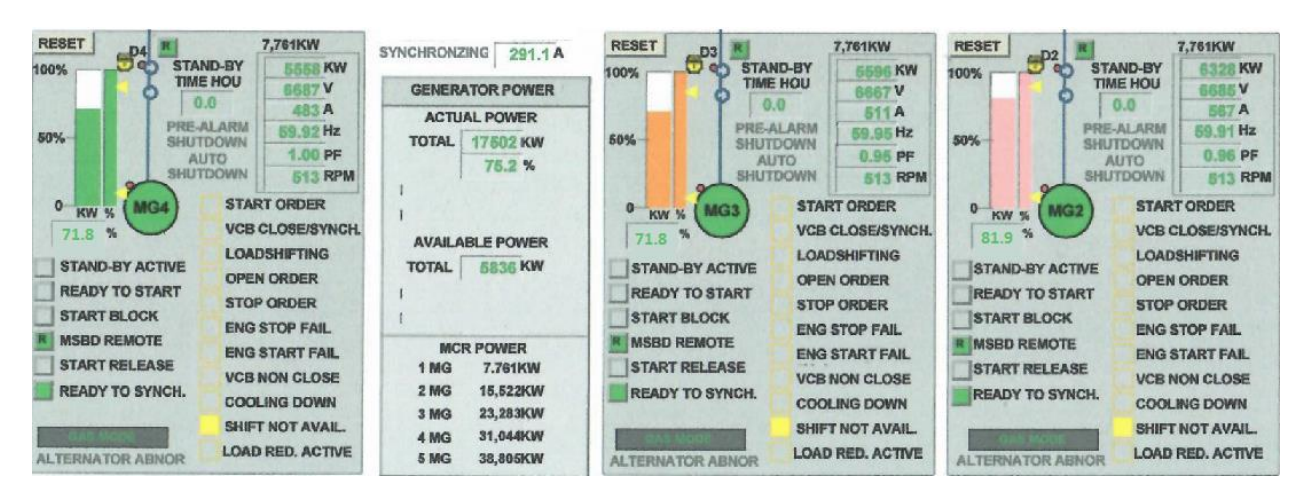


Figure 4.30 IAS representation of load distributions according to the optimization model

Figure 4.31, which shows an optimization example for LNG at 17,500 kW on three engines, shows that the calculated fuel consumption with the optimized load distribution is 2975.9 kg/h. This corresponds to a reduction of 45.1 kg/h (1.51%) compared to the conventional equal load distribution under the PMS. Converted into tons, this corresponds to a fuel saving of around 14.07 tons over the course of a 13-day ballast passage, which illustrates the considerable efficiency gains resulting from the optimization.

As the graph shows, the percentage of CO₂ emissions remains constant at 5.2% in both scenarios, just as in the previously analysed load conditions.

With the optimized load distribution, NOx emissions fall to 172.1 ppm, compared to 180.2 ppm with the same load distribution. Although the reduction is more moderate compared to the previously analyzed loaded passage, the effect remains obvious. The optimized scenario leads to a decrease in NOx emissions by 4.70%. This shows that load optimization contributes to lower emissions and more efficient engine operation even with a ballasted passage.

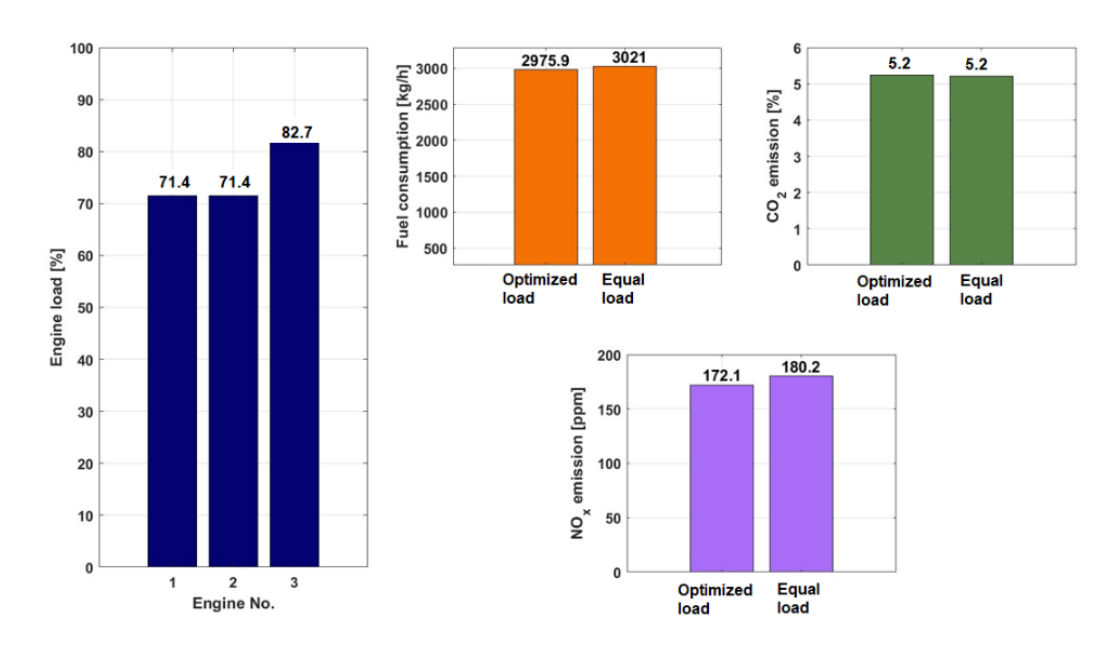


Figure 4.31 Optimization example for LNG at 17,500 kW on three engines.

4.5.3. Discharging the cargo optimization example (8,000 kW)

In unloading mode, both the unloading pumps and the ballast pumps are operated, which requires around 8,000 kW from the power plant. In this mode, two engines are in operation and the load is distributed evenly between them by the PMS. As a result, each engine operates at a load factor of 51.7%, as can be seen in the IAS screen shot in Figure 4.32.



Figure 4.32 IAS representation of load distributions according to the PMS

In order to compare the fuel consumption data determined in standard operation with the optimized scenario, the engine load was manually redistributed based on the optimization model while maintaining the same total load of 8,000 kW in the network.

The IAS screenshot in Figure 4.33 illustrates the optimized load distribution, where one engine runs at 20.1% load while the other engine runs at a higher load of 82.6%. This redistribution is in line with the recommendations of the optimization model and ensures a more efficient distribution of power while maintaining system stability.

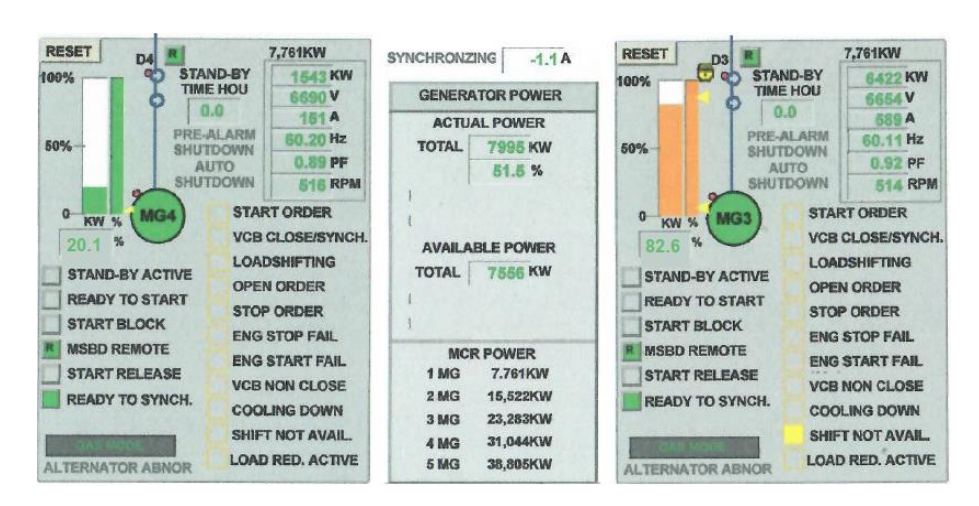


Figure 4.33 IAS representation of load distributions according to the optimization model

Figure 4.34 shows an optimization example for LNG at 8000 kW, distributed across two engines. The results show that the calculated fuel consumption with the optimized load distribution is 1397.2 kg/h, which corresponds to a reduction of 17.2 kg/h (1.23%) compared to the conventional PMS distribution with the same load. Converted into tons, this reduction corresponds to a fuel saving of approx. 0.62 MT over the 1.5 day unloading period, which illustrates the efficiency gains achieved by the load optimization.

By applying the optimized load distribution, NOx emissions are reduced to 331.5 ppm, in contrast to 432.5 ppm observed with the equal load distribution. This represents a significant reduction of 30.46% and underlines the effectiveness of the optimization model in minimizing NOx emissions during the unloading process.

In contrast to the two previously analysed ship operating modes, CO₂ emissions in this regime drop to 5.4%, compared to 5.6% with uniform load distribution. These results show that optimizing the loading when unloading the cargo effectively reduces both NOx and CO₂ emissions and thus contributes to a more environmentally sustainable ship operation.

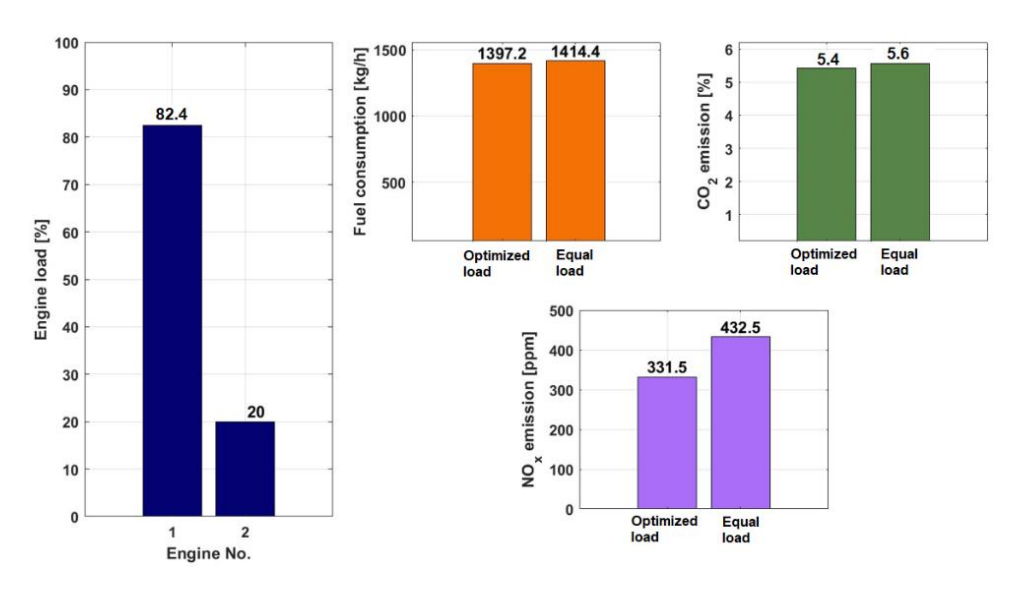


Figure 4.34 Optimization example for LNG at 8000 kW on two engines

4.5.4. Loading cargo optimization example (4,000 kW)

The cargo loading regime involves the operation of ballast pumps, which require around 4000 kW from power plant. For this mode, two engines are in operation to ensure redundancy and compliance with loading port regulations. Under the PMS-controlled distribution, the power is split evenly so that each engine operates at approximately 26% load, as shown in the IAS screenshot in Figure 4.35.

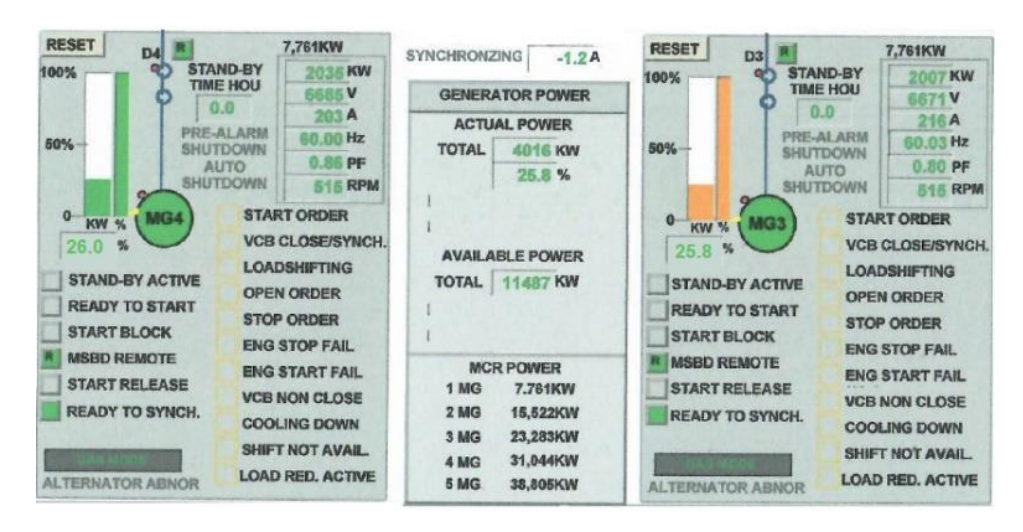


Figure 4.35 IAS representation of load distributions according to the PMS

In order to compare the measured fuel consumption with the optimized consumption, a manual redistribution of the engine load in the network was carried out according to the optimization model, while maintaining the same total load of 4000 kW.

The IAS screenshot in Figure 4.36 illustrates the optimized load distribution, where one engine runs with a load of 19.9% while the other engine runs with a higher load of 30.8%. This redistribution is in line with the recommendations of the optimization model, which aims to improve fuel efficiency and reduce emissions while maintaining stable operation.



Figure 4.36 IAS representation of load distributions according to the optimization model

Figure 4.37 shows an optimization example for LNG at 4000 kW on two engines. The calculated fuel consumption with the optimized load distribution is 796.6 kg/h, which corresponds to a reduction of 12.8 kg/h (1.60%) compared to the same load distribution under the PMS. Converted into tons, this results in a fuel saving of approx. 0.46 MT over the 1.5-day loading period, which underlines the efficiency advantages of load optimization in this operating mode.

As can be seen from the graph, the percentage of CO₂ emissions remains constant at 5.9% in both scenarios.

With the optimized load distribution, NO_x emissions fall to 679.5 ppm, compared to 756.5 ppm under equal load distribution. This represents a significant reduction of 11.33% and underlines the effectiveness of the optimization model in reducing NOx emissions for this operating mode.

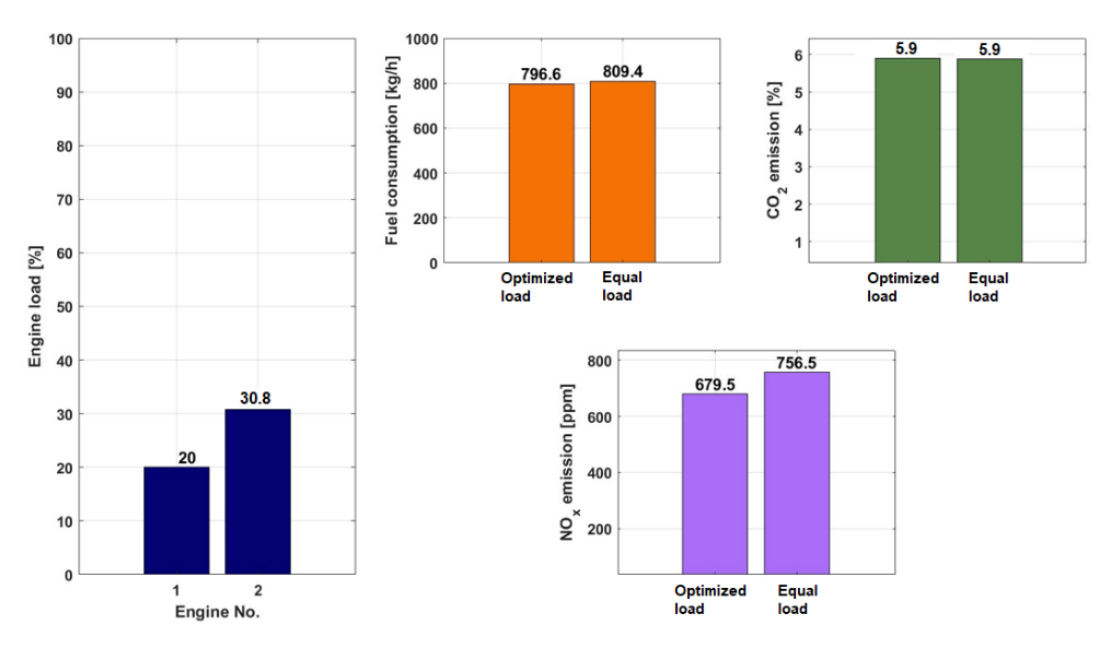


Figure 4.37 Optimization example for LNG at 4000 kW on two engines

4.5.5. Summary of observations and environmental impact

The optimization model applied to different operating conditions of the LNG vessel showed remarkable improvements in fuel efficiency. Table 4.1 summarizes the fuel savings achieved in all ship operating regimes considered, as well as the projected annual savings and cumulative savings over the duration of the ship charter.

Table 4.1 Fuel savings across different operating regimes.

Vessel Operating Regime	Duration (days)	Fuel Savings (MT)
Load port	1.5 days	0.46
Loaded passage	10 days	7.3
Discharge port	1.5 days	0.62
Ballast passage	13 days	14.07
Total for one Voyage	26 days	22.45
Annual Savings (14 voyages)	-	314.3
Charter period (25 years)	-	7857.5

Short-term saving and travel-based savings

The greatest fuel savings were observed during the ballast passage, where a reduction in fuel consumption of 1.51% led to a total saving of 14.07 MT per passage. This is due to the optimized load distribution of the engine, which ensures more efficient fuel consumption at moderate driving loads.

The second largest saving was in the loaded passage at 7.3 MT, which equates to a fuel saving of 0.74%.

For cargo handling, fuel savings were lower due to the relatively lower power requirements from an LNG power plant and the brevity of these particular ship operations. Discharging cargo resulted in fuel savings of 0.62 MT, while loading cargo resulted in fuel savings of 0.46 MT. Despite the shorter duration, these savings are still relevant, especially in terms of cumulative annual fuel savings. In total, a single 26-day voyage resulted in fuel savings of 22.45 MT. Extrapolated to an annual operating cycle (14 voyages), the fuel savings amount to 314.3 MT per year. Over the 25-year lease period, the projected fuel savings total 7,857.5 MT, underscoring the long-term economic and environmental benefits of implementing the optimization model.

Environmental impact of load optimization

The optimization model not only reduced fuel consumption but also contributed to a reduction in NOx and CO₂ emissions.

The most significant reduction was observed in the cargo unloading, where NOx emissions fell by 30.46% compared to an equal load distribution. Reductions of 11.87% and 4.70% were recorded for the loaded passage and the ballast passage respectively. Although the NOx reduction in the ballast passage was more moderate, it still shows a consistent positive trend across all regimes.

Interestingly, CO₂ emissions remained constant in three out of four operating regimes (loaded passage, ballast passage and loading) despite lower fuel consumption. However, during cargo unloading, CO₂ emissions fell from 5.6% to 5.4%, which indicates that optimizing loading in some operating modes can also contribute to a direct reduction in CO₂ emissions.

Long-term implications and relevance for industry

The results underline the practical applicability of the optimization model for LNG ships that are chartered on a long-term basis. The ability to consistently reduce fuel consumption and NOx emissions across all ship operating modes suggests that this model can be effectively integrated into real-world ship energy management strategies.

Given the increasing global focus on fuel efficiency and emissions reduction, the application of such an optimization approach is in line with regulatory requirements such as the IMO's Energy Efficiency Design Index (EEDI) and Carbon Intensity Indicator (CII).

In addition, the economic impact of reducing 7857.5 MT of fuel over a 25-year period represents a significant cost saving potential for ship owners and charterers, further underlining the benefits of load optimization in DFDE LNG propulsion systems.

In conclusion, this analysis confirms that optimizing engine load distribution in Dual-Fuel Diesel Electric (DFDE) propulsion systems significantly improves fuel efficiency and reduces emissions compared to conventional PMS. By applying this optimized approach, LNG vessels can achieve measurable fuel savings while complying with stricter environmental regulations.

Furthermore, the vessel analyzed in this study is part of a fleet of seven sister vessels, all operating under the same charter conditions. When considering the entire fleet, the potential fuel savings and emissions reductions increase significantly, highlighting the broader impact of optimizing utilization across vessels.

This study not only confirms the effectiveness of intelligent load balancing but also lays the foundation for future advances in energy management and ship sustainability.

5. EXERGY ASSESSMENT OF FUEL UTILISATION IN MARINE POWER PLANTS

In this chapter, a detailed exergy-based assessment is presented to complement the previously established energy and emissions optimization framework. Unlike conventional energy analysis, which considers only the quantity of energy, exergy analysis integrates the second law of thermodynamics to evaluate the quality and usability of energy flows. This approach enables a more rigorous quantification of system inefficiencies, irreversibility, and the true potential for optimization in dual-fuel diesel-electric (DFDE) marine power plants. The following sections outline the theoretical background, practical methodologies, and application of exergy principles to the fuels and combustion processes relevant to LNG propulsion systems.

5.1. FUEL EXERGY AND THERMODYNAMIC ASSESSMENT

Exergy is one of the fundamental concepts of thermodynamics. It enables a quantitative assessment of energy quality and the determination of the maximum available useful work that can be obtained from a particular system. In contrast to the classical approach, which focuses exclusively on energy quantities, exergy analysis takes energy quality into account through the second law of thermodynamics, which enables a more realistic perspective on energy processes and systems.

The concept of exergy is particularly important in fuel analysis, as it allows the thermodynamic potential of different energy sources to be accurately quantified. This analysis is of increasing importance in the context of growing demands for energy efficiency, sustainable development and the rational utilization of energy resources. As Dincer and Rosen [79] note, "Exergy analysis as it takes into account locations, types, and real magnitudes of wastes and loss of energy."

Exergy represents the maximum theoretical (available) work that can be achieved when a system interacts only with its environment and reaches a state of complete equilibrium with it (Bejan et al. [80]). In the context of fuels, this approach enables a deeper understanding of the chemical and physical processes that take place during combustion and the optimization of the entire energy chain from the primary source to the final application.

Energy analysis often deals with complex systems involving different forms of energy and multiple conversions. In such systems, traditional analysis based solely on the first law of

thermodynamics often does not provide an accurate picture for effective management and optimization. As highlighted by Kotas [81] and Szargut [82], exergy analysis enables the quantification of irreversibility and the identification of components with the greatest potential for improvement.

5.1.1. Comparison of energy and exergy concepts

Energy, as defined in the first law of thermodynamics, is a conserved quantity that can be transformed from one form to another but can never be destroyed. The first law can be expressed mathematically as follows:

$$dU = \delta Q - \delta W \tag{10}$$

where U is the internal energy of the system, Q is the heat exchange, and W is the work performed or consumed by the system. However, as Çengel and Boles [83] note, the first law provides no information about the quality of energy or the limitations that occur in energy conversion processes.

As described in [81] and [84], the total exergy of a system consists of kinetic, potential, physical (thermomechanical) and chemical components without taking into account the nuclear, magnetic and electrical contributions:

$$e_x = e_{x,kin} + e_{x,pot} + e_{x,ph} + e_{x,ch}$$
 (11)

The kinetic exergy is given by: $e_{x,kin} = \frac{c^2}{2}$, and the potential exergy by: $e_{x,pot} = g \cdot z$. These forms of energy are equal to their respective exergies, as both can be completely converted into work [84].

The physical exergy represents the available work that can be obtained when a system interacts with its environment and reaches a state of limited equilibrium (thermal and mechanical) through reversible processes [84]. The value of the physical exergy is calculated using the following expression:

$$e_{x,ph} = (h - h_0) - T_0(s - s_0)$$
(12)

where h and s are the specific enthalpy and the specific entropy respectively and T_0 is the temperature of the reference state. To determine the value of the physical exergy, it is necessary to define a reference condition, either $T_{\rm ref}$ and $p_{\rm ref}$ or the environmental conditions T_0 and p_0 , depending on the specific requirements of the calculation. The standard reference state is defined according to [82] at a temperature of $t_{\rm ref}$ = 25 °C ($T_{\rm ref}$ = 298.15 K) and a pressure of $t_{\rm ref}$ = 101,325 Pa.

The concept of chemical exergy refers to the available work that can be obtained when the working substance is brought from a restricted reference state (or environmental state) to the dead state. In this state, the working substance is thermally, mechanically and chemically (in terms of concentration) in complete equilibrium with its surroundings or reference environment [84]. The chemical exergy can be calculated using the following expression:

$$e_{x,ch} = \mathbb{R} \cdot T_{0/ref} \cdot \ln \frac{p_o}{p_{00}} \tag{13}$$

where \mathbb{R} is the universal gas constant, $T_{0/ref}$ is the environmental or reference temperature, p_i is the partial pressure of the working substance under consideration and p_{00} is the environmental or reference partial pressure of that substance as a component of the atmosphere.

The main difference between energy and exergy is that energy quantifies the quantity of energy in a system and cannot be destroyed (or degraded), whereas exergy quantifies the quality of that energy. This distinction is fundamental for several reasons, as explained in detail in [79] using the concept of energy degradation, i.e. energy destruction. In real (irreversible) processes, part of the exergy is effectively "destroyed", leading to an increase in entropy. This phenomenon can be quantified using the Gouy–Stodola theorem:

$$e_{x.destroyed} = T_0 \cdot s_{aen} \tag{14}$$

where is s_{gen} the entropy generated during the process.

Exergy is only fully preserved in reversible processes, whereas in irreversible processes some of the exergy is irretrievably lost. This can be expressed through the exergy balance:

$$e_{x,destroyed} = e_{x,input} - e_{x,output}$$
 (15)

Based on the two equations mentioned above, the destroyed exergy can be written as follows:

$$e_{x,destroyed} = e_{x,input} - e_{x,output} = T_0 \cdot s_{gen}$$
 (16)

5.2. EXERGY-BASED OPTIMIZATION OF ENERGY SYSTEMS

The application of exergy analysis in the optimization of energy systems offers an integrated approach that combines thermodynamic, economic and environmental aspects. As stated by Bejan et al [80], this methodology enables:

- Thermodynamic optimization reducing exergy losses through the optimal design and configuration of system components, which includes tasks such as sizing heat exchangers, selecting working fluids and determining optimal operating parameters.
- **Economic optimization** exergy can serve as the basis for a thermo-economic analysis where costs are allocated proportionally to exergy flows.
- Environmental optimization reducing exergy losses is often correlated with a reduction in emissions, particularly of harmful exhaust gases in this context.

5.3. EXERGY EFFICIENCY AND SECOND LAW THERMODYNAMICS

Exergy efficiency (ψ or η_{II}) is the ratio between the useful, obtained and utilized exergy at the output and the exergy supplied or input to the system. In contrast to energy efficiency, there are various ways of defining exergy efficiency depending on the purpose of the system, as described in [79]:

Universal definition:

$$\psi = \frac{E_{x,output \ in \ production}}{E_{x,input}} = 1 - \frac{E_{x,destruction}}{E_{x,input}}$$
(17)

Rational efficiency:

$$\psi_{ratio} = \frac{E_{x,output}}{E_{x,input}} = 1 - \frac{E_{x,consumption}}{E_{x,input}}$$
(18)

Task efficiency:

$$\psi_{ratio} = \frac{E_{x,min.required}}{E_{x,input}} \tag{19}$$

For heat engines:

$$\psi = \frac{P_{netto}}{E_x^Q} \tag{20}$$

Only the most basic exergy efficiencies are presented here, while [85] provides a range of expressions for the exergy efficiencies of thermodynamic processes.

5.4. METHODS FOR QUANTIFYING FUEL EXERGY

Fuel exergy is the maximum work that can be obtained from fuel when it is completely burnt in the presence of an oxidizer agent from the environment and the end products are brought into complete equilibrium with the environment considering the irreversibility inherent in the combustion process. According to Szargut [82], fuel exergy consists of chemical exergy and physical exergy. In most practical cases, the chemical exergy is the dominant component, while others are negligible.

5.4.1 Approximate exergy calculation method using the lower heating value (LHV)

A practical approach that has been developed is based on the ratio of the exergy and to the lower heating value of the fuel. These expressions allow a fast and sufficiently accurate calculation of the chemical exergy of the fuel based on the elemental analysis of the fuel.

Szargut proposed in [86] the following expression for liquid fuels (with C, H, O and S as compounds), for $\frac{o}{c}$ < 2:

$$\beta = \frac{ex_{ch}}{LHV} = 1.047 + 0.0154 \cdot \left(\frac{H}{C}\right) + 0.0562 \cdot \left(\frac{O}{C}\right) + 0.5904 \left(\frac{S}{C}\right) \left(1 - 0.175 \frac{H}{C}\right)$$
(21)

where H/C, O/C and S/C are the atomic ratios of hydrogen, oxygen and sulphur to carbon.

Kotas [80] proposed an expression for calculating the exergy of liquefied gases in which the composition of sulphur is taken into account, too:

$$\varphi = \frac{ex_{ch}}{LHV} = 1.0401 + 0.1728 \left(\frac{H}{C}\right) + 0.0432 \left(\frac{O}{C}\right) + 0.2169 \left(\frac{S}{C}\right) \left(1 - 3.0628 \left(\frac{H}{C}\right)\right)$$
(22)

and states that the accuracy of this expression is estimated at $\pm 0.38\%$.

In the same reference, Kotas provides φ values for industrial fuels. For natural gas, it is $\varphi = 1.04 \pm 0.5\%$, while for various fuel oils and gasoline, φ ranges from 1.04 to 1.08.

5.4.2 Stoichiometric combustion and fuel heating values

To determine the heating value of a fuel, it is necessary to define the reactants and the combustion products. In the theoretical view of combustion, the fuel is completely burnt using the stoichiometric amount of oxygen, i.e. air. The chemical reaction for the complete combustion of hydrocarbon is:

$$C_a H_b O_c + \left(a + \frac{b}{4} - \frac{c}{2} \right) O_2 \rightarrow a C O_2 + \left(\frac{b}{2} \right) H_2 0 \tag{23}$$

The stoichiometric amount of oxygen required for the combustion of fuels is calculated using the following expression:

$$n_{O_2} = \sum_{fuel} \left[\chi_{fuel} \cdot \left(N_{C,fuel} + \frac{N_{H,fuel}}{4} - \frac{N_{O,fuel}}{2} \right) \right] [kmol]$$
 (24)

where χ is the molar fraction of each fuel component and $N_{\rm C}$, $N_{\rm H}$ i $N_{\rm O}$ are the number of carbon, hydrogen and oxygen atoms in each fuel component, respectively. The amount of nitrogen contained in the air is given by $\frac{79}{21} \cdot n_{O_2}$.

In the fuel composition specified by the manufacturer, the mixture consists of: 99.82% methane (CH₄), 0.02% ethane (C₂H₆), and 0.16% nitrogen (N₂). The chemical reaction for complete combustion is:

$$0.9982 CH_4 + 0.0002 C_2H_6 + 0.0016 N_2 + 1.9971 \left(O_2 + \frac{79}{21} N_2 \right)$$

$$\rightarrow 0.9986 CO_2 + 1.997 H_2O + 7.5145 N_2.$$
(25)

Now that the reactants and combustion products have been defined, the heating values of the fuel can be calculated. Heating value of the fuel is defined as the amount of heat released when a fuel is burned completely and the products are returned to the state of the reactants. This is equal to the absolute value of the enthalpy of combustion of the fuel, h_C [83]:

$$HV = |h_c| = |H_{product} - H_{react}|$$

$$= |\sum n_{product} \cdot h_{f,product}^o - \sum n_{react} \cdot h_{f,react}^o|$$
(26)

where is h_f^o enthalpy of formation at standard reference state.

Using values from the literature [83], for the selected fuel, the lower heating value (LHV) is $801,142.414 \text{ kJ/kmol}_{\text{fuel}}$ (49,868.939 kJ/kg_{fuel}), and the higher heating value (HHV) is $889,018.402 \text{ kJ/kmol}_{\text{fuel}}$ (55,338.980 kJ/kg_{fuel}). If condensed water vapor at the reference temperature and pressure ($T_{\text{ref}} \text{ i} p_{\text{ref}}$) is taken into account, the heating value of the fuel amounts to $876,755.497 \text{ kJ/kmol}_{\text{fuel}}$ (54,575.648 kJ/kg_{fuel}). This value is between the LHV and HHV because part of water remains as vapor, determined by its saturation pressure at 25 °C, while the rest is condensed. The declared higher heating value of the fuel, according to the analysis (fuel specification), is $55,418.6 \text{ kJ/kg}_{\text{fuel}}$, which deviates by 0.144% from the calculated higher heating value.

Once the lower heating value of the fuel has been determined, the approximate standard chemical exergy of the fuel can be calculated using the expression from [81].

$$\varphi \cdot LHV = 1.04 \cdot 801,142.414 = 833,188.111 \frac{kJ}{kmol_{fuel}}$$
 (27)

5.4.3 Standard chemical exergy

The standard chemical exergy of the fuel will be determined using the Gibbs energy of formation. This approach is presented in [79], [82] and [81].

The balance of the reactants and combustion products is represented by the relation [85]:

$$\sum_{reakt} \Delta G_{f,react}^{0} - \sum_{react} n_{reakct} \cdot \bar{e}_{ch,react} =$$

$$= \sum_{product} \Delta G_{f,product}^{0} - \sum_{product} n_{product} \cdot \bar{e}_{ch,product}$$
(28)

where ΔG_f^0 is the Gibbs function of the formation, \bar{e}_{ch} is the standard chemical exergy and n is the molar amount of reactants and products in the stoichiometric mixture.

Based on the given relation, the standard chemical exergy of the fuel is calculated using the following equation:

$$\bar{e}_{ch,fuel} = \sum_{react} n_{react} \cdot \Delta G_{f,react}^{0} - \sum_{\substack{reactants \\ except \ fuel}} n_{i} \cdot \bar{e}_{ch,i}$$

$$- \sum_{product} n_{product} \cdot \Delta g G_{f,product}^{0}$$

$$+ \sum_{product} n_{product} \cdot \bar{e}_{ch,product} \left[\frac{kJ}{kmol_{fuel}} \right]$$
(29)

By using the values from tables [83] and [88] into the given expression, the standard chemical exergy of the fuel is:

$$\bar{e}_{ch,fuel} = [0.9982 \cdot (-50,790) + 0.0002 \cdot (-32,890)]$$

$$- [1.9971 \cdot 3,970 + 7.5145 \cdot 720]$$

$$- [0.9986 \cdot (-394,380) + 1.997 \cdot (-228,590) + 7.5145 \cdot 0]$$

$$+ [0.9986 \cdot 19,870 + 1.997 \cdot 9,485 + 7.5145 \cdot 720]$$
(30)

$$=830,472.182 \frac{kJ}{kmol_{fuel}}$$

The deviation of the standard chemical exergy of the fuel obtained using the approximate exergy calculation method (by correlation factor φ) is

$$\frac{833,188.111 - 830,472.182}{830,472.182} = 0.003270 \ (0.3270 \%)$$
 (31)

Since no heat or work exchange occurs during the process of delivering the fuel to the combustion chamber or during combustion itself, the sum of the stated exergies must equal the total exergy of the reactants [84].

Since the reactants are initially in equilibrium with the environment, the physical (thermomechanical) exergy is zero, and both the kinetic and potential energy are also zero. Therefore, the total exergy corresponds to the chemical exergy of the reactants and the exergy loss due to the mixing of fuel and air:

$$e_{x,reactants} = \sum_{react} \chi_{react} \cdot \bar{e}_{ch,react} + \mathbb{R} \cdot T_0 \cdot \sum_{react} \chi_{react} \cdot ln(\gamma_{react} \cdot \chi_{react}) =$$

$$= \sum_{fuel} \chi_{fuel} \cdot \bar{e}_{ch,fuel} + \sum_{air} \chi_{air} \cdot \bar{e}_{ch,air} + \mathbb{R} \cdot T_0$$

$$\cdot \sum_{react} \chi_{react} \cdot ln(\gamma_{react} \cdot \chi_{react}) \left[\frac{kJ}{kmol_{product}} \right]$$
(32)

where γ_{react} is the activity coefficient, which is equal to one for ideal mixtures. By substituting the values into the given expression, the exergy of the reactants amounts to $823,475.498 \text{ kJ/kmol}_{\text{fuel}}$ (78,351.617 kJ/kg_{fuel}).

The next step is to determine the exergy of the combustion products. To do this, it is necessary to calculate the adiabatic flame temperature. The adiabatic flame temperature is determined under the condition of enthalpy equality between the reactants and the combustion products, i.e. when no heat or work is exchanged in the observed system:

$$H_{react} = H_{product} (33)$$

By expanding the given expression, the following is obtained:

$$\sum n_{react} \cdot (\bar{h}_f^0 + \bar{h} - \bar{h}^0)_{react} = \sum N_{product} \cdot (\bar{h}_f^0 + \bar{h} - \bar{h}^0)_{product}$$
(34)

where \bar{h}_f^0 is the enthalpy of formation at the reference state, and $\bar{h} - \bar{h}^0$ represents the deviation of the specific enthalpy of the combustion products from the reference state, i.e., from the combustion temperature to the reference temperature. For the reactants, this deviation is equal to zero (as they enter the system at 25 °C), while for the combustion gases, it is used to determine the adiabatic flame temperature.

The left and right sides of the equation will be equal at a combustion product temperature of 2,053.167 °C, which represents the adiabatic flame temperature.

When determining the exergy of the combustion products, the dissociation of the combustion products caused by high temperatures is neglected and it is assumed that the chemical composition does not change during cooling to the reference temperature, i.e. that no reverse reaction of the combustion products occurs (e.g. $CO_2 \rightarrow CO + \frac{1}{2}O_2$).

Using the data from Table 5.1 at the adiabatic combustion temperature and the reference temperature, the physical exergy of the products (exhaust gases), based on the stated assumptions, amounts is 577,552.556 kJ/kmol_{fuel} (35,951.078 kJ/kg_{fuel}), while the chemical exergy of the products (exhaust gases) is 23,897.663 kJ/kmol_{fuel} (1,487.565 kJ/kg_{fuel}). The exergy destroyed (irreversibility) is 227,086.393 kJ/kmol_{fuel} (14,135.511 kJ/kg_{fuel}). The sum of these exergies is 828,536.612 kJ/kmol_{fuel} (78,832.419 kJ/kg_{fuel}).

Table 5.1 Values for the calculation of the physical exergy of combustion products [83]

	T_{ad}			T_0			
	$n_{\rm i}$	$ar{h}-ar{h}^0$	S	$\Delta s(T_{ad},p_i/p_0)$	$n_{\rm i}$	S ₀	$\Delta s(T_0,p_i/p_0)$
	$\left(\frac{kmol}{kmol_{fuel}}\right)$	$\left(\frac{kJ}{kmol}\right)$	$\left(\frac{kJ}{kmol \cdot K}\right)$	$\left(\frac{kJ}{kmol \cdot K}\right)$	$\left(\frac{kmol}{kmol_{fuel}}\right)$	$\left(\frac{kJ}{kmol \cdot K}\right)$	$\left(\frac{kJ}{kmol \cdot K}\right)$
CO ₂	0.9986	111,268.88	318.42	-19.57	0.9986	213.79	-18.09
H ₂ O _(g)	1.997	89, 832.25	272.61	-13.81	0.2787	188.84	-28.70
H ₂ O _(l)	0	/	/	/	1.7183	69.95	/
N ₂	7.5145	67, 953.20	257.52	-2.79	7.5145	191.61	-1.31

If the exergy of the reactants is compared with the exergy of the combustion products, including the destroyed exergy, the difference is 0.615%.

5.5. CARBON DIOXIDE EMISSIONS IN THE CONTEXT OF EXERGY AND REGULATIONS

According to the IMO guidelines for calculating the achieved energy efficiency index (EEDI) for new ships [88], the conversion factor between CO₂ emissions and fuel consumption is $2.750 \frac{t_{CO_2}}{t_{fuel}}$ for methane and $2.927 \frac{t_{CO_2}}{t_{fuel}}$ for ethane. For the specified fuel composition, the conversion factor between CO₂ emissions and fuel consumption is:

$$C_{F'} = \frac{n_{co_2,product} \cdot M_{Co_2}}{\sum_{fuel} (\chi \cdot M)_{fuel}}$$

$$= \frac{0.9986 \cdot 44.0095}{0.9982 \cdot 16.0425 + 0.0002 \cdot 30.0690 + 0.0016 \cdot 28.0134}$$

$$= 2.736 \frac{t_{Co_2}}{t_{fuel}}.$$
(35)

Taking into account that the average daily fuel consumption of the observed ship is around 120 tons of fuel, this results in a reduction in exhaust emissions of: $(2.750 - 2.736) \times 120 = 1.68$ tons CO₂/day.

If exhaust gas emissions are expressed per unit of fuel heating value, this is more relevant than if they are expressed per unit of fuel mass. In particular, when CO₂ emissions are analyzed per kilogram of fuel consumed, this can lead to a false advantage for low energy fuels, such as methanol, as a greater mass must be consumed to produce the same amount of energy.

According to the IMO guidelines [89], the lower heating value for LNG is 48,000 kJ/kg_{fuel}. In contrast, Regulation (EU) 2023/1805 [90] specifies a value of 49,100 kJ/kg_{fuel}, while the calculated value based on the actual fuel composition is 49,868.939 kJ/kg_{fuel}. There is a notable difference between the IMO guideline and the EU regulation: 1,100 kJ/kg_{fuel}, which corresponds to a deviation of 2.292%.

Table 5.2 shows the values of CO₂ emissions per mass and per lower heating value of the fuel from the sources listed.

Table 5.2 Heating values and carbon dioxide emissions

	LHV	$C_{\rm F}\left[\frac{t_{CO_2}}{t_{fuel}}\right]$	$CO_2 \left[\frac{g_{CO_2}}{MJ_{fuel}} \right]$	
	[kJ/kg _{fuel}]	[^t fuel]	[M] fuel]	
IMO [11]	48,000.000	2.750	57.292	
Regulation (EU)	49,100.000	2.750	56.008	
2023/1805 [12]				
This study	49,868.939	2.736	54.864	

Furthermore, if exhaust gas emissions are expressed per unit of their exergy, according to the calculation derived, the value is:

$$\frac{2736}{37.439} = 73.079 \; \frac{g_{CO_2}}{MJ}.$$

Stating CO₂ emissions per unit of energy consumed rather than per unit of mass of fuel allows for a fairer and more energy-relevant comparison between different fuels, especially when their heating values vary. This approach avoids the potential false advantage of fuels with lower energy content, such as methanol, and ensures compliance with international standards and regulations (IMO, FuelEU).

The analysis of the specific fuel blend has shown that the CO₂ emissions are lower than the reference values and that, when expressed per heating value, they provide a more realistic representation of fuel efficiency.

5.6. HEAT UTILIZATION IN HEAT ENGINES

According to [91], the power that can be obtained from a system with reactants at the inlet and combustion products at the outlet of the observed system is:

$$W = H_{react} - H_{product} - T_0 \cdot (S_{react} - S_{product}) - T_0 \cdot S_{gen} =$$

$$= B_{react} - B_{product} - T_0 \cdot S_{gen}$$
(36)

where *B* represents the work potential of the flow working fluid, i.e., of the reactants or combustion products.

The power W that can be obtained per kmol of fuel from such a system cannot exceed $B_{reakt} - B_{produkt}$, which implies that in this case $S_{gen} = 0$, and thus:

$$W_{rev} = B_{react} - B_{product} \ge W. \tag{37}$$

In the specific case where the reactants and combustion products are in the reference state, the performance of the reversible process is

$$W_{rev} = \sum_{i=1}^{m} \nu_{react,i} \cdot (\bar{h} - T_0 \cdot \bar{s})_{0,react,i}$$

$$- \sum_{i=1}^{n} \nu_{product,i} \cdot (\bar{h} - T_0 \cdot \bar{s})_{0,product,j}$$
(38)

where $(\bar{h} - T_0 \cdot \bar{s})$ is the Gibbs free energy of the reactants and combustion products at the mixture temperature and pressure T_0 i p_0 .

The case under consideration refers to the use of combustion products not inside the engine cylinder itself, but as a heat source for a Carnot engine, as shown in Figure 5.1 [91].

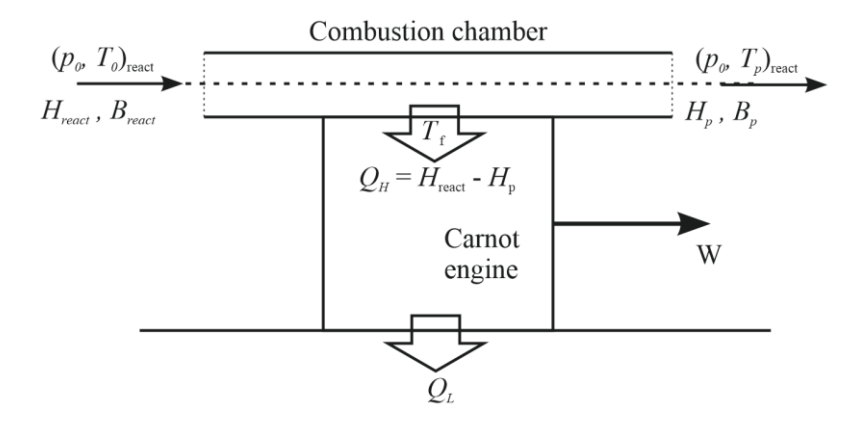


Figure 5.1 Use of combustion products as a heat source for a Carnot engine

If Figure 5.1 is observed, the Carnot engine is inserted into the system to utilized heat of combustion gases into work. The irreversibility, I, mathematically defined as $W_{\text{rev}} - W$, is caused by the combustion chamber in this configuration. The Carnot engine receives the heat $H_{\text{react}} - H_{\text{product}}$, and converts it into work W (which is equal to W_{rev} when I is equal to 0) and rejects heat to environmental $I_{\underline{0}}$. The temperature at which the combustion products transfer heat to the Carnot engine is defined as *effective flame temperature*, T_f , and the work W is [90]:

$$W = \left(H_{react} - H_{product, T_f}\right) \cdot \left(1 - \frac{T_0}{T_f}\right) \tag{39}$$

where $H_{\text{react}} - H_{\text{product}}$ is the heat transferred to the Carnot engine at the temperature T_f . Efficiency according to the second law can now be determined by considering only the combustion chamber:

$$\eta_{II} = \frac{P}{P_{rev}} = \frac{\left(H_{react} - H_{product, T_f}\right)}{\left(B_{react} - B_{product, T_f}\right)} \cdot \left(1 - \frac{T_0}{T_f}\right)$$

$$\tag{40}$$

 H_{react} and B_{react} are constant values at T_0 , while $H_{product}$ and $B_{product}$ is function of effective flame temperature.

The heat flow transferred by the combustion products to the Carnot engine is $\left(H_{product}\right)_{T_{af},p_0} - \left(H_{product}\right)_{T_{f},p_0}$, which is also equal to $\left(H_{react}\right)_{T_{0},p_0} - \left(H_{product}\right)_{T_{f},p_0}$.

In Figure 5.2, the enthalpy of the combustion products is represented by the orange line, while the blue line represents the heat flow that is extracted from the combustion chamber so that the temperature of the combustion products at the outlet corresponds to the temperature indicated on the x-axis.

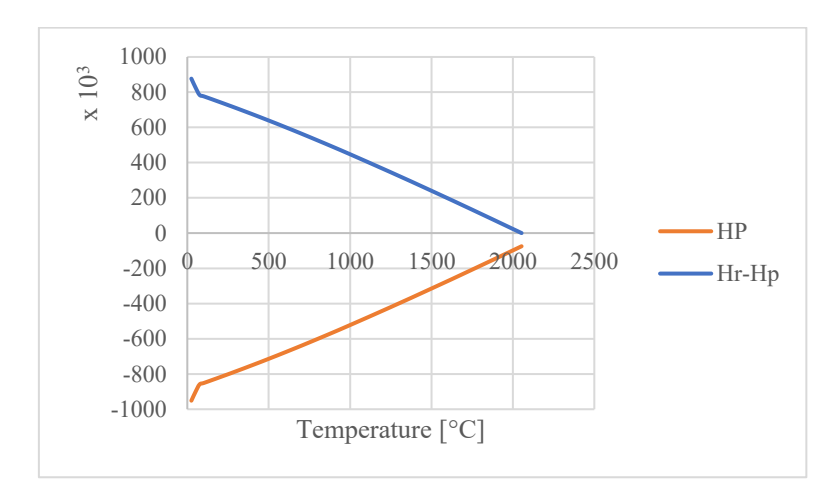


Figure 5.2 Enthalpy of combustion products and heat extraction compared to temperature

Since the enthalpy of the combustion products is almost linear from 100 °C to the adiabatic flame temperature, expression can be written as follows:

$$W = K(T_{ad} - T_f) \cdot \left(1 - \frac{T_0}{T_f}\right). \tag{41}$$

If we derive the function obtained with respect to $T_{\rm f}$ and set it equal to zero, we obtain the temperature at which the Carnot engine produces the maximum work, i.e. the temperature to which the combustion products must be cooled from the adiabatic flame temperature so that the heat transferred to the Carnot engine produces the highest possible work:

$$\frac{d}{dT_f} \left[K(T_{ad} - T_f) \cdot \left(1 - \frac{T_0}{T_f} \right) \right] = K \cdot \left(+ T_{ad} \cdot \frac{T_0}{T_f^2} - 1 \right) = 0, \tag{42}$$

from which the following is obtained: $T_f = (T_{ad} \cdot T_0)^{\frac{1}{2}}$.

According to the above expression, $T_{\rm f} = 832.612$ K, and the maximum available work is 396,365.835 kJ/kmol_{fuel}. This calculation defines the effective temperature of the gases at the outlet of the system after the heat has been transferred to the Carnot engine. This example shows that by using a heat exchanger, a significant part of the chemical exergy (38.36%) is destroyed, the usable (conserved) part of the exergy is 13.76%, while 47.88% of the chemical exergy of the fuel is converted into work by the heat engine. This analysis underlines the importance of the exergy approach for the optimization of energy systems and the precise quantification of the potential of fuels.

6. EXPECTED SCIENTIFIC CONTRIBUTION

This doctoral thesis presents a scientifically sound and practically validated approach to improving fuel efficiency and reducing emissions in dual-fuel diesel-electric (DFDE) power plants. Its contribution is not only to propose a theoretical optimization model, but also to prove its operational effectiveness by validating it in practice on an LNG tanker. The following points summarize the main scientific contributions of the dissertation:

- Development of a fuel- and emission-based model to optimize load distribution.
- The study presents a novel optimization model that dynamically distributes electrical load to DFDE generator engines based on real-time operating requirements, fuel type, and engine-specific efficiency curves. In contrast to conventional PMS, which distribute loads evenly regardless of efficiency and emissions, the proposed model integrates both economic (SFOC) and environmental (NOx, CO₂) parameters into its decision framework. This multidimensional approach contributes to advancing the theory of ocean energy system optimization.
- Integration of real-world measurement data into model development and validation.

A significant scientific contribution lies in the use of empirical data collected from an operating LNG vessel. The measurements included fuel flow rates and exhaust emissions under different loads and operating modes. This data was used both as input and to validate the model, ensuring its applicability in real marine environments. The methodological rigor applied in the development, calibration and testing of the model reflects a high degree of scientific reliability.

• Demonstration of operational gains through intelligent load allocation.

The optimization model consistently outperformed standard PMS-driven load balancing across a wide range of operating conditions and achieved measurable improvements. These results demonstrate the feasibility and benefits of implementing intelligent data-driven load sharing strategies on LNG tankers and form the basis for future integration into ship automation systems.

• Contribution to sustainable maritime technology and regulatory compliance.

By aligning the optimization strategy with international emissions regulations such as MARPOL Annex VI, the Energy Efficiency Existing Ship Index (EEXI) and the Carbon Intensity Indicator (CII), this research provides a pathway to compliance that also improves operational efficiency. The results contribute to global efforts to decarbonize the shipping

industry and provide engineers and policy makers with a practical solution to reduce the environmental impact of shipping.

• Promoting multidisciplinary research in the field of marine technology.

This dissertation bridges multiple disciplines, ocean engineering, environmental science, systems automation, thermodynamics and computational optimization. It provides a new methodology for integrating these disciplines into a coherent and practicable model for onboard energy management. As such, it provides a reproducible framework for similar studies on alternative fuels, propulsion types and hybrid marine systems.

In summary, the scientific contribution of this dissertation lies both in the novelty of the optimization model developed and in its successful validation in an operational marine environment. By focusing on the intelligent redistribution of engine loads based on fuel and emissions performance, the research fills a critical gap in existing PMS logic. The results provide a scalable, regulatory-aligned and scientifically validated solution to improve both the economic and environmental performance of modern LNG-powered vessels.

7. CONCLUSION

This dissertation has tackled a critical challenge in modern marine engineering: the inefficiency of Power Management Systems (PMS) in optimizing fuel consumption and emissions in LNG carriers powered by Dual-Fuel Diesel-Electric (DFDE) power propulsion. With tightening international regulations and a growing emphasis on environmental sustainability in the maritime industry, improving operational efficiency is no longer optional but a strategic imperative.

At the core of this research lies the development of a tailored optimization model that reallocates engine loads dynamically, considering both fuel efficiency and exhaust emissions. Through a combination of simulator analysis, real-world measurements, and MATLAB-based modeling, the dissertation provides compelling evidence that intelligent load distribution can lead to measurable reductions in fuel consumption and NOx emissions.

This research has achieved its objectives by critically examining the limitations of standard PMS-based load distribution, particularly under variable engine loads and differing fuel types. A fuel-based optimization model was created using spline-interpolated SFOC data, and its effectiveness was validated through both simulated and real-world operational data. The model was then extended into a multi-criteria framework that incorporates NOx emissions, allowing flexible prioritization between fuel efficiency and environmental goals. The algorithms were validated onboard a working LNG carrier, demonstrating their reliability and confirming their real-world applicability. The quantifiable benefits, including fuel savings of up to 5% and reductions in harmful emissions, were verified across various engine configurations and vessel operating modes.

In addition, an exergy-based assessment was introduced to deepen the thermodynamic analysis and emphasize potential efficiency improvements by considering the quality and not just the quantity of energy conversion of fuels.

The scientific and engineering contributions of this dissertation are multifaceted. Methodologically, the integration of spline interpolation into an optimization framework tailored for DFDE systems presents a novel approach. Technologically, the model is designed for integration with existing shipboard energy management systems, enabling immediate application without hardware changes. Empirically, the study enriches literature by providing real-world data and analysis on DFDE engine performance. From a regulatory perspective, the

findings support compliance with IMO standards such as MARPOL Annex VI, the Energy Efficiency Existing Ship Index (EEXI), and the Carbon Intensity Indicator (CII).

Beyond academia, this research has broader implications for various stakeholders. Engineers and operators are provided with actionable strategies to reduce fuel consumption and emissions. System designers and integrators can use the findings to enhance PMS logic or develop smarter, semi-autonomous energy systems. Policy makers may find value in the empirical basis provided for shaping emission-reduction regulations. The work contributes directly to global decarbonization efforts in maritime transport by offering a practical method to link operational decisions with emissions outcomes.

However, the study has several limitations. Environmental factors such as sea state and ambient conditions were not incorporated, which could affect engine behavior. Economic considerations, including fuel pricing and cost-benefit analysis, were not part of the model's scope but would be essential for implementation at scale. Long-term engine degradation and maintenance patterns, which may alter optimal load points over time, were also excluded. Furthermore, the model's scalability to more complex hybrid systems involving batteries or renewables remains to be tested.

Future research should explore the integration of this optimization model into real-time automation platforms, enabling dynamic adjustment of load distribution based on live operational data. Machine learning could enhance this framework by enabling predictive load optimization based on historical performance and routing data. Incorporating weather routing and sea condition data could further improve fuel efficiency. There is also strong potential to extend this research to hybrid marine energy systems that include batteries, fuel cells, or shore power. Additionally, exploring how crew interact with these optimization tools may yield insights that improve usability and adoption in mixed-automation environments.

In conclusion, this dissertation presents a scientifically grounded, empirically validated, and practically relevant framework for optimizing energy use in LNG marine power plants. It demonstrates that substantial efficiency gains and emissions reductions are achievable through improved software logic and strategic engine load management, without requiring hardware modifications. This work not only addresses an immediate operational challenge but also contributes meaningfully to the maritime sector's broader goals of sustainability and regulatory compliance.

LITERATURE

- [1] S. Martinić-Cezar, K. Bratić, M. Slišković, and N. Račić, "Exhaust emissions from marine 4-stroke engine on the three fuel types," in Proc. 2nd Int. Conf. Maritime Sci. Technol. (Naše More 2021), D. Mišković, Ed. Dubrovnik, Croatia: Maritime Dept., Univ. of Dubrovnik, 2021, pp. 227–241.
- [2] S. Martinić-Cezar, K. Bratić, Z. Jurić, and N. Račić, "Exhaust emissions reduction and fuel consumption from the LNG energy system depending on the ship operating modes," Pomorstvo Sci. J. Maritime Res., vol. 36, no. 2, pp. 338–346, 2022. doi: 10.31217/p.36.2.17
- [3] S. Martinić-Cezar, Z. Jurić, N. Assani, and B. Lalić, "Optimization of fuel consumption by controlling the load distribution between engines in an LNG ship electric propulsion plant," Energies, vol. 17, no. 15, p. 3718, 2024. doi: 10.3390/en17153718
- [4] S. Martinić-Cezar, Z. Jurić, N. Assani, and N. Račić, "Controlling engine load distribution in LNG ship propulsion systems to optimize gas emissions and fuel consumption," Energies, vol. 18, no. 3, pp. 485–506, 2025. doi: 10.3390/en18030485
- [5] International Maritime Organization. (2008, Oct. 10). MEPC.177(58): Amendments to the Technical Code on Control of Emission of Nitrogen Oxides from Marine Diesel Engines (NOx Technical Code 2008) [Online]. Available: https://www.cdn.imo.org/localresources/en/KnowledgeCentre/IndexofIMOResolutions/MEPCDocuments/MEPC.177%2858%29.pdf (accessed on 22 November 2024).
- [6] Wärtsilä Corporation. (2017). Wärtsilä 50DF Dual-Fuel Engine [Online]. Available: https://www.wartsila.com/energy/solutions/engine-power-plants/wartsila-50df-dual-fuel-engine (accessed on 15 December 2024))
- [7] MAN Energy Solutions SE. (2019, Feb. 25). MAN 51/60DF IMO Tier II / IMO Tier III,

 Project Guide Marine [Online]. Available: https://pdfcoffee.com/man-51-60df-imo-tier-iii-marine-pdf-pdf-free.html (accessed on 22 November 2024).)
- [8] T. R. Walker, O. Adebambo, M. C. Del Aguila Feijoo, E. Elhaimer, T. Hossain, S. J. Edwards, C. E. Morrison, J. Romo, N. Sharma, S. Taylor, *et al.*, "Environmental effects of marine transportation," in World Seas: An Environmental Evaluation, 2nd ed., Amsterdam, The Netherlands: Elsevier, 2018, pp. 505–530.

- [9] International Maritime Organization, "Low carbon shipping and air pollution control," [Online]. Available: http://www.imo.org/en/MediaCentre/HotTopics/GHG/Pages/default.aspx. [Accessed: Mar. 11, 2019].
- [10] L. Sastre Buades, "Implementation of LNG as marine fuel in current vessels: Perspectives and improvements on their environmental efficiency," M.S. thesis, Dept. of Nautical Sci. and Eng., Universitat Politècnica de Catalunya, Barcelona, Spain, 2017.
- [11] J. Kackur, "Shipping in the 2020 era—Selection of fuel and propulsion machinery—Business white paper," Wärtsilä, Helsinki, Finland, 2018.
- [12] I. A. Fernández, M. R. Gómez, J. R. Gómez, and A. B. Insua, "Review of propulsion systems on LNG carriers," Renew. Sustain. Energy Rev., vol. 67, pp. 1395–1411, 2017.
- [13] V. Mrzljak, P. Blecich, N. Anđelić, and I. Lorencin, "Energy and exergy analyses of forced draft fan for marine steam propulsion system during load change," J. Mar. Sci. Eng., vol. 7, p. 381, 2019.
- [14] V. Mrzljak, I. Poljak, and T. Mrakovčić, "Energy and exergy analysis of the turbogenerators and steam turbine for the main feed water pump drive on LNG carrier," Energy Convers. Manag., vol. 140, pp. 307–323, 2017.
- [15] Z. Chen, F. Zhang, B. Xu, Q. Zhang, and J. Liu, "Influence of methane content on a LNG heavy-duty engine with high compression ratio," Energy, vol. 128, pp. 329–336, 2017.
- [16] Z. Chen, B. Xu, F. Zhang, and J. Liu, "Quantitative research on thermodynamic process and efficiency of a LNG heavy-duty engine with high compression ratio and hydrogen enrichment," Appl. Therm. Eng., vol. 125, pp. 1103–1113, 2017.
- [17] T. Senčić, V. Mrzljak, P. Blecich, and I. Bonefačić, "2D CFD simulation of water injection strategies in a large marine engine," J. Mar. Sci. Eng., vol. 7, p. 296, 2019.
- [18] D. Dobrota, B. Lalić, and I. Komar, "Problem of boil-off in LNG supply chain," Trans. Marit. Sci., vol. 2, pp. 91–100, 2013.
- [19] J. Romero Gómez, M. Romero Gómez, J. Lopez Bernal, and A. Baaliña Insua, "Analysis and efficiency enhancement of a boil-off gas reliquefaction system with cascade cycle on board LNG carriers," Energy Convers. Manag., vol. 94, pp. 261–274, 2015.
- [20] D. Chang, T. Rhee, K. Nam, K. Chang, D. Lee, and S. Jeong, "A study on availability and safety of new propulsion systems for LNG carriers," Reliab. Eng. Syst. Saf., vol. 93, no. 12, pp. 1877–1885, 2008.

- [21] E. W. Lemmon, M. L. Huber, and M. O. McLinden, *NIST Reference Fluid Thermodynamic and Transport Properties REFPROP, Version 8.0*, Boulder, CO, USA: National Institute of Standards and Technology, 2007.
- [22] Y. H. Yu, B. G. Kim, and D. G. Lee, "Cryogenic reliability of the sandwich insulation board for LNG ship," Compos. Struct., vol. 95, pp. 547–556, 2013.
- [23] M. Miana, R. del Hoyo, V. Rodrigálvarez, J. R. Valdés, and R. Llorens, "Calculation models for prediction of liquefied natural gas (LNG) ageing during ship transportation," Appl. Energy, vol. 87, no. 5, pp. 1687–1700, 2010.
- [24] D. Chang, T. Rhee, K. Nam, S. Lee, B. Kwak, and J. Ha, "Economic evaluation of propulsion systems for LNG carriers: A comparative life cycle cost approach," Hydrocarb. Asia, vol. 18, no. 2, pp. 22–40, 2008.
- [25] Y. Shin and Y. P. Lee, "Design of a boil-off natural gas reliquefaction control system for LNG carriers," Appl. Energy, vol. 86, no. 1, pp. 37–44, 2009.
- [26] R. Gilmore, S. Hatzigrigoris, S. Mavrakis, A. Spertos, and A. Vordonis, "LNG carrier alternative propulsion systems," presented at SNAME Greek Section Meeting, Athens, Greece, Feb. 2005.
- [27] D. Yeo, B. Ahn, J. Kim, and I. Kim, "Propulsion alternatives for modern LNG carriers," in Proc. 15th Int. Conf. and Exhibition on Liquefied Natural Gas (LNG 15), Gas Technology Institute, vol. 15, 2007, pp. 620–635.
- [28] MAN Energy Solutions, *ME-GI Dual Fuel MAN B&W Engines: A Technical, Operational and Cost-Effective Solution for Ships Fuelled by Gas*, [Online]. Available: http://goo.gl/caO0k1. [Accessed: Mar. 28, 2015].
- [29] Wärtsilä Corporation, "Wärtsilä official website," [Online]. Available: https://www.wartsila.com. [Accessed: Jun. 16, 2015].
- [30] MAN Energy Solutions, "Marine engines and systems," [Online]. Available: https://marine.man-es.com. [Accessed: Jun. 29, 2015].
- [31] Mitsubishi Heavy Industries, "Official website," [Online]. Available: https://www.mhi.com. [Accessed: Jul. 31, 2015].
- [32] Samsung Techwin, "Official website," [Online]. Available: http://www.samsungtechwin.com. [Accessed: Jul. 26, 2015].
- [33] R. Zaccone, U. Campora, and M. Martelli, "Optimization of a diesel-electric ship propulsion and power generation system using a genetic algorithm," J. Mar. Sci. Eng., vol. 9, p. 587, 2021. doi: 10.3390/jmse9060587

- [34] P. Xie, J. M. Guerrero, S. Tan, N. Bazmohammadi, J. C. Vasquez, M. Mehrzadi, and Y. Al-Turki, "Optimization-based power and energy management system in shipboard microgrid: A review," IEEE Syst. J., vol. 16, pp. 578–590, 2022. doi: 10.1109/JSYST.2020.3047673
- [35] A. Carlsen, "Diesel-electric generator load optimization," M.S. thesis, Dept. of Marine Technology, Norwegian Univ. of Science and Technology, Trondheim, Norway, 2014.
- [36] F. D. Kanellos, G. J. Tsekouras, and N. D. Hatziargyriou, "Optimal demand-side management and power generation scheduling in an all-electric ship," IEEE Trans. Sustain. Energy, vol. 5, pp. 1166–1175, 2014. doi: 10.1109/TSTE.2014.2336973
- [37] F. D. Kanellos, J. M. Prousalidis, and G. J. Tsekouras, "Control system for fuel consumption minimization—gas emission limitation of full electric propulsion ship power systems," Proc. Inst. Mech. Eng. Part M J. Eng. Marit. Environ., vol. 228, pp. 17–28, 2014. doi: 10.1177/1475090212466523
- [38] F. D. Kanellos, A. Anvari-Moghaddam, and J. M. Guerrero, "A cost-effective and emission-aware power management system for ships with integrated full electric propulsion," Electr. Power Syst. Res., vol. 150, pp. 63–75, 2017. doi: 10.1016/j.epsr.2017.05.003
- [39] J. V. Knudsen, "Modeling, control, and optimization for diesel-driven generator sets," Ph.D. dissertation, Dept. of Energy Technology, Aalborg Univ., Aalborg, Denmark, 2017. doi: 10.5278/vbn.phd.tech.00032
- [40] J. Knudsen, J. Bendtsen, P. Andersen, K. Madsen, C. Sterregaard, and A. Rossiter, "Fuel optimization in multiple diesel driven generator power plants," in Proc. 2017 IEEE Conf. Control Technol. Appl. (CCTA), Kohala Coast, HI, USA, Aug. 27–30, 2017, pp. 493–498.
- [41] S. Solem, K. Fagerholt, S. O. Erikstad, and Ø. Patricksson, "Optimization of diesel electric machinery system configuration in conceptual ship design," J. Mar. Sci. Technol., vol. 20, pp. 406–416, 2015. doi: 10.1007/s00773-015-0307-4
- [42] M. Frisk, "On-ship power management and voyage planning interaction," M.S. thesis, Dept. of Engineering Sciences, Uppsala Univ., Uppsala, Sweden, 2015.
- [43] P. Michalopoulos, F. D. Kanellos, G. J. Tsekouras, and J. M. Prousalidis, "A method for optimal operation of complex ship power systems employing shaft electric machines," IEEE Trans. Transp. Electrif., vol. 2, pp. 547–557, 2016. doi: 10.1109/TTE.2016.2572093

- [44] C. Nuchturee, T. Li, and H. Xia, "Design of cost-effective and emission-aware power plant system for integrated electric propulsion ships," J. Mar. Sci. Eng., vol. 9, p. 684, 2021. doi: 10.3390/jmse9070684
- [45] F. Baldi, F. Ahlgren, F. Melino, C. Gabrielii, and K. Andersson, "Optimal load allocation of complex ship power plants," Energy Convers. Manag., vol. 124, pp. 344–356, 2016. doi: 10.1016/j.enconman.2016.07.009
- [46] K. Yiğit, "Examining the effect of generator load sharing practices on greenhouse gas emissions for a ship," Konya J. Eng. Sci., vol. 10, pp. 301–311, 2022. doi: 10.36306/konjes.1056500
- [47] Y. C. Shih, Y. A. Tzeng, C. W. Cheng, and C. H. Huang, "Speed and fuel ratio optimization for a dual-fuel ship to minimize its carbon emissions and cost," J. Mar. Sci. Eng., vol. 11, p. 758, 2023. doi: 10.3390/jmse11040758
- [48] B. Pang, S. Liu, H. Zhu, Y. Feng, and Z. Dong, "Real-time optimal control of an LNG-fueled hybrid electric ship considering battery degradations," Energy, vol. 296, p. 131170, 2024. doi: 10.1016/j.energy.2024.131170
- [49] B. Zhang, Y. Jiang, and Y. Chen, "Research on calibration, economy and PM emissions of a marine LNG-diesel dual-fuel engine," J. Mar. Sci. Eng., vol. 10, p. 239, 2022. doi: 10.3390/jmse10020239
- [50] Y. Cong, H. Gan, H. Wang, G. Hu, and Y. Liu, "Multiobjective optimization of the performance and emissions of a large low-speed dual-fuel marine engine based on Mnlr-Mopso," J. Mar. Sci. Eng., vol. 9, p. 1170, 2021. doi: 10.3390/jmse9111170
- [51] K. Q. Bui, L. P. Perera, and J. Emblemsvåg, "Life-cycle cost analysis of an innovative marine dual-fuel engine under uncertainties," J. Clean. Prod., vol. 380, p. 134847, 2022. doi: 10.1016/j.jclepro.2022.134847
- [52] D. Radan, T. A. Johansen, A. J. Sørensen, and A. K. Adnanes, "Optimization of load dependent start tables in marine power management systems with blackout prevention," WSEAS Trans. Circuits Syst., vol. 4, pp. 1861–1866, 2005.
- [53] International Maritime Organization, "Nitrogen oxides (NOx) Regulation 13," [Online]. Available: https://www.imo.org/en/OurWork/Environment/Pages/Nitrogen-oxides-(NOx)-Regulation-13.aspx. [Accessed: Feb. 27, 2025].
- [54] International Maritime Organization, "Res./MEPC.177(58) NOx Technical Code 2008: Technical code on control of emission of nitrogen oxides from marine diesel engines," [Online]. Available: https://puc.overheid.nl/nsi/doc/PUC_2411_14/2/. [Accessed: Feb. 25, 2025].

- [55] International Maritime Organization, "IMO and the UNFCCC policy framework,"
 [Online]. Available:
 https://www.imo.org/en/OurWork/Environment/Pages/Historic%20Background%20G
 HG.aspx. [Accessed: Feb. 25, 2025].
- [56] International Maritime Organization, NOx Technical Code 2008: Technical code on control of emission of nitrogen oxides from marine diesel engines Res. MEPC.177(58), 2008. [Online]. Available: https://www.cdn.imo.org/localresources/en/KnowledgeCentre/IndexofIMOResolutions /MEPCDocuments/MEPC.177%2858%29.pdf. [Accessed: Nov. 22, 2024].
- [57] Heywood, J. B. *Internal Combustion Engine Fundamentals*. 1st ed., New York: McGraw-Hill, 1988.
- [58] International Maritime Organization. *Guidelines for voluntary use of the ship energy efficiency operational indicator (EEOI)*. MEPC.1/Circ.850/Rev.1, 2013. Available online: https://www.imo.org
- [59] MAN Energy Solutions. *Project Guide: Marine Four-Stroke Engines*. Augsburg, Germany, 2020. Available online: https://marine.man-es.com
- [60] Marques, S., and Caprace, J.-D. "An approach for predicting the specific fuel consumption of dual-fuel two-stroke marine engines." *Ships and Offshore Structures*, vol. 14, no. 2, pp. 105–117, 2019. Available online: https://doi.org/10.1080/17445302.2018.1524924
- [61] Wärtsilä Corporation. *Wärtsilä 34DF Product Guide and Technology Review*. Helsinki, 2014. Available online: https://www.wartsila.com
- [62] Y. Gui, Study on Fuel Consumption Modeling and Optimization for Marine Engines, M.S. thesis, Dept. Energy Technology, Aalborg Univ., Aalborg, Denmark, 2023.
- [63] H. V. Pham, Y. Kim, and S. Y. Jung, "Effectiveness of the speed reduction strategy on exhaust emissions and fuel oil consumption of a marine generator engine for DC grid ships," *Journal of Marine Science and Engineering*, vol. 10, no. 7, p. 979, Jul. 2022, doi: 10.3390/jmse10070979.
- [64] E. Cuevas, A. Luque, and H. Escobar, "Spline interpolation," in *Computational Methods with MATLAB®*, Cham, Switzerland: Springer Nature, 2024, pp. 151–177. ISBN: 978-3-031-40478-8.
- [65] International Maritime Organization, 2022 Guidelines on Operational Carbon Intensity Indicators and the Calculation Methods (CII Guidelines, G1) MEPC.346(78), 2022.

[Online]. Available: https://www.cdn.imo.org/localresources/en/OurWork/Environment/Documents/Air%2 0pollution/MEPC.346(78).pdf. [Accessed: Dec. 1, 2024].

- [66] International Maritime Organization, 2022 Guidelines on Survey and Certification of the Attained Energy Efficiency Existing Ship Index (EEXI) – MEPC.351(78), 2022.
 [Online]. Available:
 https://www.cdn.imo.org/localresources/en/KnowledgeCentre/IndexofIMOResolutions/MEPCDocuments/MEPC.351(78).pdf. [Accessed: Dec. 1, 2024].
- [67] International Maritime Organization, Guidelines for Voluntary Use of the Ship Energy Efficiency Operational Indicator (EEOI) MEPC.1/Circ.684, 2005. [Online]. Available: https://gmn.imo.org/wp-content/uploads/2017/05/Circ-684-EEOI-Guidelines.pdf. [Accessed: Dec. 1, 2024].
- [68] T. Huan, F. Hongjun, L. Wei, and Z. Guoqiang, "Options and evaluations on propulsion systems of LNG carriers," in *Propulsion Systems*, London, U.K.: IntechOpen, 2019.
- [69] Wärtsilä Corporation, *Wärtsilä 50DF Engine Technology*, [Online]. Available: https://www.scribd.com/document/556733678/wartsila-50df. [Accessed: Dec. 23, 2024].
- [70] S. M. Mousavi, R. K. Saray, K. Poorghasemi, and A. Maghbouli, "A numerical investigation on combustion and emission characteristics of a dual fuel engine at part load condition," Fuel, vol. 166, pp. 309–319, 2016. doi: 10.1016/j.fuel.2015.10.052
- [71] M. C. Cameretti, R. Tuccillo, L. De Simio, S. Iannaccone, and U. Ciaravola, "A numerical and experimental study of dual fuel diesel engine for different injection timings," Appl. Therm. Eng., vol. 101, pp. 630–638, 2016. doi: 10.1016/j.applthermaleng.2015.12.071
- [72] B. Wang, T. Li, L. Ge, and H. Ogawa, "Optimization of combustion chamber geometry for natural gas engines with diesel micro-pilot-induced ignition," Energy Convers. Manag., vol. 122, pp. 552–563, 2016. doi: 10.1016/j.enconman.2016.06.027
- [73] B. Yang, C. Xi, X. Wei, K. Zeng, and M. C. Lai, "Parametric investigation of natural gas port injection and diesel pilot injection on the combustion and emissions of a turbocharged common rail dual-fuel engine at low load," Appl. Energy, vol. 143, pp. 130–137, 2015. doi: 10.1016/j.apenergy.2015.01.037
- [74] M. S. Lounici, K. Loubar, L. Tarabet, M. Balistrou, D. C. Niculescu, and M. Tazerout, "Towards improvement of natural gas-diesel dual fuel mode: An experimental

- investigation on performance and exhaust emissions," Energy, vol. 64, pp. 200–211, 2014. doi: 10.1016/j.energy.2013.10.091
- [75] G. Di Blasio, G. Belgiorno, and C. Beatrice, "Effects on performances, emissions and particle size distributions of a dual fuel (methane-diesel) light-duty engine varying the compression ratio," Appl. Energy, vol. 204, pp. 726–740, 2017. doi: 10.1016/j.apenergy.2017.07.103
- [76] W. Li, Z. Liu, and Z. Wang, "Experimental and theoretical analysis of the combustion process at low loads of a diesel natural gas dual-fuel engine," Energy, vol. 94, pp. 728–741, 2016. doi: 10.1016/j.energy.2015.11.052
- [77] N. N. Mustafi, R. R. Raine, and S. Verhelst, "Combustion and emissions characteristics of a dual fuel engine operated on alternative gaseous fuels," Fuel, vol. 109, pp. 669–678, 2013. doi: 10.1016/j.fuel.2013.03.007
- [78] B. J. Bora, U. K. Saha, S. Chatterjee, and V. Veer, "Effect of compression ratio on performance, combustion and emission characteristics of a dual fuel diesel engine run on raw biogas," Energy Convers. Manag., vol. 87, pp. 1000–1009, 2014. doi: 10.1016/j.enconman.2014.07.080
- [79] I. Dinçer and M. Rosen, *Exergy: Energy, Environment and Sustainable Development*, 2nd ed. Amsterdam, Netherlands: Elsevier, 2020. ISBN: 9780128243725.
- [80] A. Bejan, G. Tsatsaronis, and M. Moran, *Thermal Design and Optimization*, 1st ed. New York, NY, USA: Wiley-Interscience, 1995. ISBN: 0471584673.
- [81] T. J. Kotas, *The Exergy Method of Thermal Plant Analysis*. Malabar, FL, USA: Krieger Publishing Company, 1985. ISBN: 9780408013505.
- [82] J. Szargut, D. R. Morris, and F. R. Steward, Exergy Analysis of Thermal, Chemical, and Metallurgical Processes. New York, NY, USA: Hemisphere Publishing Corporation, 1988.
- [83] Y. A. Çengel and M. A. Boles, *Thermodynamics: An Engineering Approach*, 5th ed. New York, NY, USA: McGraw-Hill Science, 2005. ISBN: 978-0073107684.
- [84] S. de Oliveira, *Exergy: Production, Cost and Renewability*, vol. 63. London, UK: Springer, 2013. ISBN: 9781447141648.
- [85] M. Kanoğlu, Y. A. Çengel, and İ. Dinçer, *Efficiency Evaluation of Energy Systems*. New York, NY, USA: Springer, 2012. ISBN: 978-1-4614-2241-9.
- [86] J. Szargut, *Exergy Method: Technical and Ecological Applications*. Southampton, UK: WIT Press, 2005. ISBN: 1853127531.

- [87] M. J. Moran, H. N. Shapiro, D. D. Boettner, and M. B. Bailey, *Fundamentals of Engineering Thermodynamics*, 8th ed. Hoboken, NJ, USA: Wiley, 2014. ISBN: 1118412931.
- [88] C. Borgnakke and R. E. Sonntag, *Fundamentals of Thermodynamics*, 8th ed., SI version. Hoboken, NJ, USA: Wiley, 2014. ISBN: 978-1-118-13199-2.
- [89] International Maritime Organization, 2022 Guidelines on the Method of Calculation of the Attained Energy Efficiency Design Index (EEDI) for New Ships. London, UK: IMO, 2022, pp. 1–37.
- [90] European Parliament and Council, Regulation (EU) 2023/1805 of 13 September 2023 on the Use of Renewable and Low-Carbon Fuels in Maritime Transport and Amending Directive 2009/16/EC. Brussels, Belgium: Official Journal of the European Union, 2023.
- [91] A. Bejan, *Advanced Engineering Thermodynamics*, 3rd ed. Hoboken, NJ, USA: Wiley, 2006. ISBN: 978-0-471-67763-5.

LIST OF FIGURES AND DIAGRAMS

Figure 1.1 Simplified connection arrangement of diesel generators, main switchboards and propulsion
systems
Figure 1.2 Layout of the electrical power distribution for a DFDE-powered LNG ship11
Figure 1.3 Configuration of diesel-electric propulsion using DF engines
Figure 1.4 Schematic representation of a gas management system in a DFDE propulsion setup16
Figure 3.1 Specific Fuel Oil Consumption (SFOC) as a function of engine load for HFO, MDO, and
LNG, recorded during simulator tests
Figure 3.2 Nitrogen oxide (NO _x) emissions, measured in ppm, as a function of engine load during
simulator operation with HFO, MDO and LNG27
Figure 3.3 Carbon dioxide (CO ₂) emissions, expressed as a percentage depending on the engine load,
based on simulator tests with HFO, MDO and LNG
Figure 3.4. Example of an emission measurement while the engine is running on LNG31
Figure 3.5 Specific fuel oil consumption (SFOC) of a diesel engine over the engine load33
Figure 3.6 Specific fuel oil consumption (SFOC) for a dual-fuel engine in diesel mode33
Figure 3.7 Fuel consumption data for three different types of fuel depending on the engine load34
Figure 3.8 Exhaust gas analyzer "Testo 350 Maritime", used for measurements on an LNG ship34
Figure 3.9 CO ₂ emissions for three types of fuel depend on the engine load35
Figure 3.10 NOx emissions for three types of fuel depending on the engine load35
Figure 3.11 Position of the sampling probes during recording under real operating conditions36
Figure 3.12 SFOC on HFO
Figure 3.13 SFOC on MDO
Figure 3.14 SFOC on LNG
Figure 3.15 Optimization model flow chart
Figure 3.16 Enhanced Optimization model flow chart
Figure 4.1 Comparative analysis of HFO consumption for the power range 25,000–29,000 kW47
Figure 4.2 Engine load distribution (%) across the power range of 25,000 to 29,000 kW
Figure 4.3 Load distribution between the engines and HFO consumption at 10,000 kW load demand49
Figure 4.4 Load distribution between the engines and HFO consumption at 23,000 kW load demand49
Figure 4.5 Comparative analysis of MDO consumption for the power range $25,000-29,000 \; kW \ldots 51$
Figure 4.6 Load distribution (%) by engines for the power range 25,000–29,000 kW52
Figure 4.7 Load distribution across the engines and corresponding MDO consumption for a power
requirement of 10,000 kW53
Figure 4.8 Load distribution across the engines and corresponding MDO consumption for a power
requirement of 23,000 kW53

Figure 4.9 Comparative analysis of LNG consumption for the power range 25,000–29,000 k	W55
Figure 4.10 Engine load distribution (%) over the power range of 25,000–29,000 kW	55
Figure 4.11 Load distribution across the engines and corresponding LNG consumption for	or a power
requirement of 10,000 kW	56
Figure 4.12 Load distribution across the engines and corresponding LNG consumption for	or a power
requirement of 23,000 kW	57
Figure 4.13 Optimization example for LNG with a power requirement of 20,000 kW using for	ur engine
	58
Figure 4.14 Optimization example for MDO with a power requirement of 20,000 kW using for	ur engines
	59
Figure 4.15 Optimization example for HFO with a power requirement of 20,000 kW using fo	ur engines
	60
Figure 4.16 Fuel consumption for the power range 24,000–26,000 kW	62
Figure 4.17 CO ₂ emission share for the power range of 24,000–26,000 kW	63
Figure 4.18 Share of NOx emissions for the power range 24,000–26,000 kW	64
Figure 4.19 Percentage load distribution across the engines for the power range of 24,000-2	26,000 kW
	65
Figure 4.20 Fuel consumption as a function of weighting factors for fuel optimization	67
Figure 4.21 CO ₂ emissions based on the fuel weighting factors	68
Figure 4.22 NOx emissions based on the weighting factors	68
Figure 4.23 "Promass 80" mass flow meter	71
Figure 4.24 IAS representation of cargo Tank conditions	72
Figure 4.25 IAS representation of load distributions according to the PMS	72
Figure 4.26 IAS representation of load distributions according to the optimization model	73
Figure 4.27 Optimization example for LNG at 24,000 kW on four engines	74
Figure 4.28 IAS representation of cargo Tank conditions	75
Figure 4.29 IAS representation of load distributions according to the PMS	75
Figure 4.30 IAS representation of load distributions according to the optimization model	76
Figure 4.31 Optimization example for LNG at 17,500 kW on three engines	77
Figure 4.32 IAS representation of load distributions according to the PMS	77
Figure 4.33 IAS representation of load distributions according to the optimization model	78
Figure 4.34 Optimization example for LNG at 8000 kW on two engines	79
Figure 4.35 IAS representation of load distributions according to the PMS	79
Figure 4.36 IAS representation of load distributions according to the optimization model	80
Figure 4.37 Optimization example for LNG at 4000 kW on two engines	81
Figure 5.1 Use of combustion products as a heat source for a Carnot engine	96
Figure 5.2 Enthalpy of combustion products and heat extraction compared to temperature	97

LIST OF TABLES

Table 1.1 Specification of DF-8L 51/60 DF @ 100% load	12
Table 3.1 Different engine load distribution	29
Table 3.2 Overall result differences	29
Table 4.1 Fuel savings across different operating regimes	81
Table 5.1 Values for the calculation of the physical exergy of combustion products	93
Table 5.2 Heating values and carbon dioxide emissions	95

LIST OF ABBREVIATIONS

ABBREVIATION	DEFINITION
BOG	Boil-Off Gas
CII	Carbon Intensity Indicator
СО	Carbon Monoxide
CO ₂	Carbon Dioxide
DFDE	Dual-Fuel Diesel-Electric
DG	Diesel Generator
EEOI	Energy Efficiency Operational Indicator
EEXI	Energy Efficiency Existing Ship Index
GCU	Gas Combustion Unit
GHG	Greenhouse Gas
HFO	Heavy Fuel Oil
IAS	Integrated Automation System
IEEE	Institute of Electrical and Electronics Engineers
IMO	International Maritime Organization
LNG	Liquefied Natural Gas
MARPOL	International Convention for the Prevention of Pollution from
	Ships
MATLAB	Matrix Laboratory (Software)
MCR	Maximum Continuous Rating
MDO	Marine Diesel Oil
MEPC	Marine Environment Protection Committee
NCV	Net Calorific Value

NOx	Nitrogen Oxides
PMS	Power Management System
SFOC	Specific Fuel Oil Consumption
SOx	Sulfur Oxides
CH ₄	Methane
C ₂ H ₆	Ethane
EEDI	Energy Efficiency Design Index
EU	European Union
HHV	Higher Heating Value
LHV	Lower Heating Value
N ₂	Nitrogen
NO	Nitric Oxide
N _C	Number of Carbon Atoms in Fuel Molecule
N _H	Number of Hydrogen Atoms in Fuel Molecule
No	Number of Oxygen Atoms in Fuel Molecule

LIST OF SYMBOLS

SYMBOL	DESCRIPTION	UNIT
P	Power	kW
U	Voltage	V
I	Current	A
$cos(\varphi)$	Power factor	_
T	Torque	Nm
n	Rotational speed	rpm
SFOC	Specific Fuel Oil Consumption	g/kWh
CO_2	Carbon Dioxide emission	%
NOx	Nitrogen Oxides emission	ppm
SOx	Sulfur Oxides emission	PM
η	Efficiency	_
Q	Fuel consumption	kg/h
ṁ	Mass flow rate	kg/s
LHV	Lower Heating Value	MJ/kg
NCV	Net Calorific Value	MJ/kg
EEXI	Energy Efficiency Existing Ship Index	g CO ₂ /ton/nm
EEOI	Energy Efficiency Operational Indicator	g CO ₂ /ton/nm
CII	Carbon Intensity Indicator	g CO ₂ /ton/nm
TFC	Total Fuel Consumption	tons
MCR	Maximum Continuous Rating	kW
P_actual	Actual measured power	kW
Load (%)	Engine load as a percentage of MCR	%

x_i, y_i	Data points used for interpolation	_
S(x)	Spline interpolation function	
a_i, b_i, c_i, d_i	Polynomial coefficients for spline segments	_
lb	Lower bound for load allocation	%
ub	Upper bound for load allocation	%
wf_FC	Weight factor for fuel consumption	_
wf_NOx	Weight factor for NO _x emissions	_
То	Ambient/reference temperature	K
T_{f}	Flame (final) temperature	K
T _{ref}	Reference temperature	K
W	Work potential / available work	kJ
H _{react}	Enthalpy of reactants	kJ/kmol
H _{product}	Enthalpy of products	kJ/kmol
h	Specific enthalpy	kJ/kg
S	Specific entropy	kJ/kg·K
S	Entropy	kJ/kg·K
e _x	Specific exergy	kJ/kg
Ė _x	Exergy flow rate	kJ/s
m	Mass flow rate	kg/s
Х	Mass or mole fraction	_
у	Mole or mass fraction	_
R	Gas constant	kJ/kg·K
ηπ	Exergetic efficiency	_

n_{O2}	Amount of oxygen required	kmol
χ	Molar fraction of fuel component	_

BIOGRAPHY

Siniša Martinić-Cezar was born in Split in 1973. He obtained a bachelor's degree in Naval Mechanical Engineering from the *Faculty of Maritime Studies in Split* 2010, followed by a master's degree at the same institution in 2012.

In his professional career, Siniša Martinić-Cezar has served as a ship's engineer officer and since 2008 as chief engineer on a number of vessels, including VLCC tankers and since 2013 exclusively on LNG carriers equipped with various propulsion systems, including steam turbine, Q-Flex and DFDE technology.

Over the course of more than three decades at sea, he has gained extensive practical experience in marine propulsion, fuel efficiency optimization, maintenance management and compliance with international environmental regulations. His service on board LNG carriers and crude oil tankers, mainly with one of the world's leading shipping companies over the last two decades, has given him a deep, practical insight into the operational and technical challenges of marine engineering. This foundation has directly influenced and motivated his academic research in the areas of propulsion optimization and emission reduction.

During 2018, he enrolled in the doctoral program at the *University of Rijeka, Faculty of Maritime Studies*. In 2020, he moved to the Postgraduate Doctoral University Study "Technologies in Maritime Affairs" at the *University of Split, Faculty of Maritime Studies*.

Papers published in journals:

- Martinić-Cezar, Siniša; Jurić, Zdeslav; Assani, Nur; Račić, Nikola Controlling Engine Load Distribution in LNG Ship Propulsion Systems to Optimize Gas Emissions and Fuel Consumption // Energies (Basel), 18 (2025), 3; 485-506. doi: 10.3390/en18030485
- 2. Martinić-Cezar, Siniša; Jurić, Zdeslav; Assani, Nur; Lalić, Branko Optimization of Fuel Consumption by Controlling the Load Distribution between Engines in an LNG Ship Electric Propulsion Plant // Energies (Basel), 17 (2024), 15; 3718-3737. doi: 10.3390/en17153718
- **3. Martinić-Cezar, Siniša**; Bratić, Karlo; Jurić, Zdeslav; Račić, Nikola Exhaust emissions reduction and fuel consumption from the LNG energy system depending on the ship operating modes // Pomorstvo: scientific journal of maritime research, 36(2022) (2022), 2; 338-346. doi: 10.31217/p.36.2.17

Papers published in conference proceedings:

- 1. Martinić-Cezar, Siniša; Bratić, Karlo; Slišković, Merica; Račić, Nikola Exhaust emissions from marine 4-stroke engine on the three fuel types // 2ST INTERNATIONAL CONFERENCE OF MARITIME SCIENCE & TECHNOLOGY NAŠE MORE 2021. Dubrovnik: Pomorski odjel Sveučilišta u Dubrovniku, 2021. str. 227-241
- 2. Martinić-Cezar, Siniša; Kezić, Danko; Račić, Nikola Computer control of intelligent ship engine Sulzer RT-flex // KoREMA-Tridesetdrugi skup o prometnim sustavima s međunarodnim sudjelovanjem AUTOMATIZACIJA U PROMETU, Zagreb, Hrvatska, 14.11.2012-18.11.2012